

博士學位論文

**Studies on Photocatalytic Chemoselective Reduction
of Oxygen Containing Compounds
under Hydrogen-free Condition**

近畿大学大学院
総合理工学研究科 物質系工学専攻

中西康介

博士學位論文

Studies on Photocatalytic Chemoselective Reduction of Oxygen Containing Compounds under Hydrogen-free Condition

平成 30 年 1 月 9 日

近畿大学大学院
総合理工学研究科 物質系工学専攻

中西 康 介

Contents

General introduction	5
1. Reduction of organic compounds	5
2. Photocatalytic organic synthesis	5
3. Co-catalyst effect on photocatalytic reaction	7
4. Biomass and its transformation	7
5. Element Strategy	9
6. Outline of this work	10
References	14
Chapter 1	17
1.1. Introduction	17
1.2. Experimental	19
1.3. Results and discussion	21
1.3.1. Photocatalytic deoxygenation of diphenyl sulfoxide	21
1.3.2. The effect of the kind and amount of hole scavenger on yield and selectivity of DPSI produced in photocatalytic deoxygenation of DPSO	24
1.3.3. Action spectrum of photocatalytic deoxygenation of DPSO to DPSI	26
1.3.4. The expected reaction process of photocatalytic deoxygenation of DPSO to DPSI over TiO₂	28
1.3.5. Applicability of photocatalytic deoxygenation of sulfoxide	30
1.3.6. Effects of physical properties of TiO₂	32
1.4. Conclusions	35
References	36
Chapter 2	39
2.1. Introduction	39

2.2. Experimental	42
2.2.1. Photocatalytic hydrogenation of FAL	42
2.2.2. Adsorption of FAL and FOL on TiO₂	42
2.3. Results and discussion	43
2.3.1. Photocatalytic hydrogenation of FAL	43
2.3.2. Applicability of alcohol in chemoselective hydrogenation of FAL to FOL	47
2.3.3. Action spectrum of photocatalytic selective hydrogenation of FAL to FOL over TiO₂	50
2.3.4. Effects of various reaction conditions on reduction of FAL in ethanolic suspensions of TiO₂	52
2.3.5. The expected reaction process of photocatalytic reduction of FAL in a 2-petanol suspension of TiO₂	54
2.4. Conclusions	56
References	57
Chapter 3	58
3.1. Introduction	58
3.2. Experimental	61
3.2.1. Preparation of metal-loaded TiO₂	61
3.2.2. Characterization	61
3.2.3. Photocatalytic reaction	61
3.2.4. Adsorption of furan on TiO₂ or Metal-loaded TiO₂	62
3.2.5. Catalytic Hydrogenation of furan on TiO₂ or Metal-loaded TiO₂	62
3.3. Results and discussion	64
3.3.1. Effects of different metal co-catalysts	64
3.3.2. Effects of the Pd loadings on the yield of THF formed	69
3.3.3. TEM images and distribution of Pd nanoparticles	71

3.3.4. <i>Effects of reaction conditions on photocatalytic hydrogenation of furan</i>	73
3.3.5. <i>Photocatalytic hydrogenation of furan</i>	76
3.3.6. <i>Action spectrum and reaction process</i>	80
3.3.7. <i>The expected reaction process of photocatalytic hydrogenation of furan to THF over Pd-TiO₂</i>	82
3.4. Conclusions	84
References	85
Chapter 4	88
4.1. Introduction	88
4.2. Experimental	90
4.2.1. <i>Preparation of metal-loaded TiO₂</i>	90
4.2.2. <i>Photocatalytic reaction</i>	90
4.2.3. <i>Adsorption experiment</i>	91
4.2.4. <i>Catalytic reaction under an H₂ condition</i>	91
4.3. Results and discussion	92
4.3.1. <i>Effects of different metal co-catalysts</i>	92
4.3.2. <i>Effect of the amount of Rh loading on CCA yield</i>	96
4.3.3. <i>Photoinduced ring hydrogenation of BA in an aqueous suspension of Rh-TiO₂</i>	98
4.3.4. <i>Action spectrum</i>	100
4.3.5. <i>Effects of reaction conditions on ring hydrogenation of BA</i>	102
4.3.6. <i>Adsorption experiments</i>	107
4.3.7. <i>Dark reactions under H₂</i>	109
4.3.8. <i>Effect of pH</i>	110
4.3.9. <i>Expected reaction process</i>	112
4.4. Conclusions	114

References.....	115
Chapter 5	117
5.1. Introduction	117
5.2. Experimental	119
<i>5.2.1. Preparation of TiO₂ having two elements as a co-catalyst</i>	119
<i>5.2.2. Characterization</i>	120
<i>5.2.3. Photocatalytic reaction</i>	120
5.3. Results and Discussion	122
<i>5.3.1. Effects of the combination of two elements as a co-catalyst on ring hydrogenation</i>	122
<i>5.3.2. TEM observation</i>	125
<i>5.3.3. XPS analysis</i>	128
<i>5.3.4. XANES analysis</i>	131
<i>5.3.5. Ring hydrogenation over different types of photocatalyst with the same compositions</i>	133
<i>5.3.6. Effect of H₂ treatment of Pd-free Ru/TiO₂ on photocatalytic ring hydrogenation</i>	135
<i>5.3.7. Functions of Ru and Pd in photocatalytic ring hydrogenation</i>	137
5.4. Conclusions	139
General conclusions	142
Publication list	145
Other publication list	147
Acknowledgments	148

General introduction

1. Reduction of organic compounds

Reduction of organic compounds has several types of reaction such as electron accepting reaction, deoxygenation reaction and hydrogenation reaction. Deoxygenation is the reaction to remove oxygen atom from oxygen containing compounds such as alcohols, epoxides and sulfoxides. Hydrogenation is the reaction to insert hydrogen atom into unsaturated bonds such as alkynyl groups, alkenyl groups, carboxyl groups and nitrile groups. Stoichiometric reducing agents such as metal hydrides are conventionally used for these reductions^{1, 2}. Since the reduction with metal hydrides simultaneously gives harmful waste containing metal residue and an organic solvent, another environmentally friendly method not forming harmful waste is desired. Several metal catalysts were developed for environmentally-friendly reaction^{3, 4}; however, stoichiometry agents are required as the reducing agent even in this case. Recently, reduction of organic compounds using H₂ as "greener" reducing agent was reported^{5, 6}. The reduction method using H₂ as reducing agent has the advantage that by-product is only water in the case of removal of oxygen from substrates. Most of reactions are carried out under compressed condition at elevated temperature. Therefore, when H₂ is used as the reducing agent, special attention should be paid because of possibility of explosion. Transportation and storage of H₂ in the compressed state consume much energy. Under these circumstances, another catalytic method working under mild conditions and consuming less energy is keenly desired for more environmentally friendly reduction of organic compounds.

2. Photocatalytic organic synthesis

Organic synthesis using photocatalysts has been extensively studied as a "greener" synthesis approach of organic compounds. Titanium(IV) oxide (TiO₂) is

known as leading example of photocatalyst. When semiconductor photocatalysts such as TiO_2 are irradiated by light having an energy larger than the band gap, electron in the valence band are excited to a conduction band, resulting in formations of excited electrons (e^-) in the conduction band and positive holes (h^+) in the valence band. They cause oxidation and reduction respectively. Totally, both e^- and h^+ are consumed, simultaneously producing reduced and oxidized products. Since this redox reaction is driven only by light at room temperature, photocatalytic system does not require assists of heating and pressurization. Since photocatalyst irradiated by light has oxidizing and reducing powers, harmful oxidizing and reducing agents are generally unnecessary. For example, it is possible to use oxygen molecule (O_2) as an oxidizing agent for reactions requiring oxidizing agents such as potassium permanganate and chromium oxide. In this case, direct redox reaction between an organic compound and oxygen does not occur, in which the former is oxidized by h^+ and the latter is reduced by e^- . Similarly, alcohols are used as a reducing agent for reactions requiring reducing agents such as LiAlH_4 and NaBH_4 , in which alcohols are oxidized by h^+ and compounds are reduced by e^- . In addition, since TiO_2 is harmless to human, TiO_2 is regarded as a typical "green" catalyst material. Advantage in the separation process is also pointed out, i.e., TiO_2 is easily separated from mixtures after the reaction with filtration or centrifugation.

Many examples for application of TiO_2 photocatalyst for oxidation reactions have been reported. The examples include decomposition of environmental pollutants⁷, oxidation of hydrocarbons⁸ and amines⁹, direct oxidation of benzene to phenol¹⁰, selective oxidation of alcohols to carboxyl group¹¹, and selective oxidation of sulfide to sulfoxide¹². On the other hand, the number of reports on photocatalytic reduction is much less than that of reports on photocatalytic oxidation and most of the reports are focused on reduction of nitrobenzene¹³⁻¹⁷. Reductions of other

compounds are limited; reduction of aldehydes and ketones to alcohols^{18, 19}, dehalogenation of aromatic halide²⁰, deoxygenation of epoxides^{21, 22} and hydrogenation of unsaturated bonds²³⁻²⁵. Examples of photocatalytic reaction inducing both oxidation and reduction in the same molecule are further limited to synthesis of L-pipecolinic acid from L-lysine²⁶.

3. Co-catalyst effect on photocatalytic reaction

Some reduction reactions introduced in the previous section require the presence of co-catalyst on the surface of photocatalyst. In the cases of dehalogenation of an aromatic halide²⁰, hydrogenation of an unsaturated bonds²³⁻²⁵ and deoxygenation of epoxides²², no reactions occurred without the use of co-catalyst, i.e., the use of co-catalysts is indispensable to drive these reactions. Positions of the valence and conduction bands of semiconductors such as TiO₂ and tungsten(VI) oxide determine the oxidizing and reducing powers of the photocatalysts. No reduction occurs if the position of the conduction band is positive to the reduction potential of the target reaction. For example, the reason why no hydrogenation of the C=C double bond occurs over bare-TiO₂ is that the potential for hydrogenation of the C=C bond is more negative to the position of the conduction band of TiO₂. The C=C double bond of hydrocarbons is hydrogenated over Pd-loaded TiO₂ photocatalyst^{24, 25}. This result indicates that the Pd metal loaded on TiO₂ works as the catalyst in the photocatalytic reduction. In other words, the possibility of the photocatalytic reduction can be expanded by introducing co-catalyst to photocatalyst. However, there is still a little example reporting that photocatalytic reduction is greatly improved by introduction of co-catalyst to photocatalyst.

4. Biomass and its transformation

Biomass refers to grass, trees, agricultural crops, algae, animal excreta, waste materials, it is renewable and biological origin.²⁷ Plant-based biomass absorbs carbon dioxide in the air and water from the ground during its growth, synthesizing oxygen and sugar by photosynthesis. Carbon dioxide is known as one of greenhouse gases. When fossil resources such as petroleum are used as a fuel for thermal power generation, carbon dioxide is released into the atmosphere as exhaust gas. Recently, utilization of biomass as fuel sources and platforms of chemicals attracts much attention of chemists and conversion of biomass to biofuels has been extensively studied. Carbon dioxide released after utilization of biofuels such as combustion is absorbed again by plant-biomass during the growth. This cycle consisting of fixation of carbon dioxide by photosynthesis and release of carbon dioxide by utilization does not affect the concentration of carbon dioxide on the earth. This idea is called as "carbon neutral". At present, fats and oils are converted to biodiesel fuels that are added to diesel fuels. Biomass-derived ethanol is blended with gasoline and is solely used as fuel in some country. In addition of conversion of biomass to alternative fuels, many researchers investigate conversion of biomass to raw materials for many kinds of compounds that are now derived from petroleum. It is possible to convert biomass resources to chemicals such as alkanes, alkenes, aromatic hydrocarbons, alcohols, ethers, aldehydes, ketones, carboxylic acids, esters, nitriles, amines and amino acids^{28, 29}. However, these conversions were achieved by means of conventional catalytic or enzymatic process. Biomass conversion requires a severe condition under high temperature and high pressure of hydrogen gas, often inducing catalyst deactivation and low selectivity of target compounds. Therefore, a new method (process, catalyst) is desired to satisfy a long catalyst life and high selectivity in biomass conversion. One of the promising methods for biomass conversions is a photocatalytic process. As mentioned in the previous section, since photocatalytic reaction occurs at room

temperature under an atmospheric pressure, the catalyst deactivation due to the deposition of oligomers is suppressed. As the successful case of biomass utilization, hydrogen can be produced from an aqueous suspension of photocatalyst containing biomass and biomass is simultaneously mineralized, indicating that this method has two aspects, i.e., utilization and treatment of biomass. However, there are few kinds of conversion of biomass to other compounds and a new photocatalytic reaction system utilizing biomass is highly desired.

5. Element Strategy

Element strategy is to develop materials with high function without using rare elements and harmful elements. Element strategy is achieved by studying the role and character of elements to clarify the reaction mechanisms of the functions and properties of substances and materials. There are several types of element strategy, 1) "decreased-quantity strategy" that decreases the use of rare elements and harmful elements, 2) "alternative strategy" which uses easily available and harmless elements as alternatives to rare elements and harmful elements presently used, 3) "circulation strategy" aiming at recycling of rare elements, 4) "regulatory strategy" aiming at technological innovation by imposing regulations, and 5) "new function strategy" that develops functions which have not been known until now. Examples are developments of platinum (Pt)- and rhodium (Rh)-free three-way catalyst using palladium (Pd)³⁰, cutting usage of Rh by alloying of copper³¹, development of copper oxide catalyst for rare-metal free three-way catalyst³² and development of dysprosium-free neodymium magnetite for car motor³³.

Recently, two elements are often used especially in catalyst materials because catalyst materials consisting of two elements exhibit larger reaction rate and higher selectivity than those of catalyst materials having single element. For example,

ruthenium-palladium alloy nanoparticles showed higher activity than those consisting of a single element of ruthenium, palladium or rhodium³⁴. It is proposed that characteristics of the alloy catalyst is different from those of the single metal catalysts. Effect of alloying co-catalyst on performance of photocatalyst is also reported. When silver (Ag)-loaded zirconium oxide photocatalyst was used for reduction of nitrobenzene, aniline and azobenzene were formed³⁵. Alloying Cu with Ag resulted in the production of azoxy compounds whereas copper-loaded photocatalyst showed lower conversion and lesser selectivity. These results indicate the alloying effect. In other case, it was reported that Pt-Ru loaded TiO₂ showed higher activity than Pt-TiO₂, Ru-TiO₂ and Pt-TiO₂/Ru (Pt and Ru were isolated) in photocatalytic oxidation of carbon monoxide³⁶. However, there are still few reports and additional examples of the alloying effect are expected in co-catalysts loaded on photocatalyst.

At a viewpoint of five topics described above, the author was interested in photocatalytic reductions without the use of H₂ gas at room temperature under an atmospheric pressure, environmentally friendly new reaction systems and new catalyst systems.

6. Outline of this work

In this thesis, various photocatalytic reductions of oxygen containing compounds under H₂-free condition are described in five chapters.

In chapter 1, photocatalytic deoxygenation of sulfoxides to corresponding sulfides was examined in acetonitrile suspensions of bare TiO₂ particles at room temperature under metal-free and H₂-free conditions. Diphenylsulfide (DPSI) was obtained with a high yield (98%) in photocatalytic deoxygenation of diphenylsulfoxide (DPSO) in the presence of oxalic acid (OA) as hole scavenger under deaerated conditions. In this case, other reduced products such as H₂ were not formed,

indicating that photogenerated electrons were selectively used for deoxygenation of DPSO. Re-oxidation and degradation of DPSI did not occur after consumption of DPSO. This photocatalytic deoxygenation of DPSO proceeded with high apparent quantum efficiency (AQE) of 35% at 350 nm. The AQE was in agreement with the absorption spectrum of TiO₂. Therefore, it can be concluded that deoxygenation of DPSO in an acetonitrile suspension was induced by photoabsorption of TiO₂. Various TiO₂ samples were examined for photocatalytic deoxygenation of DPSO. A correlation was obtained for most of the TiO₂ samples between specific surface area and DPSI yield. The applicability of photocatalytic deoxygenation of sulfoxides to sulfides was investigated. Phenyl vinyl sulfoxide was chemoselectively reduced to phenyl ethyl sulfide without hydrogenation of C=C double bond.

In chapter 2, photocatalytic selective hydrogenation of furfural (FAL) to furfuryl alcohol (FOL) was examined in alcohol suspensions of TiO₂ under metal-free and H₂-free conditions. FAL is one of biomass-derived compounds, and transformation of biomass-derived compounds is one of important topics in catalytic chemistry. FAL was successfully converted to FOL in a 2-pentanol suspension of TiO₂ photocatalyst under metal-free and H₂-free conditions. FOL and 2-pentanone were formed almost stoichiometrically. During the photocatalytic reaction, hydrogenation and degradation of furan structure, and re-oxidation of the hydroxymethyl group did not occur. The applicability of alcohol as hole scavenger in chemoselective hydrogenation of FAL was investigated. Ethanol and glycerol were available in hydrogenation of FAL, indicating that biomass-derived FAL can be up-graded to FOL by using biomass-derived alcohols such as ethanol and glycerol. In other words, double up-grading of FAL and alcohol was possible by photocatalytic reaction.

In chapter 3, the author investigated the photocatalytic hydrogenation of furan,

a representative *O*-heterocyclic compound and a biomass-derived compound, in alcohol suspensions of metal-loaded TiO₂ under H₂-free condition. Among the metal-loaded TiO₂ examined for photocatalytic hydrogenation of furan, Pd-loaded TiO₂ showed a distinctive photocatalytic activity for the hydrogenation of furan and suppressed H₂ evolution. In the case of other metal co-catalysts, this excellent property was not obtained. The author examined furan adsorption on TiO₂ and metal-loaded TiO₂, and found that Pd showed the largest amount of adsorption of furan. Experiments under various reaction conditions revealed that biomass-related alcohols can be used for this photocatalytic system. Action spectrum was in agreement with absorption spectrum of TiO₂ and AQE reached 37% at 360 nm. These results show that photocatalytic hydrogenation is not limited to hydrocarbons and can be applied to *O*-heterocyclic compounds.

In chapter 4, the author examined photoinduced ring hydrogenation of benzoic acid (BA) in an aqueous suspension of metal-loaded TiO₂ in the presence of oxalic acid under H₂-free condition. Effect of different metal co-catalysts on the yield of cyclohexanecarboxylic acid (CCA) as ring hydrogenation product was discussed. Rh-loaded TiO₂ showed much higher CCA yield than other co-catalyst loaded TiO₂. Correlation between hydrogen overvoltage of metal electrodes and yield of H₂ in the photocatalytic reaction in the presence and absence of BA was observed. H₂ evolution over Rh greatly decreased when BA was present in the reaction systems. The value of electron selectivity for the CCA formation increased with the increase in the amount of oxalic acid, while the efficiency of oxalic acid utilization decreased. From the results, there is an appropriate amount of oxalic acid for this reaction. Effects of hole scavenger and solvent were also examined and no photoinduced ring hydrogenation of BA occurred when alcohols and acetonitrile were used for as the solvent. Adsorption experiments under various conditions were carried out. The

difference in the adsorption properties is one of the important reasons for the high efficiency of the Rh-loaded TiO₂ photocatalyst in the ring hydrogenation of BA.

In chapter 5, the author loaded two kinds of metals other than Rh on TiO₂ and used these photocatalysts for ring hydrogenation of BA in aqueous suspensions under H₂-free conditions. In the chapter 4, the author describes that Rh-loaded TiO₂ hydrogenated BA to CCA. However, Rh is a rare and expensive element. Therefore, a photocatalyst having cheaper element(s) free from Rh is required. Among several combinations of two elements, the author found that Ru-Pd-TiO₂ hydrogenated BA to CCA as well as Rh-TiO₂. No ring hydrogenation occurred over Pd-TiO₂, Ru-TiO₂ and physical mixture of two photocatalysts. Spectroscopic analysis suggests that Ru and RuO₂ in the particles loaded on TiO₂ are mainly distributed on the outer surface of the particles, and most of the metallic Pd is distributed inside the particles and stabilizes some of the Ru in a metallic state. Results of photocatalytic reactions and characterization of Ru-Pd-TiO₂ suggest that the stabilized metallic Ru acts as active sites for photocatalytic ring hydrogenation of BA.

References

1. A. J. Birch, *J. Chem. Soc.*, **1944**, 430-436.
2. J. Drabowicz, M. Mikolajczyk, *Synthesis*, **1976**, 527-528
3. Y. Mikami, A. Noujima, T. Mitsudome, T. Mizugaki, K. Jitsukawa, K. Kaneda, *Chem. Eur. J.*, **2011**, *17*, 1768-1772.
4. T. Mitsudome, A. Noujima, Y. Mikami, T. Mizugaki, K. Jitsukawa, K. Kaneda, *Angew. Chem. Int. Ed.*, **2010**, *49*, 5545-5548
5. F. Corvaisier, Y. Schuurman, A. Fecant, C. Thomazeau, P. Raybaud, H. Toulhoat, D. Farrusseng, *J. Catal.*, **2013**, *307*, 352-361.
6. T. Mitsudome, K. Kaneda, *Green Chem.*, **2013**, *15*, 2636-2654
7. R. Ameta, S. Benjamin, A. Ameta, S. C. Ameta, *Mater. Sci. Forum*, **2013**, *734*, 247-272.
8. I. Izumi, W. W. Dunn, K. O. Wilbourn, F. F. Fan, Allen. J. Bard, *J. Phys. Chem.*, **1980**, *84*, 3207-3210.
9. D. Sun, L. Ye, Z. Li, *Appl. Catal. B: Environ.*, **2015**, *164*, 428-432.
10. O. Tomita, R. Abe, B. Ohtani, *Chem. Lett.*, **2011**, *40*, 1405-1407.
11. S. Yurdakal, G. Palmisano, V. Loddo, O. Alagoz, V. Augugliaro, L. Palmisano, *Green Chem.*, **2009**, *11*, 510-516.
12. X. Lang, W. R. Leow, J. Zhao, X. Chen, *Chem. Sci.*, **2015**, *6*, 1075-1082
13. H. Kominami, S. Iwasaki, T. Maeda, K. Imamura, K. Hashimoto, Y. Kera, B. Ohtani, *Chem. Lett.*, **2009**, *38*, 410-411.
14. K. Imamura, S. Iwasaki, T. Maeda, K. Hashimoto, B. Ohtani, H. Kominami, *Phys. Chem. Chem. Phys.*, **2011**, *13*, 5114-5119.
15. K. Imamura, K. Hashimoto, H. Kominami, *Chem. Commun.*, **2012**, *48*, 4356-4358.
16. K. Imamura, T. Yoshikawa, K. Hashimoto, H. Kominami, *Appl. Catal. B: Environ.*, **2013**, *134-135*, 193-197.

17. H. Tada, T. Ishida, A. Takao, S. Ito, *Langmuir*, **2004**, *20*, 7898-7900.
18. M. Fukui, A. Tanaka, K. Hashimoto, H. Kominami, *Chem. Lett.*, **2016**, *45*, 985-987.
19. S. Kohtani, Y. Kamoi, E. Yoshioka, H. Miyabe, *Catal. Sci. Technol.*, **2014**, *4*, 1084-1091
20. K. Fuku, K. Hashimoto, H. Kominami, *Chem. Commun.*, **2010**, *46*, 5118-5120.
21. Y. Shiraishi, H. Hirakawa, Y. Togawa, T. Hirai, *ACS Catal.*, **2014**, *4*, 1642-1649.
22. H. Kominami, S. Yamamoto, K. Imamura, A. Tanaka, K. Hashimoto, *Chem. Commun.*, **2014**, *50*, 4558-4560.
23. K. Imamura, T. Yoshikawa, K. Nakanishi, K. Hashimoto, H. Kominami, *Chem. Commun.*, **2013**, *49*, 10911-10913.
24. K. Imamura, Y. Okubo, T. Ito, A. Tanaka, K. Hashimoto, H. Kominami, *RSC Adv.*, **2014**, *4*, 19883-19886.
25. H. Kominami, M. Higa, T. Nojima, T. Ito, K. Nakanishi, K. Hashimoto, K. Imamura, *ChemCatChem*, **2016**, *8*, 2019-2022.
26. B. Pal, S. Ikeda, H. Kominami, Y. Kera, B. Ohtani, *J. Catal.*, **2003**, *217*, 152-159.
27. P. Basu, *Biomass Gasification and Pyrolysis: Practical Design and Theory*, Academic Press, United States, **2010**, 27-28
28. A. Corma, S. Iborra, A. Velty, *Chem. Rev.*, **2007**, *107*, 2411-2502.
29. A. J. J. Straathof, *Chem. Rev.*, **2014**, *114*, 1871-1908.
30. T. Sekiba, S. Kimura, H. Yamamoto, A. Okada, *Catal. Today*, **1994**, *22*, 113-126.
31. N. Palina, O. Sakata, L. S. R. Kumara, C. Song, K. Sato, K. Nagaoka, T. Komatsu, H. Kobayashi, K. Kusada, H. Kitagawa, *Sci. Rep.*, **2017**, *7*, 41264-41272.
32. T. Fujita, H. Abe, T. Tanabe, Y. Ito, T. Tokunaga, S. Arai, Y. Yamamoto, A. Hirata, M. Chem, *Adv. Funct. Mater.*, **2016**, *26*, 1609-1616.
33. K. Hioki, A. Hattori, T. Iriyama, *J. Mag. Soc. Jpn.*, **2014**, *38*, 79-82.

34. K. Kusada, H. Kobayashi, R. Ikeda, Y. Kubota, M. Takata, S. Toh, T. Yamamoto, S. Matsumura, N. Sumi, K. Sato, K. Nagaoka, H. Kitagawa, *J. Am. Chem. Soc.*, **2014**, *136*, 1864-1871.
35. Z. Liu, Y. Huang, Q. Xiao, H. Zhu, *Green Chem.*, **2016**, *18*, 817-825.
36. T. Zhang, S. Wang, F. Chen, *J. Phys. Chem. C*, **2016**, *120*, 9732-9739.

Chapter 1

Photocatalytic deoxygenation of sulfoxides to sulfides over titanium(IV) oxide at room temperature without use of metal co-catalysts

1.1. Introduction

Deoxygenation of sulfoxides is an important reaction in both organic synthesis and biochemistry¹⁻³. However, conventional deoxygenation requires stoichiometric reagents such as phosphines, halogens, and metal hydrides⁴⁻⁸ and yields a large amount of undesirable waste, although many efforts have been devoted to improve reaction conditions and to minimize the use of toxic reagents by using catalytic systems⁹⁻¹¹. Recently, excellent catalysts for deoxygenation of sulfoxides, i.e., gold (Au) and ruthenium (Ru) supported on hydroxyapatite (HAP), were reported^{12, 13}. However, even the Au/HAP and Ru/HAP catalysts required temperatures higher than 383 K and dimethylphenylsilane as a reducing agent yielding by-product residues such as siloxanes. Therefore, a more environmentally friendly catalytic reaction system for deoxygenation of sulfoxides working at lower temperatures with “greener” reducing agents giving no residue is keenly desired.

When titanium(IV) oxide (TiO_2) is irradiated by UV light, charge separation occurs and thus-formed electrons in the conduction band and positive holes in the valence band cause reduction and oxidation, respectively. Photocatalytic reaction proceeds at room temperature and under atmospheric pressure, and the TiO_2 photocatalyst is easily separated from the reaction mixture after the reaction and can be used repeatedly without a re-activation or re-generation process. In addition, TiO_2

has been used for a long time as an indispensable inorganic material such as a pigment and UV absorber because it is inexpensive and not toxic for humans and the environment. Since photocatalytic reaction satisfies almost all of the 12 proposed requirements for green chemistry¹⁴, organic synthesis of various compounds using photocatalysts has recently been studied by many researchers¹⁵ and the number of reports on photocatalytic reduction of organic compounds by using photogenerated electrons has been increasing^{16, 17}. However, most of the reports deal with reduction (hydrogenation) of nitrobenzenes to aminobenzenes¹⁸⁻³². In this study, the author examined a new photocatalytic reduction system, i.e., deoxygenation of sulfoxides (reduction of sulfoxides to sulfides) in a suspension of metal-free TiO₂ in the presence of hole scavengers such as oxalic acid and formic acid. In this reaction, these organic acids also work as stoichiometric reagents for deoxygenation. However, oxalic acid and formic acid are recently used as green hole scavengers for photocatalytic reduction and hydrogenation because these oxalic acids are converted to carbon dioxide, which is easily separated from the solvent under acidic conditions^{33, 34}. Here the author report that corresponding sulfides were successfully produced at room temperature without the use of toxic or undesirable reagents. .

1.2. Experimental

All of the reagents were commercial materials of reagent grade and used without further purification. Ishihara ST-01 was mainly used as the TiO₂ photocatalyst in this study. In a typical run, TiO₂ (50 mg) was suspended in 5 cm³ of acetonitrile containing diphenyl sulfoxide (DPSO) and oxalic acid in a test tube, sealed with a rubber septum under argon, and then photoirradiated at $\lambda > 300$ nm by a 400-W high-pressure mercury arc (Eiko-sha, Osaka) with magnetic stirring in a water bath continuously kept at 298 K. The amounts of DPSO unreacted and diphenyl sulfide (DPSI) formed were determined with an FID-type gas chromatograph (GC-2014, Shimadzu, Kyoto) equipped with a DB-1 column. The example of the gas chromatogram output is shown in Figure 1. The amount of hydrogen gas (H₂) as the reduction product of protons (H⁺) was determined with a TCD-type gas chromatograph (GC-8A, Shimadzu, Kyoto) equipped with an MS-5A column. To obtain an action spectrum, the full arc from a xenon (Xe) lamp (Optiplex, Ushio, Tokyo) was monochromated with light width of ± 10 nm using SM-100 (Bunkoukeiki, Tokyo). The light was used for photocatalytic reaction instead of the mercury arc. Spectra and intensity of the monochromated light from the Xe lamp were determined using a spectroradiometer (USR-45D, Ushio, Tokyo).

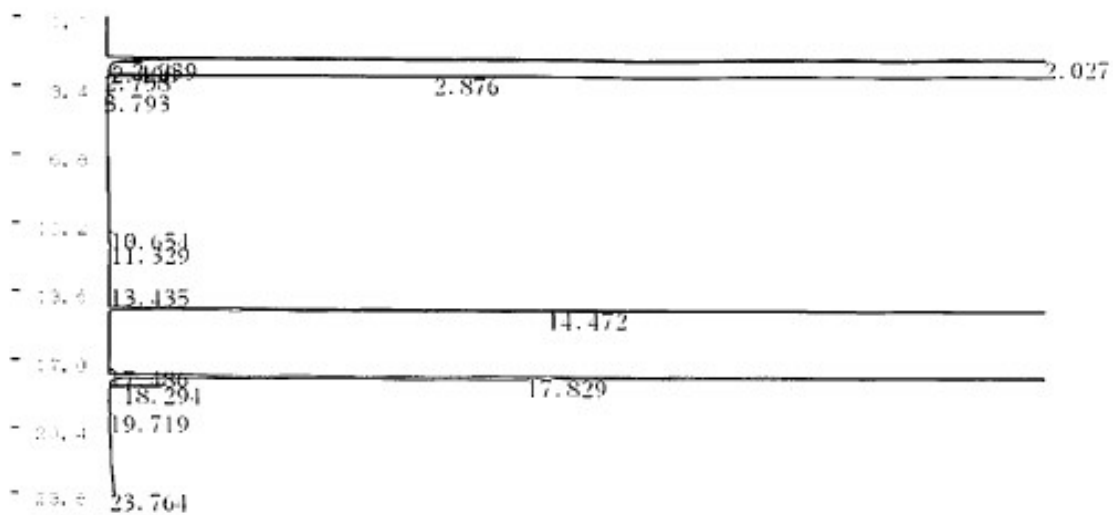


Figure 1 The gas chromatogram output at 30-min irradiation in Figure 2. 2.027 min: acetonitrile (solvent), 2.876 min: chlorobenzene (internal standard), 14.47 min: diphenylsulfide (product), 17.8 min: diphenylsulfoxide (substrate).

1.3. Results and discussion

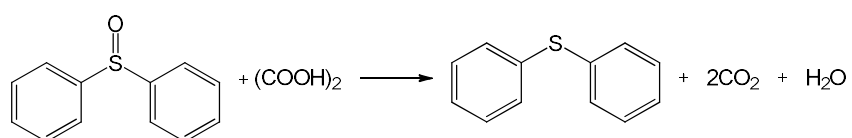
1.3.1. Photocatalytic deoxygenation of diphenyl sulfoxide

Figure 2 shows time courses of DPSO remaining and DPSI formed in an acetonitrile suspension of TiO₂ in the presence of oxalic acid under deaerated conditions. Just after photoirradiation, DPSO monotonously decreased, while DPSI was formed as the deoxygenation (reduction) product of DPSO. After 120 min, DPSO was almost completely consumed and DPSI was obtained in a high yield (98%). The results shown in Figure 2 were expressed as first-order kinetic and the rate constant was determined to be $2.15 \times 10^{-2} \text{ min}^{-1}$. Other reduced products such as H₂ were not formed, indicating that photogenerated electrons (in other words, oxalic acid) were selectively used for reduction of DPSO. No H₂ formation in the present reaction system is attributed to the use of bare (metal-free) TiO₂. This H₂-free system is attractive because there is no need to remove H₂ from the reaction system. To evaluate stoichiometry and selectivity of the reaction and side-reactions occurring under the present conditions, a new indicator, i.e., material balance (MB), was calculated by Equation (1):

$$MB = \frac{n(DPSO) + n(DPSI)}{n_0(DPSO)}, \quad \cdots(1),$$

where $n(DPSO)$ and $n(DPSI)$ are the amounts of DPSO and DPSI during the photocatalytic reaction, respectively, and $n_0(DPSO)$ is the amount of DPSO before the photocatalytic reaction. As shown in Figure 2, the values of MB were almost unity during the reaction, indicating that no other intermediates were produced under the present conditions. The author noted that 1) the amount of DPSI was unchanged, 2) the color of TiO₂ became blue (Ti³⁺ species formed), and 3) no H₂ was evolved, under excessive photoirradiation after complete consumption of DPSO. These results indicate that DPSI was not consumed by successive reactions such as re-oxidation and

degradation under the present conditions and that oxalic acid remaining was not consumed any more due to rapid recombination between photogenerated electrons and positive holes over Ti^{3+} species. From these results, the reaction, i.e., deoxygenation of DPSO to DPSI, would be shown in Scheme 1, although the author did not determine the amount of CO_2 .



Scheme 1 Photocatalytic deoxygenation of DPSO to DPSI in the presence of oxalic acid as a hole scavenger.

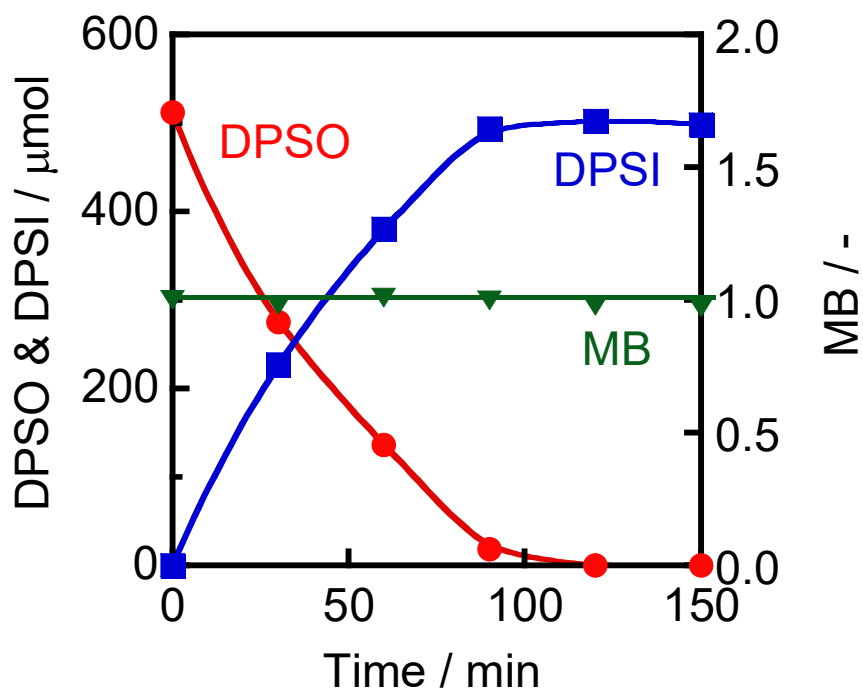


Figure 2 Time courses of DPSO remaining, DPSI formed and material balance of DPSO and DPSI in an acetonitrile suspension of TiO_2 in the presence of oxalic acid (1 mmol) under irradiation of UV light.

1.3.2. The effect of the kind and amount of hole scavenger on yield and selectivity of DPSI produced in photocatalytic deoxygenation of DPSO

Figure 3 shows the effect of the kind and amount of hole scavenger on yield and selectivity of DPSI produced in photocatalytic deoxygenation of DPSO in acetonitrile suspensions of TiO₂ for 15 min. Use of a typical alcoholic hole scavenger, 2-propanol, resulted in a low yield due to the small reaction rate. On the other hand, large yields were obtained with sufficient selectivities when organic acids (formic acid and oxalic acid) were used. These organic acids, especially oxalic acid, have been shown to be efficient hole scavengers for chemoselective reduction of 3-nitrostyrene to 3-aminostyrene over a TiO₂ photocatalyst⁹. When the amount of oxalic acid was decreased, both the yield and selectivity of DPSI decreased. Decrease in the selectivity suggests that DPSI was converted to some oxidized species other than DPSO because re-oxidation of DPSI to DPSO only decreases the yield of DPSI (the selectivity being preserved). These results indicate that twice the amount of a hole scavenger is necessary to avoid consumption of DPSI due to oxidation by positive holes.

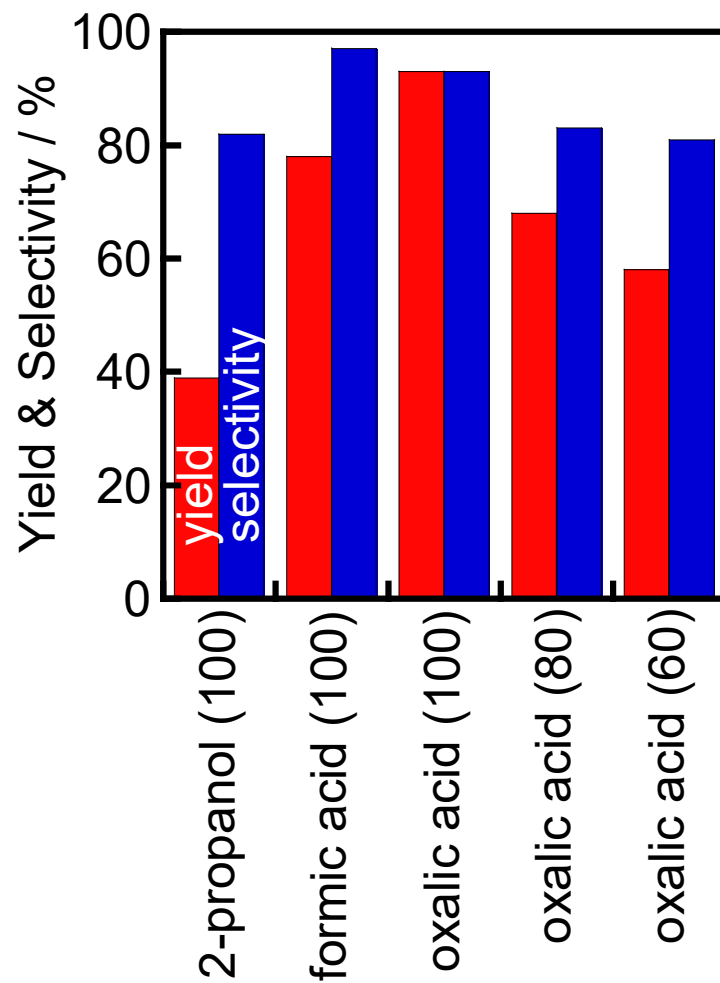


Figure 3 Effects of the kind and amount of hole scavengers on yield and selectivity of DPSI produced in photocatalytic deoxygenation of DPSO ($50 \mu\text{mol}$) in acetonitrile suspensions of TiO_2 for 15 min. The values in parentheses are the amounts of hole scavengers in μmol .

1.3.3. Action spectrum of photocatalytic deoxygenation of DPSO to DPSI

An action spectrum is a strong tool for determining whether a reaction observed occurs via a photoinduced process or a thermocatalytic process. To obtain an action spectrum in this reaction system, deoxygenation of DPSO in acetonitrile suspensions of TiO₂ (ST-01, Ishihara) was carried out at 298 K under irradiation of monochromated light from a Xe lamp with light width of ±10 nm. Apparent quantum efficiency (AQE) at each centered wavelength of light was calculated from the ratio of twice the amount of DPSI formed and the amount of photons irradiated using the following Equation (2):

$$\text{AQE} = \frac{2 \times \text{the amount of DPSI formed}}{\text{amount of incident photons}} \times 100. \quad \dots(2).$$

As shown in Figure 4, AQE was in agreement with the absorption spectrum of TiO₂. Therefore, it can be concluded that deoxygenation of DPSO in an acetonitrile suspension was induced by photoabsorption of TiO₂. As also shown in Figure 4, AQE reached 35% at 350 nm, indicating that photocatalytic deoxygenation of DPSO proceeded with high efficiency of photon utilization as well as chemical aspects such as selectivity and MB.

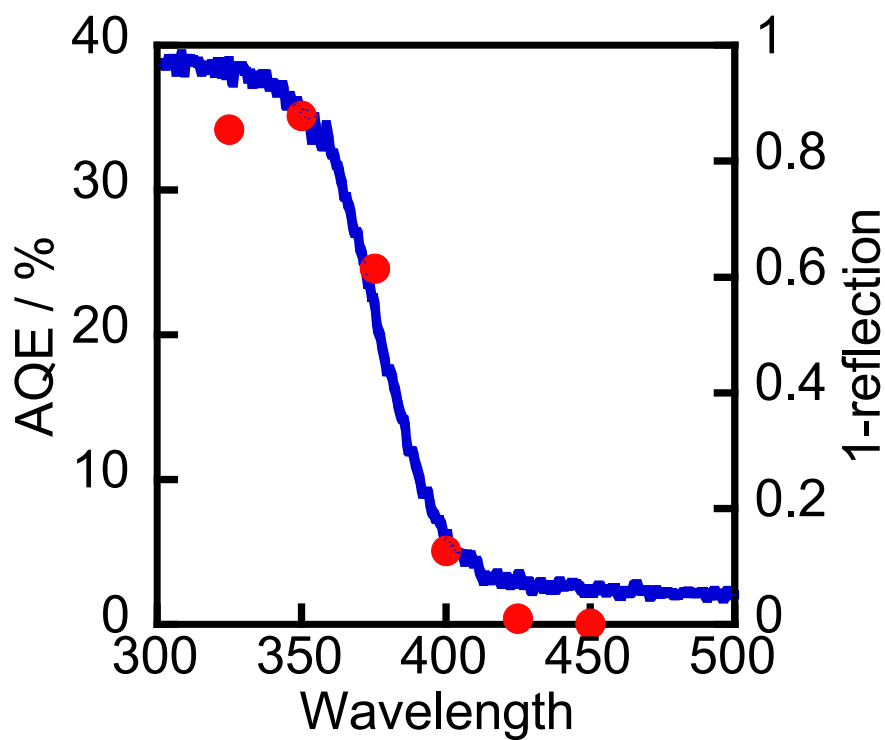


Figure 4 Absorption spectrum (right axis) and action spectrum of TiO_2 in the deoxygenation of DPSO (left axis). DPSO: 50 μmol , oxalic acid: 100 μmol .

1.3.4. The expected reaction process of photocatalytic deoxygenation of DPSO to DPSI over TiO₂

The expected reaction process of photocatalytic deoxygenation of DPSO to DPSI over TiO₂ is shown in Figure 5: 1) By irradiation of UV light, photogenerated electrons (e⁻) and positive holes (h⁺) are formed in the conduction and valence bands of TiO₂, and oxalic acid (or oxalate) is oxidized by h⁺, and 2) DPSO is reduced by e⁻, resulting in the formation of DPSI. However, H₂ formation by reduction of H⁺ does not occur under a metal-free condition because H₂ evolution generally requires loading of co-catalysts such as platinum and Pd.

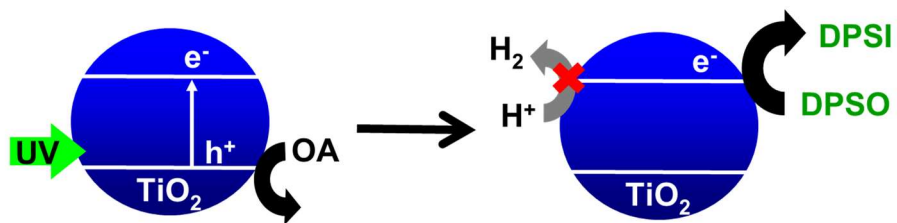
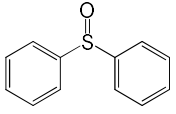
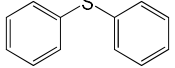
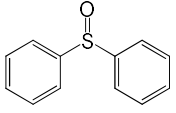
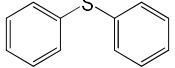
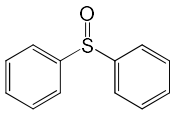
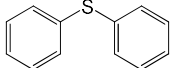
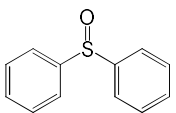
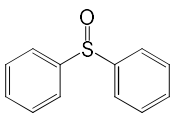
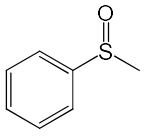
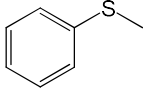



Figure 5 Expected reaction process of photocatalytic deoxygenation of DPSO to DPSI over metal-free TiO₂ in the presence of oxalic acid (OA).

1.3.5. Applicability of photocatalytic deoxygenation of sulfoxide

The applicability of photocatalytic deoxygenation of sulfoxide to sulfide was investigated, and the results are summarized in Table 1. Results of entries 1-3 indicate that the TiO₂ photocatalyst can be used repeatedly for deoxygenation of DPSO to DPSI without deactivation. The reusability of TiO₂ is attributable to its stability. Since the TiO₂ photocatalyst is used without modification with a metal co-catalyst, the present reaction system is free from changes in states such as size, dispersion and oxidation states of the co-catalyst during the photocatalytic reaction. Almost quantitative deoxygenation of DPSO occurred under a ten-times concentrated condition (entry 4) as shown in Figure 2. Methyl phenyl sulfoxide was more easily deoxygenated to methyl phenyl sulfide (entry 5). The author found that phenyl vinyl sulfoxide was chemoselectively reduced to phenyl vinyl sulfide without hydrogenation of a C=C double bond (entry 6). Kominami *et al.* have reported that 3-nitrostyrene was chemoselectively reduced to 3-aminostyrene without reduction of a C=C double bond to 3-ethylaniline in a suspension of a TiO₂ photocatalyst in the presence of oxalic acid as hole scavengers at room temperature³². The high reduction potential of vinyl group accounts for the chemoselective reduction of 3-nitrostyrene and phenyl vinyl sulfoxide. The use of TiO₂ without a metal co-catalyst strongly contributed to the chemoselectivity. If TiO₂ modified with a metal co-catalyst is used, hydrogenation of a C=C double bond³⁵ would occur as well as deoxygenation. Photocatalytic deoxygenation was also applicable for sulfoxide of an acyclic compound (entry 7), though a longer reaction time was required.

Table 1 Photocatalytic deoxygenation of sulfoxides to corresponding sulfides over TiO₂ at 298 K.^[a]

Entry	Sulfoxides	Sulfides	t / min	Yield / % ^[b]	Sel. / % ^[b]
1			20	93	95
2 ^[c]			20	98	98
3 ^[d]			20	>99	>99
4 ^[e]			120	98	98
5			15	99	99
6			15	82	82
7			30	91	91

[a] Reaction conditions: TiO₂ (50 mg), substrate (50 μmol), acetonitrile (5 cm³), oxalic acid (100 μmol), room temperature, under Ar. [b] Determined by GC using an internal standard. [c] Second use. [d] Third use. [e] Diphenyl sulfoxide (500 μmol), oxalic acid (1 mmol).

1.3.6. Effects of physical properties of TiO₂

To evaluate the effects of physical properties of TiO₂, representative commercial TiO₂ samples, which were registered at the Catalysis Society of Japan as Japan Reference Catalysts (JRC-TIO series), were used for photocatalytic deoxygenation of DPSO under the same conditions. Phase of TiO₂ and specific surface area of the TiO₂ samples are summarized in Table 2. Figure 6 shows the effect of specific surface area of TiO₂ samples on yields of DPSI produced. A clear correlation was observed for most of the TiO₂ samples between specific surface area and DPSI yield, though there were some exceptions. These results also mean that TiO₂ structure (anatase or rutile) had little effect on the photocatalytic deoxygenation of DPSO; however, bi-phase of anatase and rutile in the TiO₂ sample may be effective. The author are now investigating adsorption properties of these TiO₂ samples toward DPSO, DPSI and oxalic acid.

Table 2 Crystalline phase and specific surface area
of TiO₂ samples

TiO ₂	Phase	S _{BET} / m ² g ⁻¹ [a]
JRC-TIO-1	A	72
JRC-TIO-2	A	18
JRC-TIO-3	R	48
JRC-TIO-4 (P 25) ^[b]	A&R	54
JRC-TIO-5	R&A	2.6
JRC-TIO-6	R	100
JRC-TIO-7	A	270
JRC-TIO-8 (ST-01) ^[c]	A	313
JRC-TIO-9	A	290
JRC-TIO-10	A	311
JRC-TIO-11	A&R	97
JRC-TIO-12	A	290
JRC-TIO-13	A	59
MT-150A ^[d]	R	93

[a] Determined by BET method. [b] Supplied from Degussa. [c] Supplied from Ishihara. [d] Supplied from Tayca.

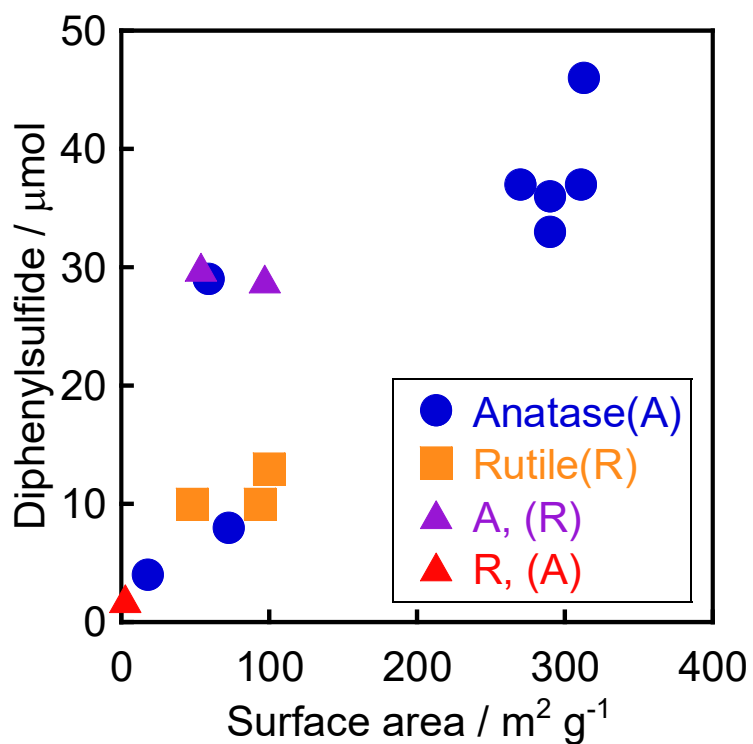


Figure 6 Effect of specific surface area of TiO₂ samples on yields of DPSI produced in photocatalytic deoxygenation of DPSO (50 μmol) for 10 min in acetonitrile solutions containing oxalic acid (100 μmol). Minor form in bi-phase samples is shown in parenthesis.

1.4. Conclusions

Photocatalytic deoxygenation of sulfoxides to corresponding sulfides was examined in acetonitrile suspensions of bare TiO₂ particles at room temperature without the use of a metal co-catalyst and toxic reagents. Organic acids, especially oxalic acid, worked efficiently as hole scavengers. The use of an excess of organic acids was effective for achieving high yields of sulfide and for avoiding fruitless degradation of sulfides. The present photocatalytic method can be applied for deoxygenation of various sulfoxides to corresponding sulfides. Chemoselective reduction of phenyl vinyl sulfoxide to phenyl vinyl sulfide was also achieved because the metal-free TiO₂ photocatalyst had no ability for hydrogenation of the C=C double bond.

References

1. G. Solladie, *Synthesis*, **1981**, 3, 185-196.
2. M. C. Carreno, *Chem. Rev.*, **1995**, 95, 1717-1760.
3. J. R. Debaun, J. J. Menn, *Science*, **1976**, 191, 187-188.
4. K. Bahrami, M. M. Khodaei, M. S. Arabi, *J. Org. Chem.*, **2010**, 75, 6208-6213.
5. G. S. Bhatia, P. P. Graczyk, *Tetrahedron Lett.*, **2004**, 45, 5193-5195.
6. K. Bahrami, M. M. Khodaei, A. Karimi, *Synthesis*, **2008**, 16, 2543-2546.
7. J. Drabowjcz, M. Mikolajczyk, *Synthesis*, **1976**, 527-528.
8. J. Zhang, X. Gao, C. Zhang, C. Zhang, J. Luan, D. Zhao, *Synth. Commun.*, **2010**, 40, 1794-1801.
9. K. Ogura, M. Yamashita, G. Tsuchihashi, *Synthesis*, **1975**, 385-387.
10. P. Geneste, M. Bonnet, C. Frouin, D. Levache, *J. Catal.*, **1980**, 61, 277-278.
11. N. Garcia, P. G-Garcia, M. R. Pedrosa, F. J. Arnaiz, R. Sanz, *Green Chem.*, **2013**, 15, 999-1005.
12. Y. Mikami, A. Noujima, T. Mitsudome, T. Mizugaki, K. Jitsukawa, K. Kaneda, *Chem. Eur. J.*, **2011**, 17, 1768-1772.
13. Y. Takahashi, T. Mitsudome, T. Mizugaki, K. Jitsukawa, K. Kaneda, *Chem. Lett.*, **2014**, 43, 420-422.
14. P. T. Anastas, J. C. Warner, *Green Chemistry: Theory and Practice*, Oxford University Press, **1998**.
15. M. A. Fox, M. T. Dulay, *Chem. Rev.*, **1993**, 93, 341-357.
16. G. Palmisano, V. Augugliaro, M. Pagliarob, L. Palmisano, *Chem. Commun.*, **2007**, 3425-3437.
17. G. Palmisano, E. Garcia-Lopez, G. Marci, V. Loddo, S. Yurdakal, V. Augugliaro, L. Palmisano, *Chem. Commun.*, **2010**, 46, 7074-7089.
18. F. Mahdavi, T. C. Bruton, Y. Li, *J. Org. Chem.*, **1993**, 58, 744-746.

19. V. Brezova, A. Blazkova, I. Surina, B. Havlinova, *J. Photochem. Photobio. A*, **1997**, *107*, 233-237.
20. J. L. Ferry, W. H. Glaze, *Langmuir*, **1998**, *14*, 3551-3555.
21. J. L. Ferry, W. H. Glaze, *J. Phys. Chem. B*, **1998**, *102*, 2239-2244.
22. V. Makarova, T. Rajh, M. C. Thurnauer, A. Martin, P. A. Kemme, D. Cropek, *Environ. Sci. Tech.*, **2000**, *34*, 4797-4803.
23. V. Brezova, P. Tarabek, D. Dvoranova, A. Stařsko, S. Biskupiřc, *J. Photochem. Photobio. A: Chem.*, **2003**, *155*, 179-198.
24. H. Tada, T. Ishida, A. Takao, S. Ito, *Langmuir*, **2004**, *20*, 7898-7900.
25. H. Tada, T. Ishida, A. Takao, S. Ito, S. Mukhopadhyay, T. Akita, K. Tanaka, H. Kobayashi, *ChemPhysChem*, **2005**, *6*, 1537-1543.
26. T. Zhang, L. You, Y. Zhang, *Dyes and Pigments*, **2006**, *68*, 95-100.
27. S. O. Flores, O. R.-Bernij, M. A. Valenzuela, I. Cordova, R. Gomez, R. Gutierrez, *Top. Catal.*, **2007**, *44*, 507-511.
28. S. Chen, H. Zhang, X. Yu, W. Liu, *Chinese Journal of Chemistry*, **2010**, *28*, 21-26.
29. H. Kominami, S. Iwasaki, T. Maeda, K. Imamura, K. Hashimoto, Y. Kera, B. Ohtani, *Chem. Lett.*, **2009**, *15*, 410-411.
30. K. Imamura, S. Iwasaki, T. Maeda, K. Hashimoto, B. Ohtani, H. Kominami, *Phys. Chem. Chem. Phys.*, **2011**, *13*, 5114-5119.
31. K. Imamura, T. Yoshikawa, K. Hashimoto, H. Kominami, *Appl. Catal. B, Environ.*, **2013**, *134-135*, 193-197.
32. K. Imamura, K. Hashimoto, H. Kominami, *Chem. Commun.*, **2012**, *48*, 4356-4358.
33. H. Kominami, A. Furusho, S.-y. Murakami, H. Inoue, Y. Kera and B. Ohtani, *Catal. Lett.*, **2001**, *76*, 31-34.
34. H. Kominami, T. Nakaseko, Y. Shimada, A. Furusho, H. Inoue, S.-y. Murakami, Y. Kera and B. Ohtani, *Chem. Commun.*, **2005**, 2933-2935.

35. K. Imamura, Y. Okubo, T. Ito, A. Tanaka, K. Hashimoto, H. Kominami, *RSC Adv.* **2014**, *4*, 19883-19886.

Chapter 2

Photocatalytic selective hydrogenation of furfural to furfuryl alcohol over titanium(IV) oxide under metal-free and hydrogen-free conditions at room temperature

2.1. Introduction

Furfural (FAL) is produced from non-edible plant-derived biomass resources such as corncobs and bagasse and is one of the most important platform chemicals with which the conversion of biomass to chemicals starts.¹⁻² Reduction, oxidation and condensation have been reported as methods for conversion of FAL to useful chemicals, and reduction is most important because there are two C-C double bonds and an aldehyde group in FAL. There are various reduced products of FAL such as furfuryl alcohol (FOL), tetrahydrofurfural and tetrahydrofurfuryl alcohol as hydrogenation products, 2-methylfuran and 2-methyltetrahydrofuran as side-chain hydrogenolysis products, and 1,2-pentanediol, 1-5-pentanediol and 1-pentanol as ring-opening hydrogenolysis products.³⁻⁴ Among these compounds, FOL is a useful compound and is used as raw material for solvents, various chemicals and pharmaceuticals.² Conversion of FAL to FOL is a chemoselective reaction, i.e., the aldehyde group should be reduced without hydrogenation of the furan ring. There are several reports on chemoselective reduction of FAL to FOL.⁵⁻⁶ However, reported hydrogenation of FAL was achieved over metal catalysts at an elevated temperature in the presence of hydrogen (H₂) as a reducing agent. Therefore, a more environmentally friendly system for FOL synthesis from FAL is highly desired.

When a semiconductor photocatalyst such as titanium(IV) oxide (TiO₂) is

irradiated by light having an energy larger than the band gap, electrons in the valence band are excited to a conduction band, resulting in the formation of excited electrons (e^-) in the conduction band and positive holes (h^+) in the valence band. Over the surface of the photocatalyst, e^- are accepted by an adsorbed reactant to be reduced, while h^+ are captured by another reactant to be oxidized. Totally, both e^- and h^+ are consumed, simultaneously producing reduced and oxidized products. Since this redox reaction is driven only by light at room temperature, photocatalytic reaction has attracted the interest of chemists, and the application of photocatalytic reaction to a green organic reaction system has recently been studied.⁷⁻⁹ However, most of studies have focused on either a reduced or oxidized product, with other products not being considered, and in the case of a reduction system, the reaction is almost limited to simple hydrogenation (reduction) of nitrobenzene. In the course of studies on application of photocatalysis to a green organic conversion, Kominami *et al.* reported new possibilities of photocatalytic reactions over TiO_2 under metal-free and hydrogen-free conditions at room temperature. For example, almost complete chemoselectivity was achieved in hydrogenation of a nitro group to an amino group of nitrobenzenes having reducible functional groups.¹⁰ Almost complete chemoselectivity was also achieved in hydrogen transfer from aliphatic alcohols to benzaldehydes, i.e., Meerwein-Ponndorf-Verley-type reaction.¹¹ In two hydrogenation (reduction) reactions, reducible functional groups attached to a benzene ring were preserved even though nitro and carbonyl groups are completely reduced to amino and hydroxymethyl ($-CH_2OH$) groups, respectively. Through these studies, Kominami *et al.* also found another important characteristic of photocatalytic reduction (hydrogenation) over metal-free TiO_2 i.e., an aromatic ring is also preserved. The author thus became interested in determining whether a heterocycle is hydrogenated or not over a metal-free TiO_2 photocatalyst. The author think that FAL is a suitable model

compound to evaluate chemoselectivity in biomass resources because FAL consists of a furan structure and carbonyl group. In this study, the author examined photocatalytic hydrogenation of FAL in alcohol suspensions of TiO₂ under metal-free and hydrogen-free conditions to evaluate the possibility of up-grading of FAL. Here we briefly report 1) chemoselectivity in hydrogenation to a furan structure and carbonyl group, 2) expandability of alcohols, and 3) reaction mechanism.

2.2. Experimental

2.2.1. Photocatalytic hydrogenation of FAL

TiO₂ (ST-01, Ishihara, anatase, 313 m²g⁻¹, 50 mg) was suspended in 5 cm³ of an alcohol containing FAL (*ca.* 50 μmol) in a test tube, which was sealed with a rubber septum and then photoirradiated under Ar at 298 K with a high-pressure mercury lamp. The amounts of FAL and FOL were determined with an FID-type gas chromatograph (GC-2025, Shimadzu) equipped with a DB-1 column. Chlorobenzene was used as an internal standard sample. Chlorobenzene (7 mm³) was added to the reaction solution (3 cm³). After the mixture had been stirred for 7 min, FAL and FOL were analyzed. The amounts of FAL and FOL were determined from the ratios of the peak areas to the peak area of chlorobenzene. The amount of H₂ as the reduction product of protons (H⁺) and the amount of CO₂ were determined with a TCD-type gas chromatograph (GC-8A, Shimadzu) equipped with an MS-5A column and Porapak QS column. A multi-wavelength irradiation monochromator (MM-3, Bunkoukeiki Co., Ltd) was used to obtain apparent quantum efficiency (AQE), and light intensity was determined by using a spectroradiometer (USR-45D, Ushio Inc.).

2.2.2. Adsorption of FAL and FOL on TiO₂

TiO₂ (ST-01, 200 mg) was suspended in 5 cm³ of ethanol containing FAL and/or FOL (each 100 μmol) in a test tube. The test tube was sealed with a rubber septum under argon and the mixture was stirred in a water bath at 293 K for 30 hours in the dark. The amounts of FAL and FOL were determined with an FID-type gas chromatograph (GC-2025, Shimadzu) equipped with a DB-1 column. Chlorobenzene was used as an internal standard sample. Chlorobenzene (7 mm³) was added to the reaction solution (3 cm³). After the mixture had been stirred for 7 min, FAL and FOL were analyzed. The amounts of FAL and FOL were determined from the ratios of the peak areas to the peak area of chlorobenzene.

2.3. Results and discussion

2.3.1. Photocatalytic hydrogenation of FAL

Figure 1 shows time courses of photocatalytic reduction of FAL in a 2-pentanol suspension of TiO₂. The amount of FAL decreased with photoirradiation and FOL was formed, indicating that the carbonyl group of FAL was chemoselectively hydrogenated to a -CH₂OH group. After 30-min irradiation of UV light, FAL was almost completely consumed and the yield of FOL reached >99%. The amount of FOL did not decrease after consumption of FAL. Almost quantitative formation of FOL and no change in the amount of FOL also mean that the following reactions did not occur: 1) hydrogenation of the furan structure, 2) degradation of the furan structure, and 3) re-oxidation of the -CH₂OH group of FOL. From the results of previous study and the present results, it can be concluded that benzene and furan rings are not hydrogenated over a metal-free TiO₂ photocatalyst. The reason why reactions 2) and 3) did not occur is that the use of 2-pentanol as a solvent minimized the possibility of reactions 2) and 3). Adsorption of FAL and/or FOL on TiO₂ in ethanol was examined and results were shown in Figure 2. Competitive adsorption of FAL and FOL revealed that FAL was preferentially adsorbed on TiO₂, which accounts for the high selectivity and yield of FOL in this reaction system. The author noted that there was no other reduced product during the whole reaction. As a reduced product, H₂ can be formed by reduction of protons (H⁺), but it was not formed. Material balance (MB) was calculated by Equation (1). The value of MB can be used to evaluate the selectivity of FOL and the presence of intermediates in the reaction.

$$MB = \frac{n(FAL) + n(FOL)}{n_0(FAL)}, \quad (1)$$

Where $n(FAL)$ and $n(FOL)$ are the amounts of FAL and FOL during the photocatalytic reaction, respectively, and $n_0(FAL)$ is the amount of FAL before the photocatalytic

reaction. The value of MB was slightly smaller than unity in the initial stage of the reaction, suggesting that FAL was adsorbed on TiO₂ and/or that an intermediate(s) was formed. After 20-min photoirradiation, the value became almost unity, indicating that the intermediate(s) was converted to FOL and/or FOL was not adsorbed on TiO₂. The author also analyzed the oxidation product in this reaction. 2-Pentanone was formed as the oxidized product of 2-pentanol. The amount of 2-pentanone increased with irradiation time and was saturated at around 50 μmol. As the fully oxidized product, CO₂ was not formed as is expected from no change in the amounts of FOL and 2-pentanone with prolonged photoirradiation. The balance between oxidation and reduction (redox balance, RB) was evaluated by Equation (2).

$$\text{Redox balance} = \frac{n(2 - \text{pentanone})}{n(\text{FOL})} \quad (2)$$

During the reaction, the value of redox balance was almost unity. These results clarified the characteristics of this reaction system: 1) stoichiometric reaction of FAL and 2-pentanol to FOL and 2-pentanone occurs, 2) the stoichiometric reaction ceases when FAL is consumed, and 3) no other reactions occur.

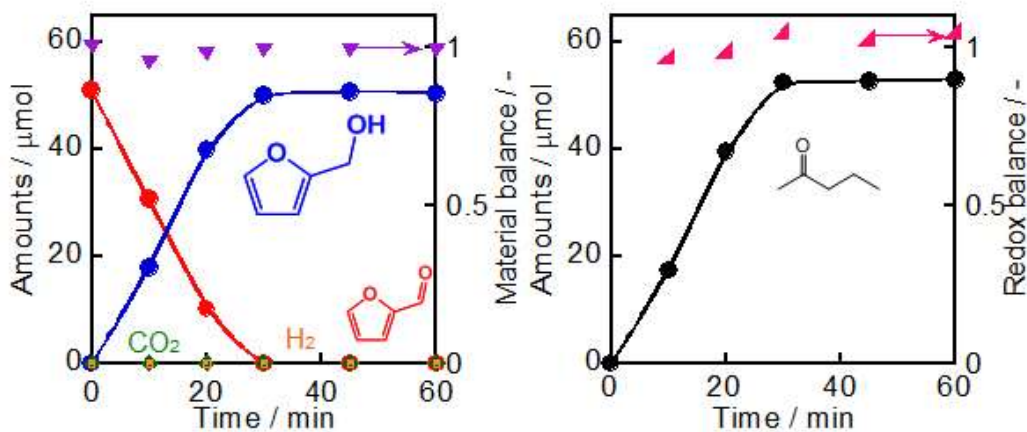


Figure 1 Time courses of (a) FAL, FOL, H_2 , CO_2 , and material balance and (b) 2-pentanone and redox balance in a 2-pentanol suspension of a TiO_2 photocatalyst under irradiation of UV light at 298 K.

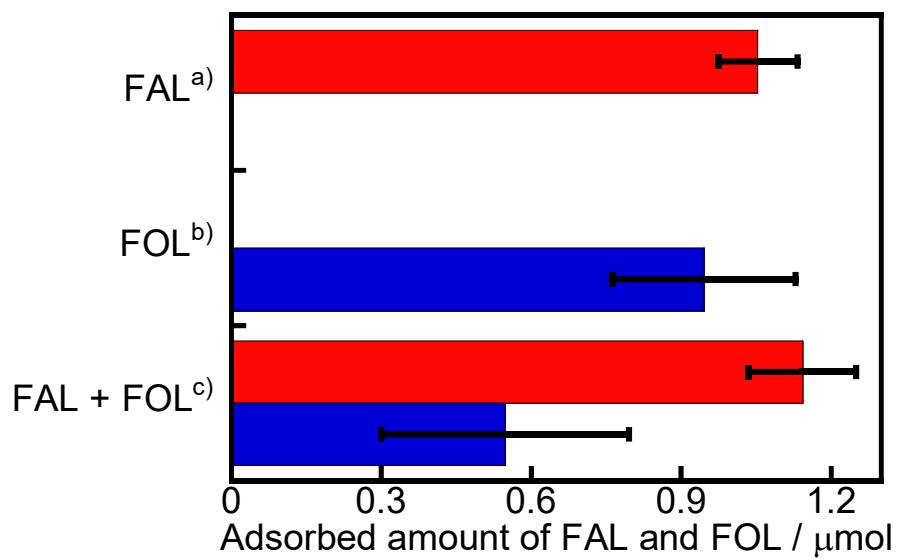
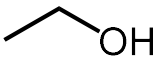
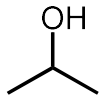
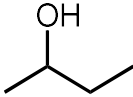
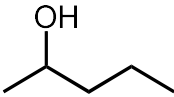
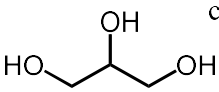


Figure 2 Amount of FAL and/or FOL adsorbed onto TiO_2 in ethanol containing a) FAL, b) FOL and c) FAL and FOL for 30 h in the dark.

2.3.2. Applicability of alcohol in chemoselective hydrogenation of FAL to FOL

Table 1 shows the applicability of alcohol as a hole scavenger in the photocatalytic reduction of FAL to FOL. FOL was obtained in high yields in all cases. The reaction rate was dependent on the reactivity of alcohol with holes because similar tendency was observed in photocatalytic hydrogen formation along with alcohol oxidation.¹² The author noted that ethanol and glycerin were available in the hydrogenation of FAL, indicating that biomass-derived FAL can be up-gradated to FOL by using biomass-derived compounds. Figure 3 shows the results of re-use tests of photocatalytic reduction of FAL to FOL in ethanolic suspensions of TiO₂. The photocatalyst was reusable at least twice without notable loss of activity.

Table 1 Applicability of alcohol in chemoselective hydrogenation of FAL to FOL over a TiO₂ photocatalyst under metal-free and hydrogen-free conditions at 298 K.

Alcohols	Time / min	Conv. ^a / %	Sel. ^b / %
CH ₃ OH	10	>99	>99
	15	>99	>99
	20	>99	98
	20	>99	92
	30	>99	99
	120	>99	92

^aConversion of FAL; Conv. = decrement of FAL / initial amount of FAL × 100.

^bSelectivity of FOL from FAL; Sel. = amount of FOL / decrement of FAL × 100.

^cGlycerol (500 μmol) was dissolved in water.

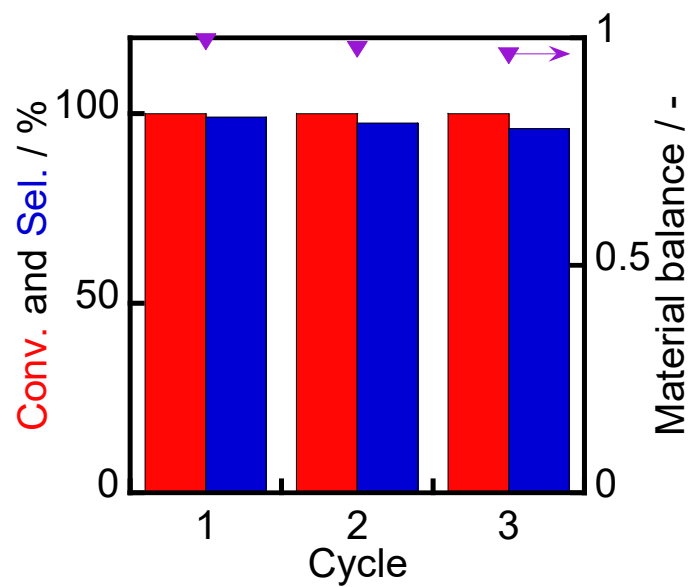


Figure 3 Cycle test of TiO_2 in photocatalytic reduction of FAL to FOL in ethanolic suspensions for 15-min photoirradiation from a high-pressure mercury lamp.

2.3.3. Action spectrum of photocatalytic selective hydrogenation of FAL to FOL over TiO₂

An action spectrum is a strong tool for determining whether a photoinduced process is the rate-determining step in the reaction observed. To obtain an action spectrum in this reaction system, hydrogenation of FAL in ethanolic suspensions of TiO₂ was carried out at 298 K under irradiation of monochromated light from a Xe lamp. Apparent quantum efficiency (AQE) at each centered wavelength of light was calculated from the ratio of twice the amount of FOL formed and the amount of photons irradiated using Equation (3):

$$\text{AQE} = \frac{2 \times \text{amount of FOL formed}}{\text{amount of incident photons}} \times 100 \quad (3).$$

As shown in Figure 4, AQE was in agreement with the absorption spectrum of TiO₂. Therefore, it can be concluded that reduction of FAL in ethanolic suspensions was induced by photoabsorption of TiO₂. As also shown in Figure 4, AQE reached 17% at 330 nm, indicating that photocatalytic reduction of FAL to FOL occurred with high efficiency of photon utilization.

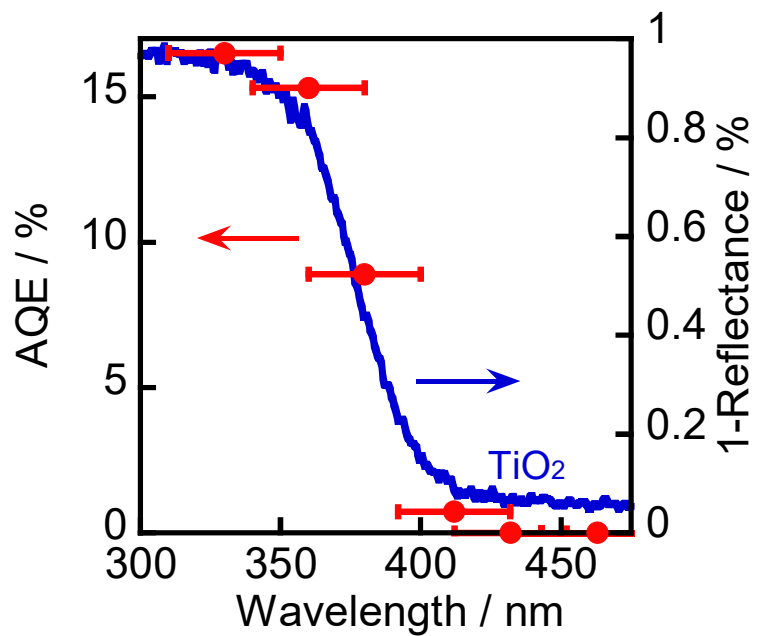


Figure 4 Absorption spectrum (right axis) and action spectrum of TiO_2 in hydrogenation of FAL to FOL in an ethanolic suspension of TiO_2 (left axis).

2.3.4. Effects of various reaction conditions on reduction of FAL in ethanolic suspensions of TiO₂

The effects of various reaction conditions on reduction of FAL in ethanolic suspensions of TiO₂ are shown in Figure 5. Entries 1, 2 and 3 show the results of three blank reactions: 1) in the absence of TiO₂ in the dark (non-catalytic thermal reaction between FAL and ethanol, entry 1), 2) in the absence of TiO₂ with irradiation of light (photochemical reaction, entry 2), and 3) in the presence of TiO₂ in the dark (thermocatalytic reaction between FAL and ethanol over TiO₂, entry 3). The results indicate that the TiO₂ photocatalyst and photoirradiation are indispensable for the reduction of FAL. The dark reaction under 1 atm of H₂ (thermocatalytic reaction between FAL and H₂ over TiO₂) was examined in an ethanolic suspension at 298 K (entry 5); however, no reaction occurred, suggesting that H₂ was not activated over metal-free TiO₂ at 298 K. The result of entry 5 clarifies that the photocatalytic method is effective for chemoselective conversion of FAL to FOL under H₂-free and metal-free conditions at around room temperature.

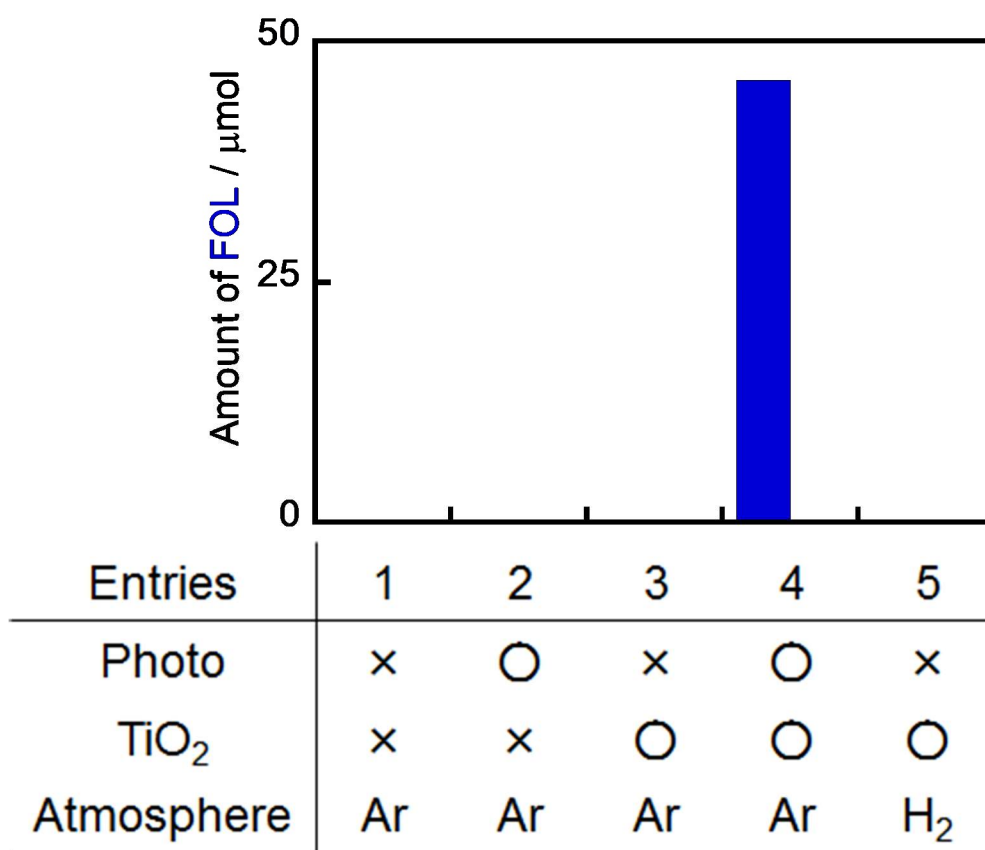


Figure 5 Effects of various reaction conditions on reduction of FAL in ethanolic suspensions of TiO₂.

2.3.5. The expected reaction process of photocatalytic reduction of FAL in a 2-petanol suspension of TiO₂

The expected reaction process of photocatalytic reduction of FAL in a 2-petanol suspension of TiO₂ under H₂-free and metal-free condition is shown in Figure 6: 1) By irradiation of UV light, e⁻ and h⁺ are formed in the conduction and valence bands of TiO₂, and 2-petanol is oxidized to 2-pentanone by h⁺ and 2) the carbonyl group of FAL is reduced to -CH₂OH groups by e⁻, resulting in the formation of FOL. The furan ring is not hydrogenated, probably because the activation energy of this process over metal-free TiO₂ is large. No hydrogenation of FAL even in the presence of H₂ (entry 5 in Figure 5) indicates that dissociative adsorption of H₂ is difficult over metal-free TiO₂.

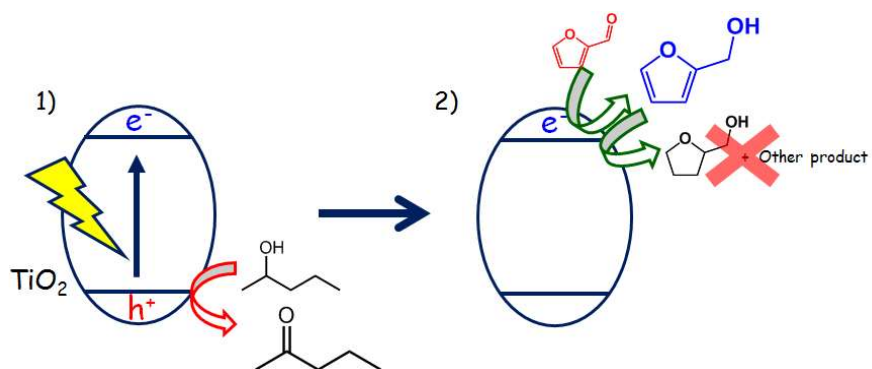


Figure 6 An expected reaction process of chemoselective hydrogenation of FAL to FOL and oxidation of 2-pentanol to 2-pentanone over a TiO₂ photocatalyst under metal-free and hydrogen-free conditions.

2.4. Conclusions

In conclusion, FAL was chemoselectively and quantitatively converted to FOL in a 2-pentanol suspension of a TiO₂ photocatalyst under metal-free and hydrogen-free conditions. Oxidation of 2-pentanol to 2-pentanone simultaneously occurred with a high stoichiometry, and various alcohols such as glycerol and ethanol were used for this reaction, indicating that double up-grading of FAL and alcohol was possible.

References

1. Corma, S. Iborra, A. Velty, *Chem. Rev.*, **2007**, *107*, 2411.
2. Ullman's Encyclopedia of industrial Chemistry, ed. by H. E. Hoydonckx, W. M. V. Rhijn, W.V. Rhijin, D. E. D. Vos, P. A. Jacobs, *Wiley-VCH*, **2007**.
DOI: doi.org/10.1002/14356007.a12-119.pub2.
3. Y. Nakagawa, M. Tamura, K. Tomishige, *J. Jpn. Petrol. Inst.*, **2017**, *60*, 1.
4. Takagaki, S. Nishimura, K. Ebitani, *Catal. Surv. Asia*, **2012**, *16*, 164.
5. X. Chen, L. Zhang, B. Zhang, X. Guo, X. Mu, *Sci. Rep.*, **2016**, *6*, 28558.
6. S. Sitthisa, D. E. Resasco, *Catal. Lett.*, **2011**, *141*, 784.
7. Palmisano, E. Garcia-Lopez, G. Marci, V. Loddo, S. Yurdakal, V. Augugliaro, L. Palmisano, *Chem. Commun.*, **2010**, *46*, 7074.
8. Palmisano, V. Augugliaro, M. Pagliaro, L. Palmisano, *Chem. Commun.*, **2007**, 3425.
9. M. A. Fox, M. T. Dulay, *Chem. Rev.*, **1993**, *93*, 341.
10. Imamura, T. Yoshikawa, K. Hashimoto, H. Kominami, *Appl. Catal. B Environ.*, **2013**, *134-135*, 193.
11. M. Fukui, H. Kouda, A. Tanaka, K. Hashimoto, H. Kominami, *Chem. Select*, **2017**, *2*, 2293.
12. Z. H. N. Al-Azri, W. Chen, A. Chan, V. Jovic, T. Ina, H. Idriss, G. I. N. Waterhouse, *J. Catal.*, **2015**, *329*, 355.

Chapter 3

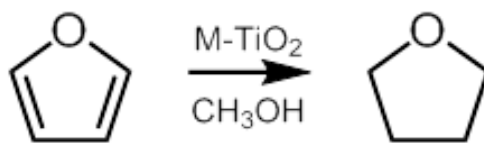
Photocatalytic hydrogenation of furan to tetrahydrofuran in alcoholic suspensions of metal-loaded titanium(IV) oxide without addition of hydrogen gas

3.1. Introduction

Tetrahydrofurans (THFs) are important compounds as intermediates of chemical products, and they are produced by dehydration of diols and hydrogenation of corresponding furans.^{1,2} Hydrogenation of furans to THFs is more attractive because furans can be produced from biomass. Hydrogenation of the furans is achieved by catalytic hydrogenation using a metal catalyst such as nickel or palladium (Pd) supported on a suitable support.² However, these catalyst systems require the addition of an excess amount of dihydrogen (H₂) gas as a hydrogen source in a closed reactor. Therefore, a more environmentally friendly catalytic reaction system for hydrogenation of furans utilizing a “greener” hydrogen source is desired.

Since titanium(IV) oxide (TiO₂) is inexpensive and not toxic for humans and the environment, TiO₂ has been used for a long time as an indispensable inorganic material such as a pigment and UV absorber. Another important application of TiO₂ is the use as a photocatalyst. When TiO₂ is irradiated by UV light, charge separation occurs and thus-formed electrons in the conduction band and positive holes in the valence band cause reduction and oxidation, respectively. The photocatalytic reaction satisfies almost all of the 12 proposed requirements for green chemistry³ because of its characteristics shown below. First, TiO₂ functions as a catalyst. The TiO₂-photocatalyzed reaction occurs at room temperature. Solar energy can be used

to drive the reaction. Since TiO_2 is a typical solid catalyst, energy consumption for separation of TiO_2 from the reaction mixture is much smaller than that for separation of a homogeneous catalyst. In addition, a TiO_2 photocatalyst can be used repeatedly free from a special re-activation process because of its excellent chemical and physical stability. Therefore, photocatalytic material transformation has been studied by many researchers.⁴⁻⁶ Recently, photocatalytic reduction of organic compounds has attracted the attention of researchers^{5, 6}, and much interest has been shown in reduction of nitrobenzenes to aminobenzenes.⁷⁻²¹ The author and Imamura *et al.*, recently found that benzonitrile and styrene were successfully hydrogenated in alcohol suspensions of a palladium-loaded TiO_2 (Pd-TiO_2) photocatalyst, although the reduction potentials of benzonitrile and styrene are believed to be much higher than the potential of the conduction band of TiO_2 .^{22,23} The reason why Pd-TiO_2 exhibited good performance in photocatalytic hydrogenation is the high “catalytic” activity for hydrogenation of unsaturated bonds such as $\text{C}=\text{C}$ and $\text{C}\equiv\text{N}$ bonds.^{26,27} Two results have shown that 1) hydrogenation occurs without the use of H_2 because alcohol works as an electron and hydrogen source in the photocatalytic reaction, 2) a Pd co-catalyst strongly contributes to the reduction, and 3) the applicability of photocatalytic reduction is not limited by the conduction band position of semiconductor photocatalysts. Kominami *et al.* other co-catalyst effects in chemoselective reduction of (2,3-epoxypropyl)benzene to allylbenzene (silver co-catalyst)²⁴ and semihydrogenation of alkynes to alkenes (copper co-catalyst)²⁵, indicating that photocatalytic H_2 -free reduction can be broadened by the use of metal co-catalysts. In this study, the author examined photocatalytic hydrogenation of furan, a representative heterocyclic compound, to THF in an alcoholic suspension of metal-loaded TiO_2 (Scheme 1) to expand the possibility of photocatalytic hydrogenation. Here the author report 1) effects of metal co-catalysts and 2) effects of various parameters on H_2 -free hydrogenation of furan, and 3) details of the reaction.



Scheme 1 Photocatalytic hydrogenation of furan to THF in a methanolic suspension of metal (M)-loaded TiO₂ under an H₂-free condition.

3.2. Experimental

3.2.1. Preparation of metal-loaded TiO₂

Various metals as co-catalysts (Au, Ag, Cu, Pd and Pt) were loaded on TiO₂ (MT-150A, Tayca, Osaka, Japan) by using the photodeposition method. Some TiO₂ samples were selected from Japan Reference Catalysts (JRC-TIO series) registered at the Catalysis Society of Japan and used to examine the effects of different kinds of TiO₂. Unloaded TiO₂ powder was suspended in 10 cm³ of an aqueous methanol solution (10 vol%) containing a metal source in a test tube. HAuCl₄, AgNO₃, CuCl₂, PdCl₂ and H₂PtCl₆ were used as metal sources. Each test tube was sealed with a rubber septum under argon (Ar) and then photoirradiated for 90 min at $\lambda > 300$ nm by a 400-W high-pressure mercury arc (Eiko-sha, Osaka) with magnetic stirring in a water bath continuously kept at 298 K. The resulting powder was washed repeatedly with distilled water and dried for 1 h in *vacuo*.

3.2.2. Characterization

The morphology of Pd-TiO₂ particles was observed under a JEOL JEM-2100F transmission electron microscope (TEM) operated at 200 kV in the Joint Research Center of Kindai University.

3.2.3. Photocatalytic reaction

In a typical run, Pd-TiO₂ (50 mg) was suspended in 5 cm³ of methanol containing furan (40 ± 4 μ mol) in a test tube, which was sealed with a rubber septum and then photoirradiated under Ar at 298 K with the same high-pressure mercury lamp or a UV-LED (UV-LED, PJ-1505-2CA, CCS Inc., Kyoto, maximum energy at $\lambda = 365$ nm). The amounts of furan and THF were determined with an FID-type gas chromatograph (GC-2025, Shimadzu) equipped with a DB-1 column. Chlorobenzene

was used as an internal standard sample. Chlorobenzene (7 mm³) was added to the reaction solution (3 cm³). After the mixture had been stirred for 7 min, furan and THF in the mixture solution were analyzed. The amounts of furan and THF were determined from the ratios of the peak areas to the peak area of chlorobenzene. The amount of H₂ as the reduction product of protons (H⁺) was determined with a TCD-type gas chromatograph (GC-8A, Shimadzu) equipped with an MS-5A column. A multi-wavelength irradiation monochromator (MM-3, Bunkoukeiki Co., Ltd) was used to obtain apparent quantum efficiency (AQE), and light intensity was determined by using a spectroradiometer (USR-45D, Ushio Inc.).

3.2.4. Adsorption of furan on TiO₂ or Metal-loaded TiO₂

TiO₂ (MT-150A) or metal-loaded TiO₂ (200 mg) was suspended in 5 cm³ of methanol containing furan (40 ± 4 μmol) in a test tube. The test tube was sealed with a rubber septum under argon and the mixture was stirred in a water bath at 293 K for 18 hours in the dark. The amount of furan was determined with an FID-type gas chromatograph (GC-2025, Shimadzu) equipped with a DB-1 column. Chlorobenzene was used as an internal standard sample. Chlorobenzene (7 mm³) was added to the reaction solution (3 cm³). After the mixture had been stirred for 7 min, furan in the mixture solution was analyzed. The amount of furan was determined from the ratios of the peak areas to the peak area of chlorobenzene.

3.2.5. Catalytic Hydrogenation of furan on TiO₂ or Metal-loaded TiO₂

TiO₂ (MT-150A) or metal-loaded TiO₂ (50 mg) was suspended in 5 cm³ of methanol in a test tube. The test tube was sealed with a rubber septum under H₂ and injected methanol (500 μmol) containing furan (40 ± 4 μmol). The mixture was stirred in a water bath at 293 K for 5 min in the dark. The amount of THF was

determined with an FID-type gas chromatograph (GC-2025, Shimadzu) equipped with a DB-1 column. Chlorobenzene was used as an internal standard sample. Chlorobenzene (7 mm³) was added to the reaction solution (3 cm³). After the mixture had been stirred for 7 min, furan in the mixture solution was analyzed. The amount of THF was determined from the ratios of the peak areas to the peak area of chlorobenzene.

3.3. Results and discussion

3.3.1. Effects of different metal co-catalysts

In the hydrogenation of furan, H₂ may be formed as the product of reduction of H⁺ by photogenerated electrons ($2\text{H}^+ + 2\text{e}^- \rightarrow \text{H}_2$). Therefore, hydrogenation of furan competes with the reduction of H⁺, and the selectivity of two products (THF and H₂) is also an important indicator for evaluation of photocatalysts as well as the yields of THF and H₂. Figure 1 shows the effects of metal co-catalysts (1.0 wt%) on the yields of THF and H₂ produced in photocatalytic hydrogenation of furan in methanolic suspensions of metal-loaded TiO₂ (MT-150A) for 10 min under Ar with irradiation of UV light from an LED. When bare TiO₂ was used as the photocatalyst, no THF or H₂ was formed. Just after photoirradiation, the color of TiO₂ became blue, indicating that Ti⁴⁺ in TiO₂ was reduced to Ti³⁺ by photogenerated electrons. These results mean that without the aid of a co-catalyst, photoirradiated TiO₂ has no ability to reduce (hydrogenate) a C=C double bond in a heterocyclic compound as well as a C=C double bond in hydrocarbons.²³ In the case of Au-, Ag- and Cu-loaded TiO₂ samples, no THF was formed, indicating that these metals were inactive as co-catalysts for furan hydrogenation. H₂ was evolved over Au- and Ag-loaded TiO₂ samples. Formation of H₂ will be discussed at the end of this section. In contrast to these metal-loaded TiO₂ samples, a small amount of THF was formed when Pt-loaded TiO₂ (Pt-TiO₂) was used, although a large amount of H₂ was simultaneously evolved. The author noted that Pd-loaded TiO₂ (Pd-TiO₂) showed a distinctive photocatalytic activity for the largest production of THF and suppressed evolution of H₂. As clearly shown, Pd-TiO₂ possessed a favorable catalytic property in hydrogenation of furan in contrast to Pt-TiO₂. Bradley *et al.*²⁸ reported that Pd can readily adsorb a furan ring due to a strong interaction between the Pd and π bonds in furan. The strong interaction between Pd and furan is attributed to the high activity of Pd-TiO₂. As shown in Figure 1, H₂

was formed when Au, Ag, Pt and Pd were used as co-catalysts. It is known that co-catalysts such as Pt loaded on a photocatalyst act as sites for storage of photogenerated electrons and as active sites for reaction, resulting in reduced activation energy of the reaction and formation of hydrogenated products.^{29, 30} In previous papers on photocatalytic NH₃ decomposition in aqueous suspensions of TiO₂ having co-catalysts, the author reported that the rate of H₂ evolution was drastically changed depending on the type of co-catalyst and that the effect as a co-catalyst became smaller with increase in hydrogen over-voltage of the co-catalyst metal when used as an electrode.^{31, 32} A similar tendency was observed in the evolution of H₂ from methanol in the presence of furan in this study as shown in Figure 2. However, the use of a Pd co-catalyst resulted in a very small yield of H₂ that was much different from the value predicted from the hydrogen overvoltage. The second smallest value of hydrogen overvoltage means that the activation energy for H₂ evolution over Pd particles is rather small. The much smaller H₂ yield in furan hydrogenation indicates that the Pd co-catalyst provides an excellent route with very small activation energy for hydrogenation of furan to THF.

Supported Pd nanoparticles are often used for catalytic hydrogenation with H₂ as a hydrogen source. In thermocatalytic hydrogenation, H₂ molecules are adsorbed dissociatively on Pd particles, and thus-formed active hydrogen species are inserted into the C=C double bond.^{33, 34} Therefore, active hydrogen species formed reductively from H⁺ in the photocatalytic process and formed dissociatively from H₂ gas would be essentially the same. It can be concluded that hydrogenation of furan to THF under the present conditions consists of two processes: 1) photocatalytic production of active hydrogen species and 2) thermocatalytic hydrogenation of furan over Pd particles. As can be seen in Figures 1 and 2, only thermocatalytic properties of metal particles decide whether hydrogenation of furan to THF occurs or not. Strictly speaking, the

observed hydrogenation should be called a combination reaction by photocatalysis and thermocatalysis, although the author call this reaction simply photocatalytic hydrogenation hereafter.

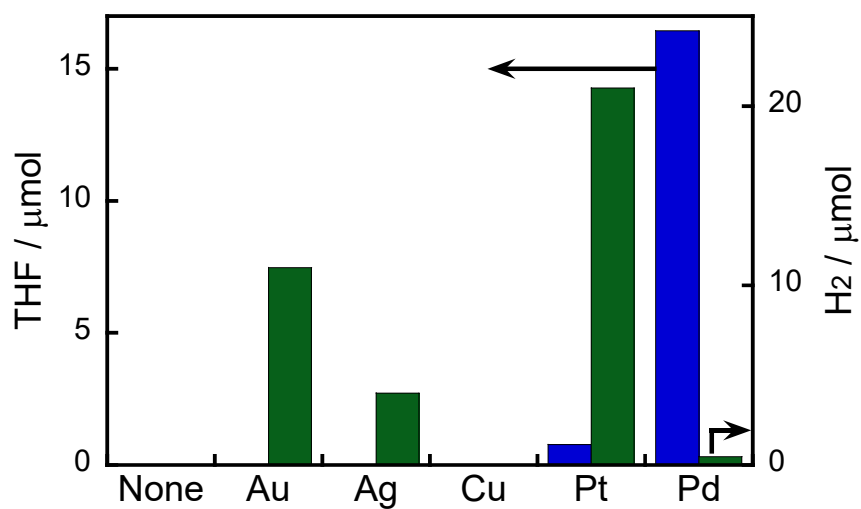


Figure 1 Effects of different metal co-catalysts (1.0 wt%) on the yields of THF and H₂ produced in photocatalytic hydrogenation of furan ($40 \pm 4 \mu\text{mol}$) in methanolic suspensions of metal-loaded TiO₂ (MT-150A) for 10 min under irradiation of UV light from an LED.

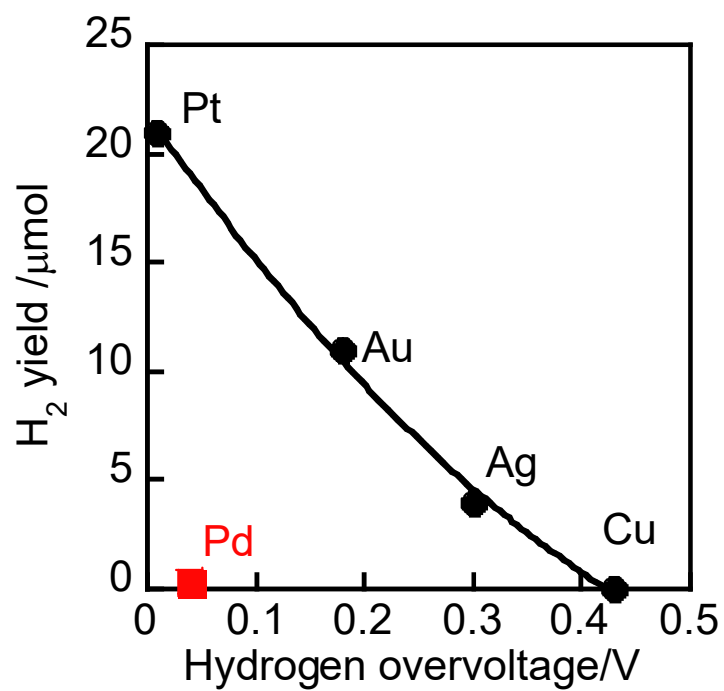


Figure 2 Correlation between yield of H₂ produced in photocatalytic hydrogenation of furan and hydrogen overvoltage of metal electrodes. Reaction conditions are shown in Figure 1

3.3.2. Effects of the Pd loadings on the yield of THF formed

Figure 3 shows effects of the Pd loadings on the yield of THF formed by photocatalytic hydrogenation of furan in methanolic suspensions after 5-min photoirradiation from a high-pressure mercury lamp. The yield of THF increased with increase in the amount of Pd up to 1.0 wt% probably because the number of reduction sites for hydrogenation of furan increased with an increase in the Pd content. However, the yield was saturated over 1.0 wt%. There are some possible reasons for the saturation: 1) dispersion of Pd on the TiO₂ surface was saturated, 2) the rate-determining step changed from the reduction process to oxidation process, and 3) the overall reaction was limited by photon flux.

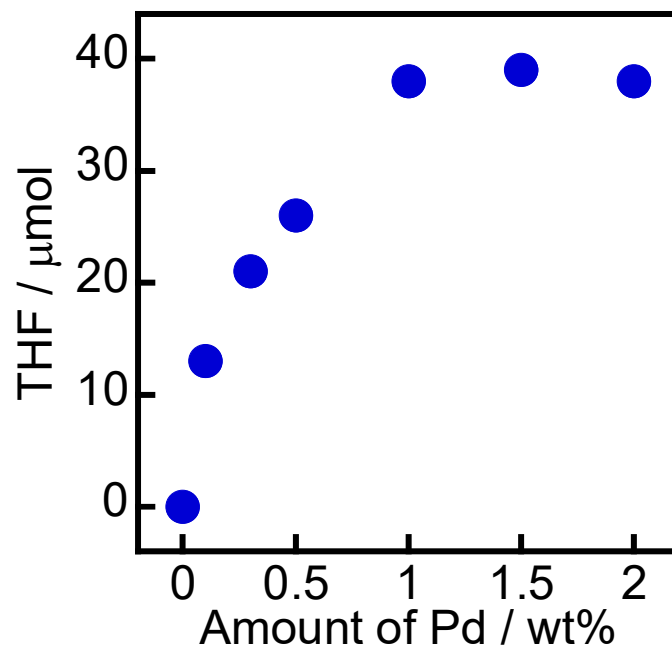


Figure 3 Effects of amount of Pd loading on TiO₂ in photocatalytic hydrogenation of furan ($40 \pm 4 \mu\text{mol}$) in methanolic suspensions for 5 min under irradiation of UV light from a high-pressure mercury lamp.

3.3.3. TEM images and distribution of Pd nanoparticles

TEM photographs of bare TiO₂ (MT-150A) and 1.0 wt% Pd-TiO₂ and the distribution of Pd particles in 1.0 wt% Pd-TiO₂ are shown in Figure 4a), b) and c), respectively. Fine Pd particles can be seen in the TEM photograph (Figure 4b)), and the average diameter was determined to be 3.4 nm, indicating that Pd nanoparticles were deposited on the TiO₂ surface by the photodeposition method. The amount of THF (40 μmol) after photoirradiation for 5 min was larger than the amount of Pd (4.7 μmol) loaded on TiO₂, indicating that Pd metal works as a catalyst for the hydrogenation of furan.

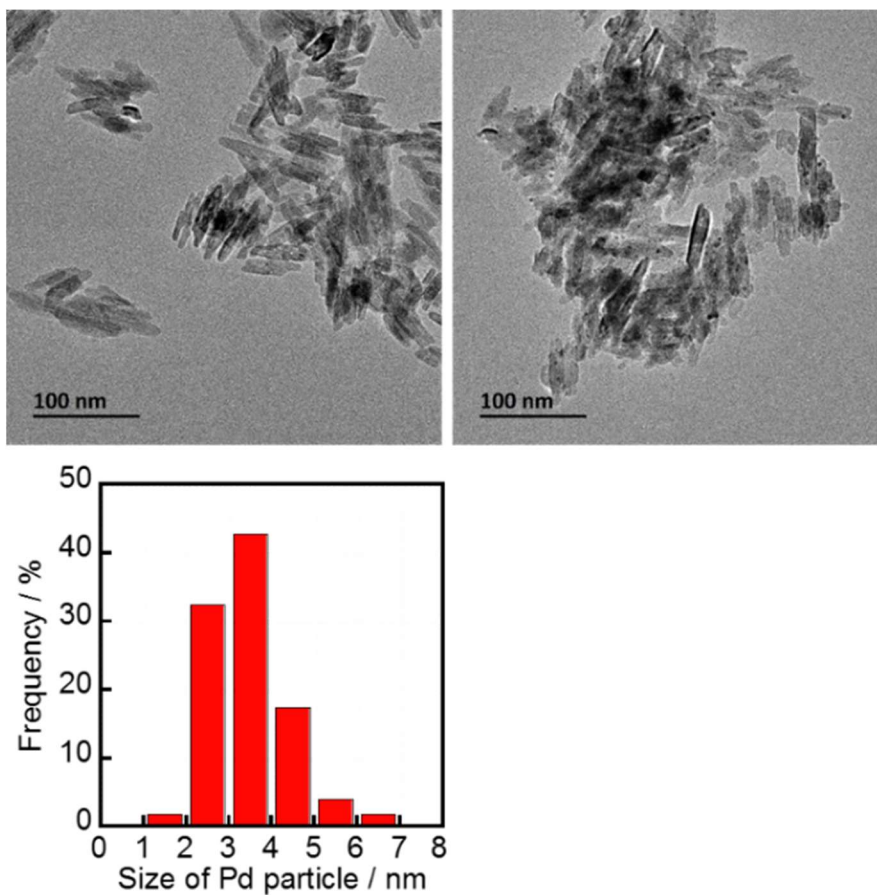


Figure 4 TEM photographs of (a) TiO₂ (MT-150A) and (b) 1.0 wt%Pd-TiO₂, and (c) distribution of Pd particles in 1.0wt%Pd-TiO₂.

3.3.4. Effects of reaction conditions on photocatalytic hydrogenation of furan

The effects of various reaction conditions on photocatalytic hydrogenation of furan to THF were investigated, and the results are summarized in Table 1. First, the effects of different kinds of commercial TiO₂ were examined (Entries 1-7). In addition to MT-150A TiO₂, six samples were selected from Japan Reference Catalysts (JRC-TIO series) registered at the Catalysis Society of Japan. Rutile TiO₂ (R, entries 6 and 7) showed THF yields higher than those by anatase TiO₂ (A, entries 1-3) and those of TiO₂ consisting of two phases (A/R, entries 4 and 5). In the case of photocatalytic hydrogenation of nitro compounds, rutile phase TiO₂ was active, though the reason is not clear.^{20, 35} An increase in Pd loading up to 1.0 wt% resulted in an increase in THF yield (Entry 8) as has already been shown in Figure 3. Prolonging the reaction time increased the yield as expected (Entry 9). To examine the durability of the Pd-TiO₂ photocatalyst in this reaction system, Pd-TiO₂ was used repeatedly. After reaction for 10 min (Entry 9), Pd-TiO₂ particles were recovered by simple filtration from the reaction mixture and were re-used. Entries 10 and 11 show that Pd-TiO₂ photocatalysts were reusable at least twice without notable loss of activity. Entries 12, 13 and 14 show results of three blank reactions: 1) in the absence of Pd-TiO₂ in the dark (non-catalytic thermal reaction between furan and methanol, entry 12), 2) in the absence of Pd-TiO₂ with irradiation of light (photochemical reaction, entry 13), and 3) in the presence of Pd-TiO₂ in the dark (thermocatalytic reaction over Pd-TiO₂, entry 14). These results indicate that the Pd-TiO₂ photocatalyst and photoirradiation were indispensable for the hydrogenation of furan. In the dark at 298 K, THF was formed in the presence of Pd-TiO₂ and H₂ (1 atm) (Entry 15), indicating that H₂ was used for hydrogenation of furan over Pd-TiO₂. In other words, Pd particles loaded on TiO₂ showed thermocatalytic activity for hydrogenation of furan as discussed earlier. When the amount of H₂ added in the reactor was reduced to 50 μmol, THF was not

formed in the dark at 298 K (Entry 16). Results of the dark reactions under H₂ (Entries 15 and 16) mean that a large excess of H₂ is necessary to obtain a sufficient rate of THF production at 298 K. Dark reactions over metal-free TiO₂ and TiO₂ modified with other metal co-catalysts under H₂ (1 atm) were negligible (entries 17-21). To examine the effects of different kinds of alcohol, ethanol, 2-propanol, 2-butanol, 2-pentanol and glycerol were chosen (Entries 22-26). Ethanol and glycerol have attracted much attention as typical biomasses and by-products in biomass utilization (saponification and transesterification of fats and oils). When these alcohols were used, THF was formed, indicating that various alcohols can be used as solvents and electron sources for hydrogenation of furan. The results for ethanol and glycerol indicate another important possibility of two alcohols: biomass alcohols can be used as hydrogen sources without another H₂-producing process for upgrading of another biomass (hydrogenation of furan to THF in this study). In the reaction in 2-pentanol, oxidation product was analyzed as well as THF and H₂ (Entry 25). 2-Pentanone was formed and redox balance (RB) was calculated to be 0.97 from Equation (1). The value indicates that photogenerated electrons and positive holes were equally used in the photocatalytic reaction,

$$RB = \frac{2 \times n(\text{THF}) + n(\text{H}_2)}{n(2 - \text{Pentanone})} \quad (1).$$

Table 1 Effects of various reaction conditions on photocatalytic production of THF from furan in alcoholic suspensions of Pd-TiO₂ at 298 K^a.

Entries	TiO ₂ ^b	Phase ^c	S _{BET} ^d / m ² g ⁻¹	Pd / wt%	Alcohol	UV	Time / min	Gas phase	Yield / □mol
1	JRC-TIO-1	A	72	0.5	MeOH	On	5	Ar	17
2	JRC-TIO-8	A	313	0.5	MeOH	On	5	Ar	16
3	JRC-TIO-13	A	59	0.5	MeOH	On	5	Ar	18
4	JRC-TIO-4	A, (R)	54	0.5	MeOH	On	5	Ar	9
5	JRC-TIO-11	A, (R)	97	0.5	MeOH	On	5	Ar	20
6	JRC-TIO-3	R	48	0.5	MeOH	On	5	Ar	21
7	MT-150A	R	93	0.5	MeOH	On	5	Ar	26
8	MT-150A	R	93	1.0	MeOH	On	5	Ar	38
9	MT-150A	R	93	1.0	MeOH	On	10	Ar	40
10 ^e	MT-150A	R	93	1.0	MeOH	On	5	Ar	33
11 ^f	MT-150A	R	93	1.0	MeOH	On	5	Ar	36
12	-	-	-	-	MeOH	(Dark)	10	Ar	-
13	-	-	-	-	MeOH	On	5	Ar	-
14	MT-150A	R	93	1.0	MeOH	(Dark)	5	Ar	-
15	MT-150A	R	93	1.0	MeOH	(Dark)	5	H ₂	39
16	MT-150A	R	93	1.0	MeOH	(Dark)	5	H ₂ ^g /Ar	-
17	MT-150A	R	93	-	MeOH	(Dark)	5	H ₂	-
18	MT-150A	R	93	1.0 (Au)	MeOH	(Dark)	5	H ₂	-
19	MT-150A	R	93	1.0 (Ag)	MeOH	(Dark)	5	H ₂	-
20	MT-150A	R	93	1.0 (Cu)	MeOH	(Dark)	5	H ₂	-
21	MT-150A	R	93	1.0 (Pt)	MeOH	(Dark)	5	H ₂	0.6
22	MT-150A	R	93	1.0	EtOH	On	10	Ar	19
23	MT-150A	R	93	1.0	2-PrOH	On	10	Ar	22
24	MT-150A	R	93	1.0	2-BuOH	On	10	Ar	29
25	MT-150A	R	93	1.0	2-PnOH	On	10	Ar	13 ^h
26	MT-150A	R	93	1.0	Glycerol	On	10	Ar	35

^aAlcohol solution (5 cm³) of furan (40 ± 4 μmol) and 50 mg of photocatalyst under irradiation of UV light from a high-pressure mercury lamp. ^bJRC-TIO series registered at the Catalysis Society of Japan as Japan Reference Catalysts. MT-150A was supplied from Tayca. ^cA: Anatase, R: Rutile, Minor form in bi-phase samples is shown in parenthesis. ^dDetermined by BET method. ^eSecond use. ^fThird use. ^gH₂: 50 μmol. ^hH₂ formed: 6 μmol, 2-pentanone formed: 33 μmol.

3.3.5. Photocatalytic hydrogenation of furan

Figure 5 shows time courses of furan remaining and THF and H₂ formed in a methanolic suspension of 1.0 wt%Pd-TiO₂ (MT-150A) under deaerated conditions. The amount of furan decreased almost linearly with photoirradiation, while THF as the hydrogenation product of furan was formed with decrease in the amount of furan. After 25 min, furan was almost completely consumed and THF was obtained in a high yield (97%). To evaluate the selectivity of THF and intermediates in the furan hydrogenation, an indicator, i.e., material balance (MB), was calculated by Equation (2):

$$MB = \frac{n(\text{furan}) + n(\text{THF})}{n_0(\text{furan})} \dots(2)$$

where $n(\text{furan})$ and $n(\text{THF})$ are the amounts of furan and THF during the photocatalytic reaction, respectively, and $n_0(\text{furan})$ is the amount of furan before the photocatalytic reaction. In the initial stage of the reaction, the value of MB was *ca.* 0.9. The author examined furan adsorption on TiO₂ and metal-loaded TiO₂ in the dark (Figure 6), and the results indicated that furan was adsorbed on both TiO₂ and some metals (Pd, Pt and Au), and Pd-TiO₂ showed the highest amount of adsorption. The value of MB in the early stage can be attributed to adsorption of furan on Pd-TiO₂. Formation of an intermediate(s) may also be one of the reasons for the value of MB. Since species other than furan and THF were not detected in GC, the author cannot discuss the possibility of adsorption of an intermediate(s). As also shown in Figure 5, H₂ evolution was predominant under excessive photoirradiation after consumption of furan, indicating that active hydrogen species were continuously formed over the Pd co-catalyst. The author noted that the amount of THF slightly decreased after complete consumption of furan. Since a large excess of methanol used as a solvent effectively consumes positive holes, the possibility of THF re-oxidation can be eliminated. Results after consumption of furan suggest the occurrence of a reductive

process of THF in which a part of the active hydrogen species was probably used for catalytic hydrogenolysis of THF, resulting in consumption of THF. Mizugaki *et al.* reported formation of butanol in the ring opening reaction of furfural that has a furan ring.³⁶ Since butanol was not detected in GC, butanol was probably adsorbed on Pd-TiO₂. The high yield of THF at 25 min indicates that the activation energy of catalytic hydrogenolysis of THF over Pd is larger than that of catalytic hydrogenation of furan. Therefore, furan hydrogenation predominantly occurred at 298 K when furan was present in the reaction system.

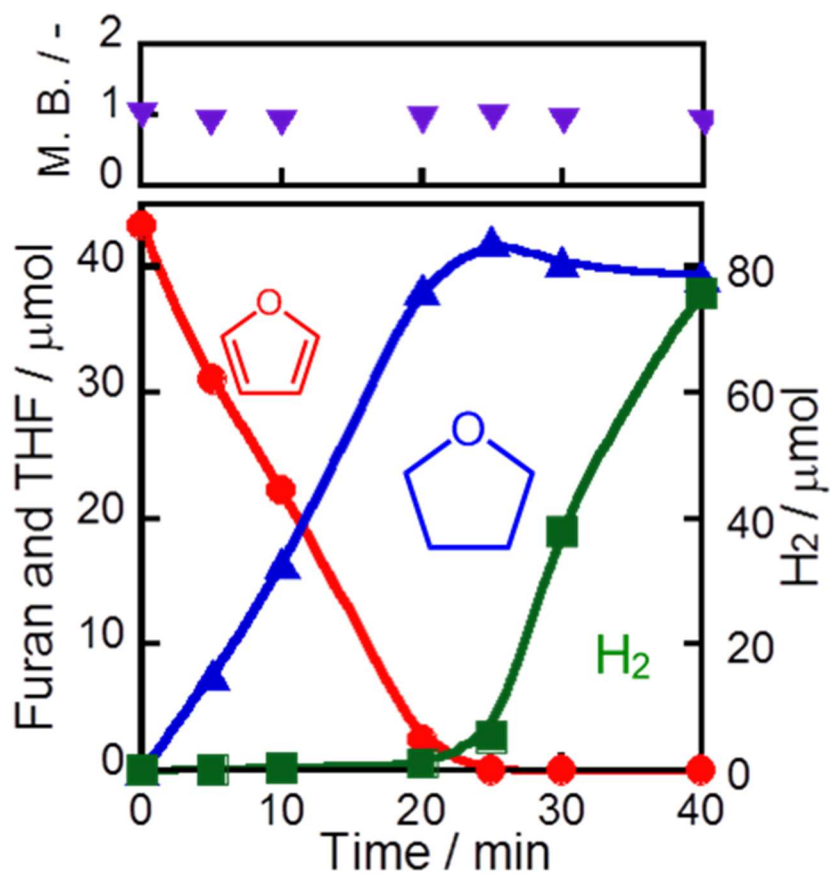


Figure 5 Time courses of furan remaining, THF formed and material balance of furan and THF in a methanolic suspension of 1.0 wt% Pd-TiO₂ under irradiation of UV light from an LED.

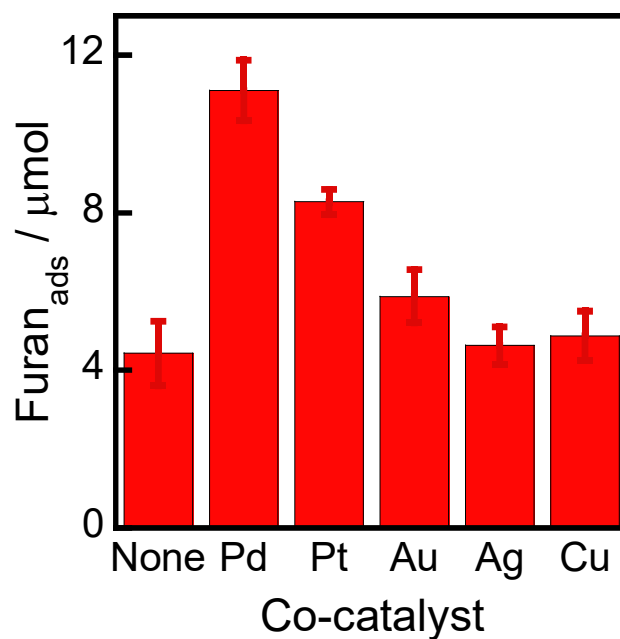


Figure 6 Effects of different kinds of photocatalysts (each 200 mg) on amount of furan adsorbed in methanolic suspensions for 18 h in the dark.

3.3.6. Action spectrum and reaction process

An action spectrum is a strong tool for determining whether a photoinduced process is the rate-determining step in the reaction observed. To obtain an action spectrum in this reaction system, hydrogenation of furan in methanolic suspensions of 1.0 wt% Pd-TiO₂ (MT-150A) was carried out at 298 K under irradiation of monochromated light from a Xe lamp. Apparent quantum efficiency (AQE) at each centered wavelength of light was calculated from the ratio of quadruple the amount of THF formed and the amount of photons irradiated using Equation (3):

$$\text{AQE} = \frac{4 \times \text{the amount of THF formed}}{\text{amount of incident photons}} \times 100 \quad \dots(3).$$

As shown in Figure 7, AQE was in agreement with the absorption spectrum of TiO₂. Therefore, it can be concluded that hydrogenation of furan in a methanolic suspension was induced by photoabsorption of TiO₂. As also shown in Figure 7, AQE reached 37% at 360 nm, indicating that photocatalytic hydrogenation of furan to THF occurred with high efficiency of photon utilization in addition to high selectivity and MB close to unity. The result indicates that photoabsorption at 410 nm does not contribute to the reaction, in other words, this photoabsorption does not induce the band-gap excitation of TiO₂. Electrons in the trap site below the bottom of the conduction band of TiO₂ have no potential to reduce protons to H₂.

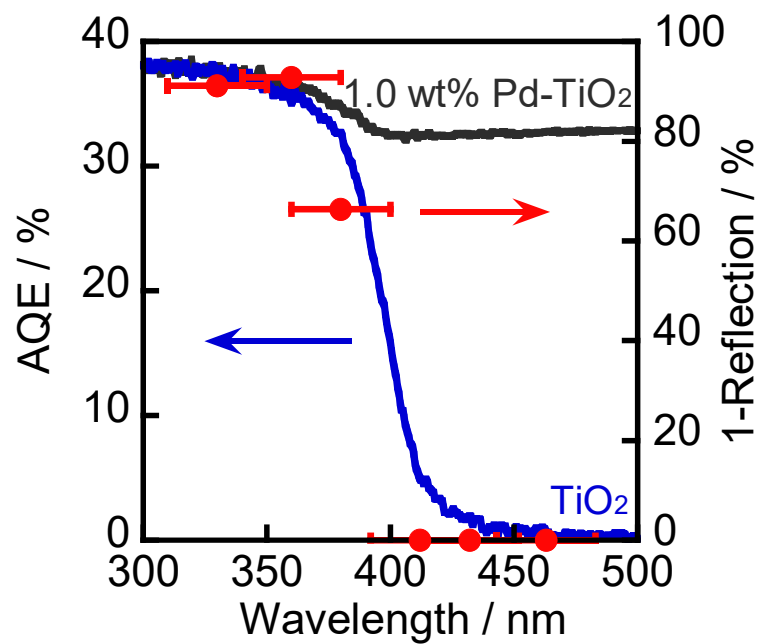


Figure 7 Absorption spectrum (right axis) and action spectrum of TiO₂ and 1.0wt% Pd-TiO₂ in the hydrogenation of furan (left axis).

3.3.7. The expected reaction process of photocatalytic hydrogenation of furan to THF over Pd-TiO₂

The expected reaction process of photocatalytic hydrogenation of furan to THF over Pd-TiO₂ is shown in Figure 8: 1) By irradiation of UV light, photogenerated electrons (e⁻) and positive holes (h⁺) are formed in the conduction and valence bands of TiO₂, and methanol is oxidized by h⁺, 2) H⁺ is reduced by e⁻, resulting in the formation of active hydrogen species over Pd particles and 3) two C=C double bonds of furan are successively hydrogenated by the active hydrogen species over Pd particles, resulting in the formation of THF. Higher adsorption ability of Pd is one of the most important reasons for the large yield of THF in the photocatalytic hydrogenation of furan. Since THF was formed in the presence of H₂ in the dark at 298 K, the active hydrogen species would be essentially the same as those formed in the photocatalytic process. Active hydrogen species also induce other reactions, i.e., H₂ evolution by self-coupling and hydrogenolysis of THF; however, these reactions are negligible as long as furan to be reacted with active hydrogen species is present in the reaction system. The negligible production of H₂ in the photocatalytic hydrogenation of furan means that the active species formed on Pd are very active for hydrogenation of furan, and the equilibrium between the active species formed on Pd and H₂ in the gas phase greatly shifts toward the left side (formation of the active species).

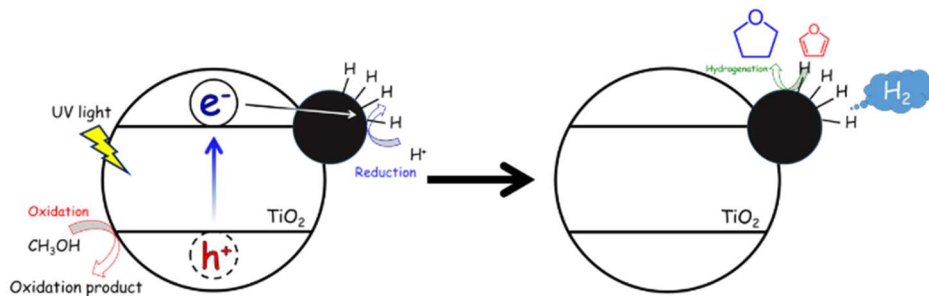


Figure 8 Expected reaction process of photocatalytic hydrogenation of furan to THF over Pd-TiO₂.

3.4. Conclusions

The author examined photocatalytic hydrogenation of furan, a representative heterocyclic compound and a compound derived from biomass, in an alcoholic suspension of metal-loaded TiO₂ under an H₂-free condition, in which alcohol worked as a solvent, electron donor and hydrogen source. Among the metal-loaded TiO₂ samples examined in this study, Pd-loaded TiO₂ (Pd-TiO₂) showed a distinctive photocatalytic activity for the largest production of THF and suppressed evolution of H₂, with apparent quantum efficiency reaching 37% at 360 nm. Hydrogenation of furan to THF under the present condition consisted of two processes: 1) photocatalytic production of active hydrogen species and 2) thermocatalytic hydrogenation of furan over Pd particles. Biomass-related alcohols (ethanol, butanol and glycerol) can also be used for hydrogenation of furan. The results obtained in this study show that photocatalytic hydrogenation is not limited to hydrocarbons and can be applied to heterocyclic compounds.

References

1. Mitsubishi Chemical Corporation, *Jpn. Pat.*, JP2013-60429A, **2013**.
2. (a) Q. Yuan, F. Ye, T. Xue and Y. Guan, *Appl. Catal. A-Gen.*, **2015**, *507*, 26. (b) C. Godawa, A. Gaset, P. Kalck and Y. Maire, *J. Mol. Catal.*, **1986**, *34*, 199. (c) T. J. Connolly, J. L. Considine, Z. Ding, B. Forsatz, M. N. Jennings, M. F. MacEwan, K. M. McCoy, D. W. Place, A. Sharma and K. Sutherland, *Org. Process Res. Dev.*, **2010**, *14*, 459-465.
3. P. T. Anastas and J. C. Warner, *Green Chemistry: Theory and Practice*, Oxford University Press, **1998**.
4. M. A. Fox and M. T. Dulay, *Chem. Rev.*, **1993**, *93*, 341-357.
5. G. Palmisano, V. Augugliaro, M. Pagliarob and L. Palmisano, *Chem. Commun.*, **2007**, 3425-3437.
6. G. Palmisano, E. Garcia-Lopez, G. Marci, V. Loddo, S. Yurdakal, V. Augugliaro, L. Palmisano, *Chem. Commun.*, **2010**, *46*, 7074-7089.
7. F. Mahdavi, T. C. Bruton and Y. Li, *J. Org. Chem.*, **1993**, *58*, 744-746.
8. V. Brezova, A. Blažkova, I. Šurina and B. Havlinova, *J. Photochem. Photobio. A*, **1997**, *107*, 233-237.
9. J. L. Ferry and W. H. Glaze, *Langmuir*, **1998**, *14*, 3551-3555.
10. J. L. Ferry and W. H. Glaze, *J. Phys. Chem. B*, **1998**, *102*, 2239-2244.
11. O. V. Makarova, T. Rajh, M. C. Thurnauer, A. Martin, P. A. Kemme and D. Cropek, *Environ. Sci. Tech.*, **2000**, *34*, 4797-4803.
12. V. Brezova, P. Tarabek, D. Dvoranova, A. Staško, S. Biskupič, *J. Photochem. Photobio. A: Chem.*, **2003**, *155*, 179-198.
13. H. Tada, T. Ishida, A. Takao and S. Ito, *Langmuir*, **2004**, *20*, 7898-7900.
14. H. Tada, T. Ishida, A. Takao, S. Ito, S. Mukhopadhyay, T. Akita, K. Tanaka and H. Kobayashi, *ChemPhysChem*, **2005**, *6*, 1537-1543.

15. T. Zhang, L. You and Y. Zhang, *Dyes and Pigments*, **2006**, *68*, 95-100.
16. S. O. Flores, O. R.-Bernij, M. A. Valenzuela, I. Cordova, R. Gomez and R. Gutierrez, *Top. Catal.*, **2007**, *44*, 507-511.
17. S. Chen, H. Zhang, X. Yu and W. Liu, *Chinese J. Chem.*, **2010**, *28*, 21-26.
18. H. Kominami, S. Iwasaki, T. Maeda, K. Imamura, K. Hashimoto, Y. Kera and B. Ohtani, *Chem. Lett.*, **2009**, *15*, 410-411.
19. K. Imamura, S. Iwasaki, T. Maeda, K. Hashimoto, B. Ohtani and H. Kominami, *Phys. Chem. Chem. Phys.*, **2011**, *13*, 5114-5119.
20. K. Imamura, T. Yoshikawa, K. Hashimoto and H. Kominami, *Appl. Catal. B, Environ.*, **2013**, *134-135*, 193-197.
21. K. Imamura, K. Hashimoto and H. Kominami, *Chem. Commun.*, **2012**, *48*, 4356-4358.
22. K. Imamura, T. Yoshikawa, K. Nakanishi, K. Hashimoto and H. Kominami, *Chem. Commun.*, **2013**, *49*, 10911-10913.
23. K. Imamura, Y. Okubo, T. Ito, A. Tanaka, K. Hashimoto and H. Kominami, *RSC Adv.*, **2014**, *4*, 19883-19886.
24. H. Kominami, S. Yamamoto, K. Imamura, A. Tanaka and K. Hashimoto, *Chem. Commun.*, **2013**, *49*, 4558-4560.
25. H. Kominami, M. Higa, T. Nojima, T. Ito, K. Nakanishi, K. Hashimoto and K. Imamura, *ChemCatChem*, **2016**, *8*, 2019-2022.
26. F. Corvaisier, Y. Schuurman, A. Fecant, C. Thomazeau, P. Raybaud, H. Toulhoat and D. Farrusseng, *J. Catal.*, **2013**, *307*, 352-361.
27. J. J. W. Bakker, A. G. van der Neut, M. T. Kreutzer, J. A. Moulijn and F. Kapteijn, *J. Catal.*, **2010**, *274*, 176-191.
28. M. Bradley, J. Robinson and D.P. Woodruff, *Surf. Sci.*, **2010**, *604*, 920-925.
29. K. Shimura and H. Yoshida, *Energy Environ. Sci.*, **2011**, *4*, 2467-2481.

30. T. Sakata and T. Kawai, *Chem. Phys. Lett.*, **1981**, *80*, 341-344.
31. H. Kominami, H. Nishimune, Y. Ohta, Y. Arakawa and T. Inaba, *Appl. Catal. B: Environ.*, **2012**, *111–112*, 297–302.
32. H. Kominami, A. Furusho, S.-Y. Murakami, H. Inoue, Y. Kera and B. Ohtani, *Catal. Lett.*, **2001**, *76*, 31-34.
33. M. P. Latusek, B. P. Spigarelli, R. M. Heimerl and J. H. Holles, *J. Catal.*, **2009**, *263*, 306-314
34. Y. Nakagawa, K. Takada, M. Tamura and K. Tomishige, *ACS Catal.*, **2014**, *4*, 2718-2726.
35. Y. Shiraishi, Y. Togawa, D. Tsukamoto, S. Tanaka and T. Hirai, *ACS Catal.*, **2012**, *2*, 2475-2481.
36. T. Mizugaki, T. Yamakawa, Y. Nagatsu, Z. Maeno, T Mitsudome, K. Jitsukawa and K. Kaneda, *ACS Sustainable Chem. Eng.*, **2014**, *2*, 2243-2247.

Chapter 4

Ring hydrogenation of aromatic compounds in aqueous suspensions of an Rh-loaded TiO₂ photocatalyst without use of H₂ gas

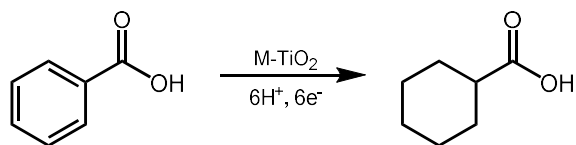
4.1. Introduction

Since a photocatalytic reaction satisfies almost all of the 12 proposed requirements for green chemistry,¹ photocatalytic conversion of various organic compounds has recently been studied by many researchers.² Recently, the number of reports on reductive conversion of organic compounds by using photogenerated electrons has been increasing.^{3, 4} However, most of the reports deal with reduction (hydrogenation) of nitrobenzenes to aminobenzenes.⁵⁻¹⁵ Kominami *et al.* has explored new photocatalytic reduction systems under a hydrogen (H₂)-free condition with focus on a) selective and chemoselective photocatalytic reduction and b) co-catalyst-assisted photocatalytic reduction (CPR). As a typical case of a), 3-nitrostyrene was chemoselectively reduced to 3-aminostyrene without hydrogenation of a C=C double bond to 3-ethylaniline in a suspension of a TiO₂ photocatalyst.¹⁶ As a case of a), Kominami *et al.* also found that *p*-chlorobenzaldehyde was chemoselectively converted to *p*-chlorobenzyl alcohol in an alcoholic suspension of TiO₂ in which the chloro group was preserved.¹⁷ As a case of b), benzonitrile and styrene were successfully hydrogenated to benzyl amine and ethyl benzene, respectively, in alcohol suspensions of a palladium-loaded TiO₂ photocatalyst, although the reduction potentials of benzonitrile and styrene are believed to be much higher than the potential of the conduction band of TiO₂.^{18, 19} As a case that satisfies both a) and b), *i.e.*, chemoselective CPR (CCPR),

Kominami *et al.* reported chemoselective reduction of (2,3-epoxypropyl)benzene to allylbenzene (silver co-catalyst)²⁰ and semihydrogenation of alkynes to alkenes (copper co-catalyst).²¹ The author think that various possibilities are included in CCPR because many metal co-catalysts can be applied for photocatalytic reaction.

Ring hydrogenation of aromatics is an important method to produce compounds consisting of a cyclohexane structure. For example, cyclohexanecarboxylic acid (CCA) which is an important intermediate of pharmaceutical and related compounds, is generally produced by ring hydrogenation of benzoic acid (BA).²² In the case of substituted aromatics, hydrogenation (reduction) of the functional groups also occurs as a side-reaction and produces aromatic compounds of which the functional group is reduced. In the case of BA, benzaldehyde and benzyl alcohol were formed by hydrogenation of the carboxyl group of BA.²³ Ring hydrogenation of BA was achieved over metal catalysts supported on suitable supports such as rhodium (Rh), ruthenium and NiZrB.²⁴⁻²⁷ However, these catalyst systems require the addition of an excess amount of H₂ gas as a hydrogen source in a closed reactor. Since special care should be paid during a reaction using H₂, a safer catalytic reaction system driving selective ring hydrogenation without the use of H₂ is desired. As described above, there are various possibilities of CCPR, and H₂-free CCPR can be applied for ring hydrogenation of aromatics having a carboxyl group to corresponding alicyclic compounds.

In this study, the author chose BA as a model compound of aromatics having a carboxyl group and examined photoinduced H₂-free ring hydrogenation of BA over metal-loaded TiO₂, in the presence of a hole scavenger that works as an electron and hydrogen source (Scheme 1).



Scheme 1 Photoinduced ring hydrogenation of benzoic acid in an aqueous suspension of metal (M)-loaded TiO₂ under an H₂-free condition.

4.2. Experimental

4.2.1. Preparation of metal-loaded TiO₂

Various metals as co-catalysts (Au, Ag, Cu, Pt and Rh) were loaded on TiO₂ (ST-01, Ishihara) by using the photodeposition method. TiO₂ powder was suspended in 10 cm³ of an aqueous methanol solution (10 vol%) containing a metal source in a test tube. HAuCl₄, AgNO₃, CuCl₂, PdCl₂, H₂PtCl₆ and RhCl₃ were used as metal sources. Each test tube was sealed with a rubber septum under argon (Ar) and then photoirradiated for 90 min at $\lambda > 300$ nm by a 400-W high-pressure mercury lamp (Eiko-sha, Osaka) with magnetic stirring in a water bath continuously kept at 298 K. The resulting powder was washed repeatedly with distilled water and dried for 2 h in vacuo.

4.2.2. Photocatalytic reaction

In a typical run, metal-loaded TiO₂ (50 mg) was suspended in 5 cm³ of water containing BA (*ca.* 50 μ mol) and OA (*ca.* 300 μ mol) as a hole scavenger in a test tube, which was sealed with a rubber septum and then photoirradiated under Ar at 298 K with the high-pressure mercury lamp. The amounts of BA and CCA were determined with an FID-type gas chromatograph (GC-2025, Shimadzu) equipped with a DB-1 column. Chlorobenzene was used as an internal standard sample. Chlorobenzene (7 mm³) and diethyl ether (2 cm³) were added to the reaction solution (3 cm³). After the mixture

had been stirred for 7 min, BA and CCA in the diethyl ether phase were analyzed. The amounts of BA and CA were determined from the ratios of the peak areas to the peak area of chlorobenzene. The amount of H₂ as the reduction product of protons (H⁺) and the amount of CO₂ as the oxidation product of OA were determined with a TCD-type gas chromatograph (GC-8A, Shimadzu) equipped with an MS-5A column and Porapak QS column. A multi-wavelength irradiation monochromator (MM-3, Bunkoukeiki Co., Ltd) was used to obtain apparent quantum efficiency (AQE), and light intensity was determined by using a spectroradiometer (USR-45D, Ushio Inc.).

4.2.3. Adsorption experiment

Rh-loaded TiO₂ (200 mg) was suspended in 5 cm³ of water containing BA (*ca.* 50 μmol) and OA (*ca.* 300 μmol), methanol containing BA or acetonitrile containing BA (*ca.* 50 μmol) and OA (*ca.* 300 μmol) in a test tube. The test tube was sealed with a rubber septum under Ar and the mixture was stirred in a water bath at 293 K for 20 hours in the dark. The amount of BA was determined in the same way as that for the photocatalytic reaction (section 2.2). When methanol and acetonitrile were used as solvents, no diethyl ether was added. The amount of OA in the liquid phase was determined with a Jasco PU-2800 plus ion chromatograph equipped with an IC NI-424 column (Shodex, Japan). Before analysis with the ion chromatograph, the pH value of the solution containing OA was adjusted to 10 with an aqueous solution of sodium hydroxide.

4.2.4. Catalytic reaction under an H₂ condition

Rh-loaded TiO₂ (50 mg) was placed in a test tube. The test tube was sealed with a rubber septum under H₂. Into the sealed test tube, 5 cm³ of water containing BA (*ca.* 50 μmol) and OA (*ca.* 300 μmol), water containing BA (*ca.* 50 μmol) and

methanol (*ca.* 300 μmol) or methanol containing BA (*ca.* 50 μmol) was injected with another needle being inserted into the rubber septum to keep the internal pressure at 1 atm. After injection of the reaction solution, the mixture was stirred in a water bath at 293 K in the dark. The amount of BA was determined in the same way as that for the photocatalytic reaction.

4.3. Results and discussion

4.3.1. Effects of different metal co-catalysts

Figure 1 shows the effects of different metal co-catalysts (1.0 wt%) on the yields of CCA produced in photoinduced ring hydrogenation of BA in aqueous suspensions of metal-loaded TiO₂ under irradiation of UV light for 15 min. No CCA was formed when bare TiO₂ was used as the photocatalyst. The color of bare TiO₂ became blue just after photoirradiation, indicating that parts of Ti⁴⁺ in TiO₂ were reduced to Ti³⁺ by photogenerated electrons. When Au-, Ag-, Cu- and Pd-loaded TiO₂ samples were used, no CCA was formed, indicating that bare TiO₂ and these metals were inactive for ring hydrogenation of BA. In contrast to these metal-loaded TiO₂ samples, when Pt and Rh were loaded on TiO₂, these photocatalysts, *i.e.*, Pt-TiO₂ and Rh-TiO₂, hydrogenated BA, resulting in the production of CCA. Rh-TiO₂ showed a much higher CCA yield than those of the other co-catalysts loaded on TiO₂ samples. In the case of Au, Cu, Pd, Pt and Rh, H₂ was formed as the product of reduction of H⁺ by photogenerated electrons ($2\text{H}^+ + 2\text{e}^- \rightarrow \text{H}_2$), although the amount of H₂ was dependent on the type of co-catalyst. Formation of CCA and/or H₂ means that two types of reaction (BA hydrogenation and H₂ formation) compete over metal-loaded TiO₂ photocatalysts.

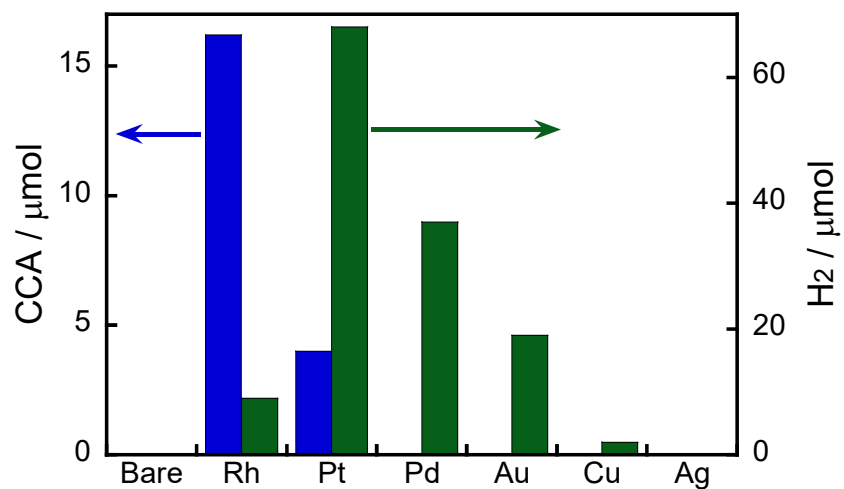


Figure 1 Effects of different metal co-catalysts (1.0 wt%) on the yields of CCA and H₂ produced in photoinduced ring hydrogenation of BA in aqueous suspensions of metal-loaded TiO₂ for 15 min under irradiation of UV light from a high-pressure mercury lamp.

Figure 2(a) shows the correlation between the yield of H₂ produced in photocatalytic ring hydrogenation of BA (Y₁) and hydrogen overvoltage (HOV) of metal electrodes. The use of an Rh co-catalyst resulted in a very small yield of H₂ that was much different from the value predicted from HOV. For comparison, photocatalytic reaction in the absence of BA was also examined and only reduction of H⁺ by e⁻ occurred under this condition. The yield of H₂ produced in photocatalytic reaction in the absence of BA (Y₂) was plotted against HOV (Figure 2(b)), showing that the yield gradually decreased with increase in HOV including Rh. Change in H₂ yield without exception means that reduction of H⁺ by e⁻ occurred on the metal co-catalyst and the reaction rate is determined by HOV of the co-catalyst. Figure 2(c) shows the correlation between H₂ yields in the presence and absence of BA. A linear correlation with a slope close to unity was observed for all of the co-catalysts except Rh. This correlation means that H₂ formation, *i.e.*, reduction of H⁺ by e⁻, occurs regardless of whether BA is present or not. In other words, these co-catalysts have no or little interaction with BA. On the other hand, H₂ evolution over Rh greatly decreased when BA was present in the reaction system, suggesting that Rh interacts with BA and provides a new route with small activation energy for ring hydrogenation of BA to CCA.

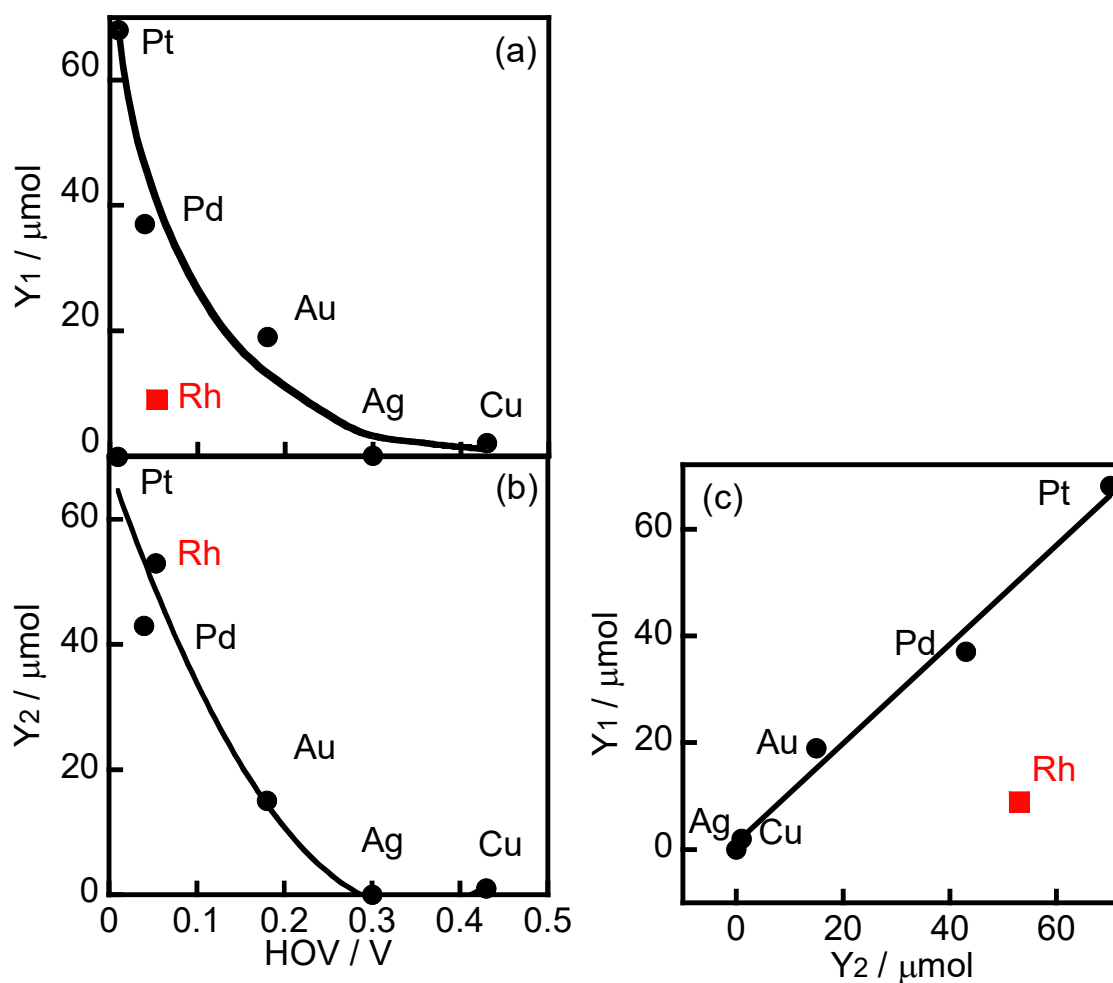


Figure 2 (a) Correlation between hydrogen overvoltage (HOV) of metal electrodes and yield of H₂ produced in photocatalytic ring hydrogenation of BA in the presence of OA (Y₁, Figure 1), (b) correlation between HOV and yield of H₂ produced under a BA-free condition (Y₂), and (c) correlation between Y₁ and Y₂.

4.3.2. Effect of the amount of Rh loading on CCA yield

The effect of the amount of Rh loading on CCA yield was examined, and the results for 15-min photoirradiation are shown in Figure 3. The highest CCA yield was obtained at 1.0 wt%, indicating that photocatalytic performance was affected positively and negatively by Rh particles loaded on TiO₂. The number of reduction sites for ring hydrogenation increased and the light-shading effect also increased with increase in Rh loading.

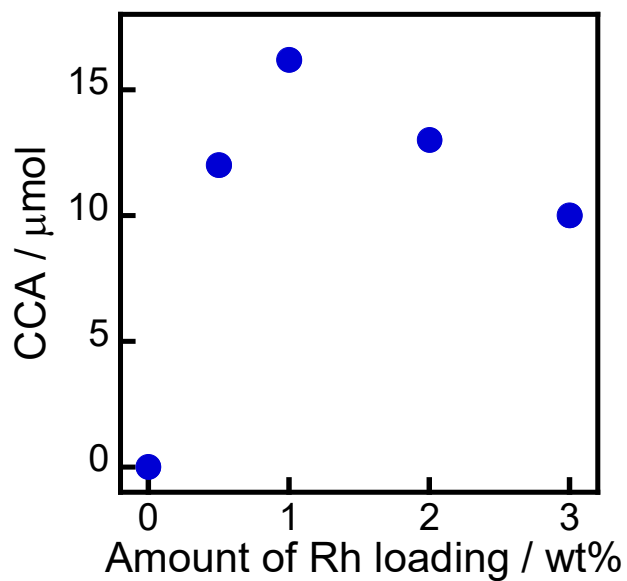


Figure 3 Effects of different amounts of Rh loading on photoinduced ring hydrogenation of BA to CCA in aqueous suspensions for 15 min under irradiation of UV light from a high-pressure mercury lamp.

4.3.3. Photoinduced ring hydrogenation of BA in an aqueous suspension of Rh-TiO₂

Figure 4 shows time courses of BA remaining, CCA formed, and H₂ and CO₂ evolved in an aqueous suspension of 1.0 wt% Rh-TiO₂ under irradiation of UV light. Just after irradiation, the amount of BA monotonously decreased, while CCA was formed. After 60 min, BA was almost completely consumed and CCA was obtained in a high yield (93%). To evaluate the selectivity of CCA and intermediates in the BA hydrogenation, an indicator, i.e., material balance (MB), was calculated by Equation (1):

$$MB = \frac{n(BA) + n(CCA)}{n_0(BA)}, \quad (1)$$

where $n(BA)$ and $n(CCA)$ are the amounts of BA and CCA during the photocatalytic reaction, respectively, and $n_0(BA)$ is the amount of BA before the photocatalytic reaction. During the reaction, the value of MB was *ca.* 0.9. However, no other product such as benzaldehyde, benzyl alcohol or toluene was detected in the reaction mixture. The author believe that a small amount of a water-soluble by-product may be produced. As also shown in Figure 4, H₂ evolution was predominant under excessive photoirradiation after consumption of BA, indicating that active hydrogen species (AHS) over Rh were continuously formed by proton reduction over the Rh co-catalyst. The author noted that the amount of CCA did not decrease after complete consumption of BA. Since an excess of OA used as a hole scavenger effectively consumes positive holes, the possibility of CCA re-oxidation and over-hydrogenation was eliminated.

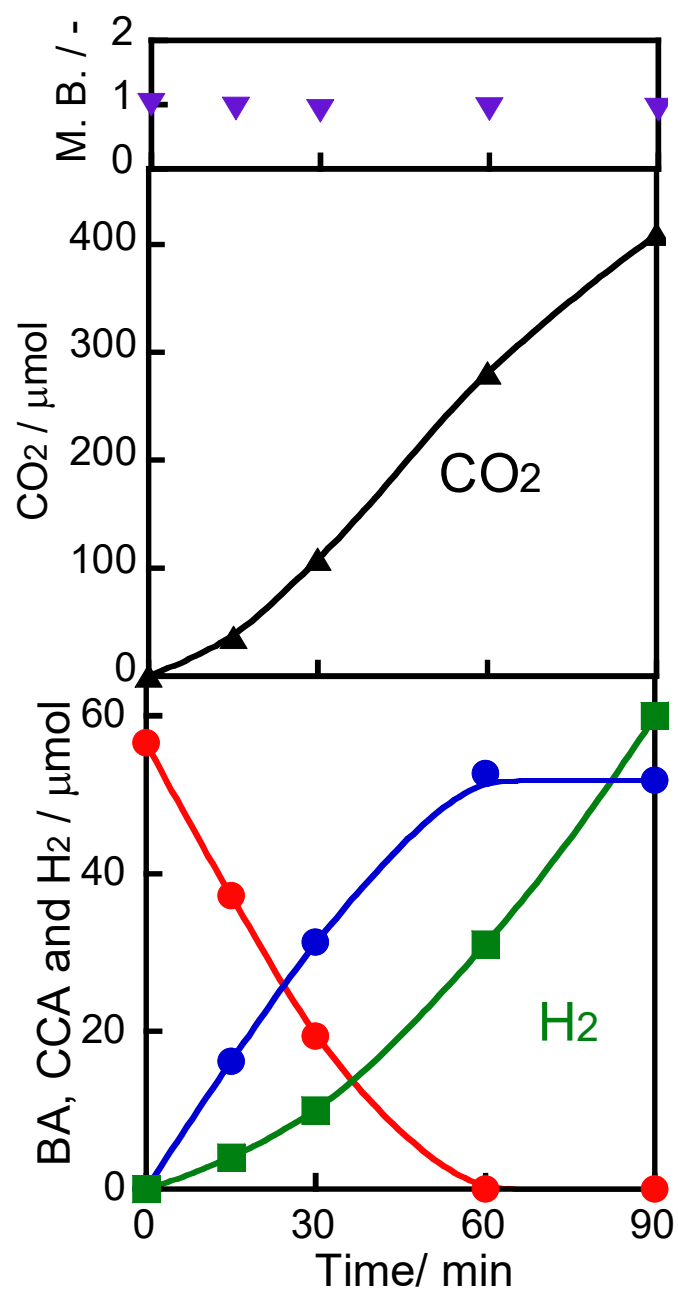


Figure 4 Time courses of BA remaining, CCA formed, and H₂ and CO₂ evolved in an aqueous suspension of 1.0 wt% Rh-TiO₂ under irradiation of UV light from a high-pressure mercury lamp.

4.3.4. Action spectrum

An action spectrum is a strong tool for determining whether a photoinduced process is the rate-determining step in the reaction observed. To obtain an action spectrum in this reaction system, ring hydrogenation of BA in aqueous suspensions of 1.0 wt% Rh-TiO₂ was carried out at 298 K under irradiation of monochromated light from a Xe lamp. Apparent quantum efficiency (AQE) at each centered wavelength of light was calculated from the ratio of sextuple the amount of CCA formed and the amount of photons irradiated using Equation (2):

$$AQE = \frac{6 \times \text{the amount of CCA formed}}{\text{amount of incident photons}} \times 100. \quad (2)$$

As shown in Figure 5, AQE was in agreement with the absorption spectrum of TiO₂. Therefore, it can be concluded that ring hydrogenation of BA in an aqueous suspension was induced by photoabsorption of TiO₂. As also shown in Figure 5, AQE reached 16% at 360 nm, indicating that photoinduced ring hydrogenation of BA to CCA occurred with high efficiency of photon utilization.

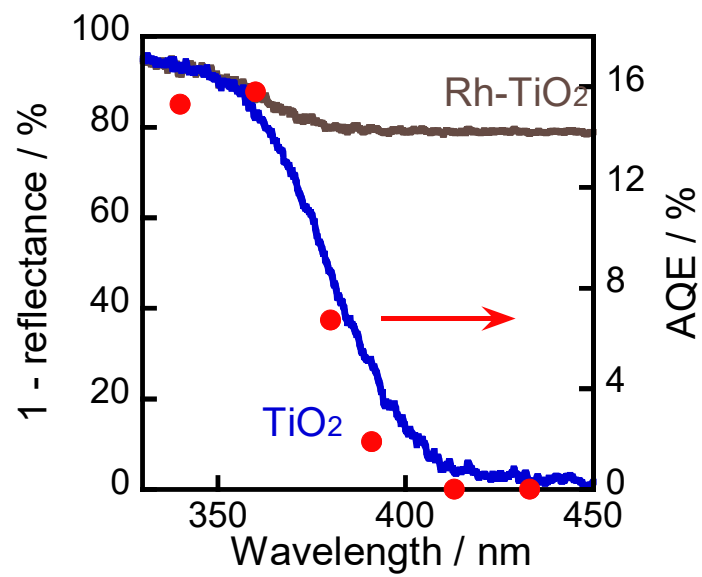


Figure 5 Absorption spectrum (right axis) and action spectrum of TiO₂ and 1.0wt% Rh-TiO₂ in ring hydrogenation of BA (left axis).

4.3.5. Effects of reaction conditions on ring hydrogenation of BA

The effects of various reaction conditions on ring hydrogenation of BA to CCA in aqueous suspensions of Rh-TiO₂ at 298 K are shown in Table 1. First, in order to examine the durability of the Rh-TiO₂ photocatalyst in this reaction system, Rh-TiO₂ was used repeatedly. After reaction for 60 min (entry 1), Rh-TiO₂ particles were recovered by simple filtration from the reaction mixture and were re-used. Entries 2 and 3 show that Rh-TiO₂ photocatalysts were reusable at least twice without notable loss of activity. According to Scheme 1, conversion of one molecule of BA to CCA requires six electrons, which corresponds to three molecules of OA ($3(\text{COOH})_2 = 6\text{CO}_2 + 6\text{H}^+ + 6\text{e}^-$). Therefore, at least, 150 μmol of OA is necessary for hydrogenation of 50 μmol of BA. The effects of different amounts of OA were also examined, and the results are shown in entries 5-8 in Table 1. High yields of CCA were obtained when the amount of OA was reduced to 250 and 200 μmol (entries 5 and 6). Under the stoichiometric condition (150 μmol), the yield of CCA decreased because a competitive reaction (H_2 evolution) consuming photogenerated electrons simultaneously occurred as shown in Figure 3 (Entry 7). When the reaction was carried out under 50 μmol of OA, the CCA yield further decreased due to the shortage of the hole scavenger for this reaction. The effect of the amount of OA on this reaction is further discussed on the basis of utilization of photogenerated electrons shown Figure 6. The amount of electrons used for ring hydrogenation of BA (production of CCA, $n(\text{CCA})$) increased with increase in the amount of OA (Figure 6(a)). Here, a new indicator, *i.e.*, electron selectivity for CCA formation ($\text{ES}(\text{CCA})$), was calculated according to Equation (3):

$$\text{ES}(\text{CAA}) = \frac{n(\text{CCA})}{n(\text{CCA}) + n(\text{H}_2)}, \quad (3)$$

where $n(\text{H}_2)$ is the amount of electrons used for H_2 evolution (Figure 6(b)). The value of $\text{ES}(\text{CCA})$ increased with increase in the amount of OA. However, efficiency

of OA utilization (EOU) determined by Equation (4),

$$EOU = \frac{n(CCA) + n(H_2)}{2 \times \text{initial amount of OA}}, \quad (4)$$

decreased, probably because unreacted OA remained after 60-min reaction (also shown in Figure 6(b)). From the results of ES(CCA) and EOU, it can be concluded that the appropriate amount of OA is about 200 μmol , satisfying both high ES(CCA) (0.80) and EOU (0.89). Entry 4 shows the result after 15-min photoirradiation. Entries 9, 10 and 11 show results of three blank reactions: 1) in the presence of Rh-TiO₂ in the dark (thermocatalytic reaction over Rh-TiO₂, entry 9), 2) in the absence of Rh-TiO₂ with irradiation of light (photochemical reaction, entry 10), and 3) in the absence of Rh-TiO₂ in the dark (non-catalytic thermal reaction between BA and OA, entry 11). These results indicate that the Rh-TiO₂ photocatalyst and photoirradiation are indispensable for the ring hydrogenation of BA. Photoinduced ring hydrogenation of phthalic acid to 1, 2-cyclohexanedicarboxylic acid was achieved over Rh-TiO₂ (entry 12). However, benzene and toluene were not converted to corresponding alicyclic compounds and only H₂ was evolved (entries 13 and 14), indicating high chemoselectivity of the Rh-TiO₂ photocatalyst to ring hydrogenation of carboxylic acids. Effects of the hole scavenger and solvent were also examined in entries 15, 16, 17, 18 and 19. When methanol was used as a hole scavenger instead of OA in an aqueous suspension of Rh-TiO₂, the reaction rate for ring hydrogenation of BA was very small (entry 15), probably due to the small amount of adsorption on the surface of TiO₂. In other words, OA is an excellent hole scavenger for this reaction. The adsorption behavior of OA and BA will be discussed in the next section. No hydrogenation occurred in photoirradiation to BA in an acetonitrile suspension of Rh-TiO₂ in the presence of OA, although H₂ was evolved (entry 19). This result means that the reaction medium is also an important factor to drive the ring hydrogenation of BA and

that an aqueous medium and OA as the hole scavenger are an indispensable combination for efficient hydrogenation of BA. When alcohols are used as solvents, they act as hole scavengers in addition to the reaction medium. In previous studies, the author found that alcohols worked well as solvents and hole scavengers for photocatalytic hydrogenation of unsaturated carbon-carbon bonds.^{24, 26} However, in the case of ring hydrogenation in alcohols in the absence of OA, only H₂ was produced with no CCA being formed (entries 16, 17 and 18). The results support the importance of the combination of an aqueous medium and OA as the hole scavenger for photocatalytic ring hydrogenation of BA.

Table 1 Effect of various reaction conditions on hydrogenation of BA to CCA in aqueous suspensions of Rh-TiO₂ at 298 K

Entries	Substrate	Hole scavenger		Solvent	Photo-catalyst	UV light	Time / min	Atmosphere	Yield ^a / μ mol	H ₂ / μ mol
		Type	Amount / μ mol							
1	BA	OA	300	H ₂ O	Rh-TiO ₂	On	60	Ar	53	31
2 ^b	BA	OA	300	H ₂ O	Rh-TiO ₂	On	60	Ar	52	34
3 ^c	BA	OA	300	H ₂ O	Rh-TiO ₂	On	60	Ar	53	32
4	BA	OA	300	H ₂ O	Rh-TiO ₂	On	15	Ar	16	4
5	BA	OA	250	H ₂ O	Rh-TiO ₂	On	60	Ar	48	42
6	BA	OA	200	H ₂ O	Rh-TiO ₂	On	60	Ar	47	36
7	BA	OA	150	H ₂ O	Rh-TiO ₂	On	60	Ar	32	33
8	BA	OA	50	H ₂ O	Rh-TiO ₂	On	60	Ar	10	15
9	BA	OA	300	H ₂ O	Rh-TiO ₂	(Dark)	15	Ar	n. d. ^d	n. d.
10	BA	OA	300	H ₂ O	-	On	15	Ar	n. d.	n. d.
11	BA	OA	300	H ₂ O	-	(Dark)	15	Ar	n. d.	n. d.
12	PA ^e	OA	300	H ₂ O	Rh-TiO ₂	On	60	Ar	49	37
13	Benzene	OA	300	H ₂ O	Rh-TiO ₂	On	60	Ar	n. d.	42
14	Toluene	OA	300	H ₂ O	Rh-TiO ₂	On	60	Ar	n. d.	47
15	BA	Methanol	300	H ₂ O	Rh-TiO ₂	On	15	Ar	1	7
16	BA	Methanol	-	Methanol	Rh-TiO ₂	On	15	Ar	n. d.	62
17	BA	Ethanol	-	Ethanol	Rh-TiO ₂	On	15	Ar	n. d.	85
18	BA	2-Propanol	-	2-Propanol	Rh-TiO ₂	On	15	Ar	n. d.	41
19	BA	OA	300	Acetonitrile	Rh-TiO ₂	On	15	Ar	n. d.	22
20	BA	OA	300	H ₂ O	Rh-TiO ₂	(Dark)	15	H ₂	18	-
21	BA	OA	300	H ₂ O	-	(Dark)	15	H ₂	n. d.	-
22	BA	Methanol	300	H ₂ O	Rh-TiO ₂	(Dark)	15	H ₂	10	-
23	BA	Methanol	300	Methanol	Rh-TiO ₂	(Dark)	15	H ₂	2	-

^a Yield of corresponding alicyclic compound. ^b Second use. ^c Third use. ^d Not detected. ^e Phthalic acid.

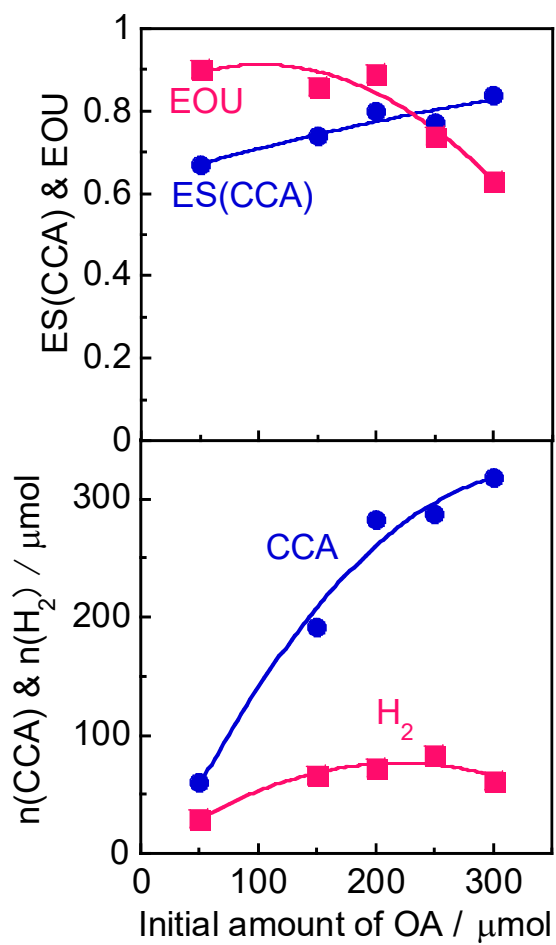


Figure 6 Effect of the amount of OA on this reaction is further discussed on the basis of utilization of photogenerated electrons.

4.3.6. Adsorption experiments

Some adsorption experiments were carried out to understand the effects of OA and solvent on BA adsorption to Rh-TiO₂, and the results are shown in Figure 7. A large amount of OA molecules was adsorbed on Rh-TiO₂ in water regardless of the presence or absence of BA (entries A and C). A large concentration of OA molecules on the surface of Rh-TiO₂ greatly contributes to hole scavenging under light irradiation, resulting in a large reaction rate of the ring-hydrogenation of BA. On the other hand, adsorption behavior of BA in water was affected by the presence of OA, and the amount of BA greatly decreased in the presence of OA (entries A and B). These results indicate that adsorption of BA and OA on Rh-TiO₂ was competitive and that OA adsorption was predominant under the condition of a photocatalytic reaction. However, 2.0 μmol of BA was adsorbed on Rh-TiO₂ even in the presence of OA. The balanced adsorption of OA and BA is one of the reasons for the effective ring hydrogenation of BA. The amounts of BA adsorbed on Rh-TiO₂ in methanol and acetonitrile were under the detection limit (entries D and E). Therefore, negligible adsorption of BA to Rh-TiO₂ in methanol and acetonitrile can be attributed to predominant H₂ formation without ring hydrogenation of BA in alcohol suspensions (entries 16, 17, 18 and 19 in Table 1).

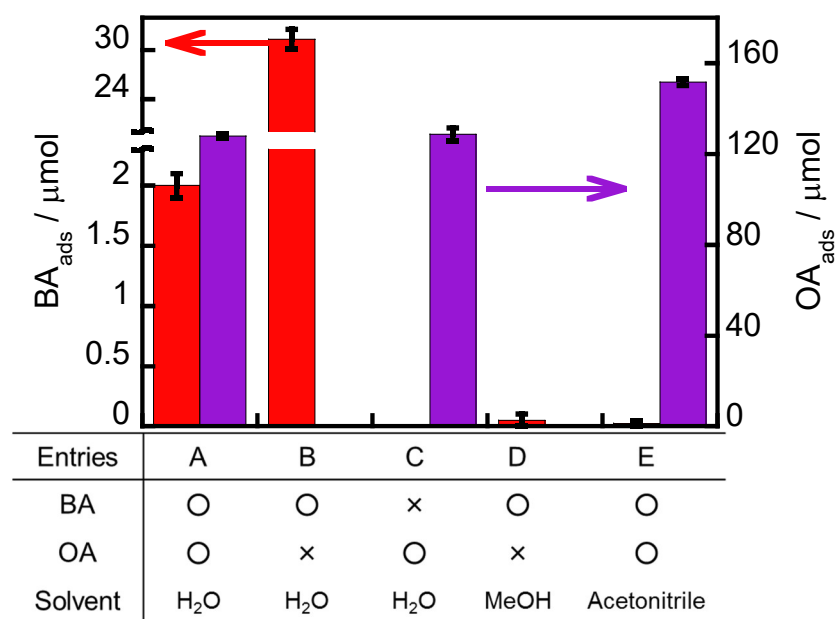


Figure 7 Amounts of BA and/or OA adsorbed onto Rh-TiO₂ for 20 h in the dark.

4.3.7. Dark reactions under H₂

Since H₂ is formed as a by-product in photocatalytic ring hydrogenation of BA in the presence of a hole scavenger, some dark reactions (thermal reactions) under H₂ (1 atm) were examined at 298 K to understand this reaction (entries 20, 21, 22, 23). In the dark, CCA was formed in an aqueous suspension of Rh-TiO₂ (entry 20) but was not formed in the absence of Rh-TiO₂ (entry 21), indicating that supported Rh particles were active for ring hydrogenation in the presence of H₂. This process consists of 1) formation of AHS on the surface of Rh particles by dissociative adsorption of H₂ and 2) insertion of AHS into the aromatic ring of BA. A thermal catalytic reaction under H₂ also occurred in an aqueous suspension of Rh-TiO₂ in the presence of methanol (Entry 22). The author noted that the reaction rate of the thermal reaction in the methanol suspension of Rh-TiO₂ under H₂ was very small (entry 23) compared with the reaction rate in aqueous media (entries 20 and 22). The adsorption experiment described in the previous section clearly showed that BA was hardly adsorbed on Rh-TiO₂ in methanol. Therefore, the result of entry 23 can be explained by this adsorption effect.

4.3.8. Effect of pH

Figure 8(a) shows the effects of initial pH of the aqueous suspension of Rh-TiO₂ on CCA yield (Y(CCA)) and H₂ yield (Y(H₂)), indicating that an acidic condition is appropriate for ring hydrogenation of BA. On the other hand, H₂ evolution was less affected by pH of the suspension. To understand the effect of pH on Y(CCA), adsorption experiments were carried out under various pH conditions (Figure 8(b)). The amount of OA adsorbed gradually decreased with increase in pH in an acidic condition; however, the amount was still large in the basic condition. The amount of BA adsorbed was much smaller than that of OA as shown in Figure 7, and the amount of BA adsorbed decreased with increase in pH of the suspension. The author noticed that the behavior of BA adsorption against pH was similar to that of Y(CCA), and a relatively clear correlation was observed between BA adsorption and Y(CCA), especially in acidic conditions (Figure 8(c)). This plot indicates that the reaction rate of BA hydrogenation was decided by the adsorption of BA, at least in an acidic condition.

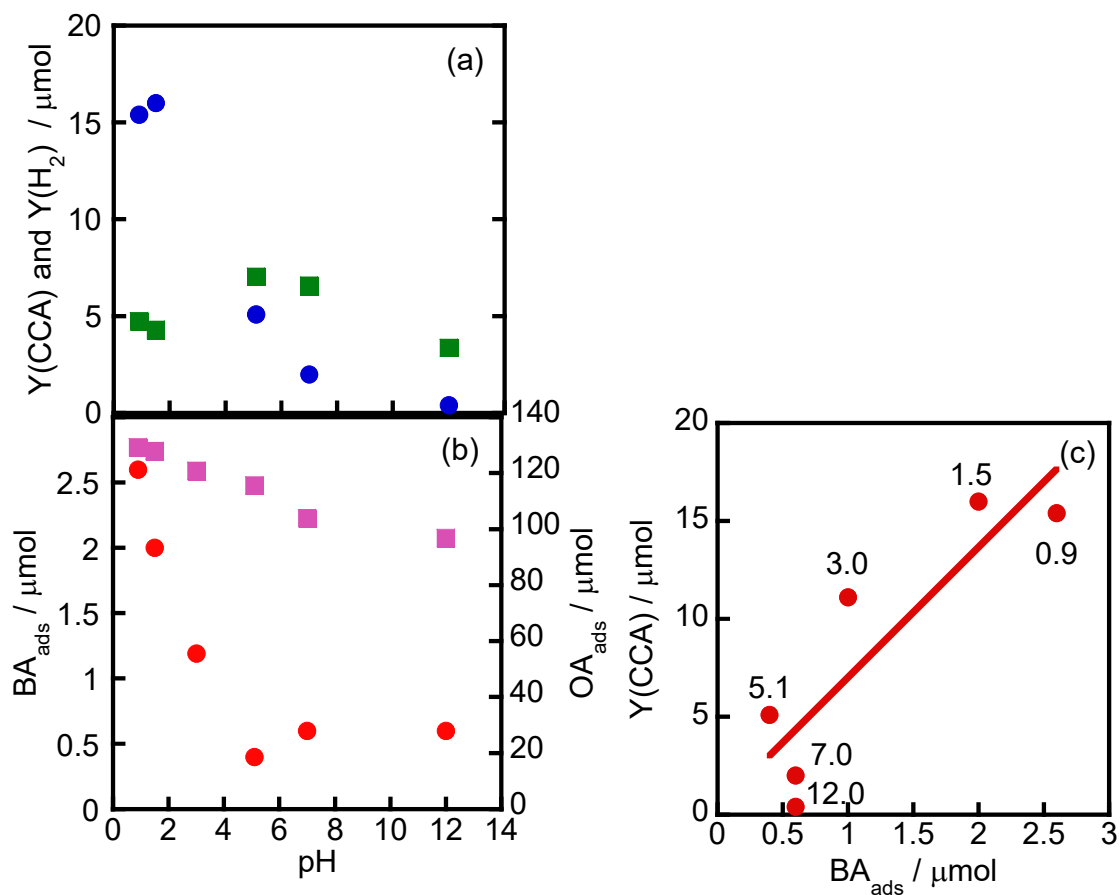


Figure 8 Effects of initial pH of the aqueous suspension of Rh-TiO₂ on (a) CCA yield (Y(CCA), circles) and H₂ yield (Y(H₂), squares), (b) amounts of BA (BA_{ads}, circles) and OA (OA_{ads}, squares) adsorbed and (c) correlation between Y(CCA) and BA_{ads}. Reaction conditions except pH were the same as those in the experiment for which results are shown in Figure 1. The pH of the reaction solution was adjusted with an aqueous solution of sulfuric acid and sodium hydroxide. Values shown in Figure 8(c) are pH value of the suspensions.

4.3.9. Expected reaction process

The expected reaction process of photoinduced ring hydrogenation of BA to CCA over Rh-TiO₂ is shown in Figure 9: 1) By irradiation of UV light, photogenerated electrons (e⁻) and positive holes (h⁺) are formed in the conduction and valence bands of TiO₂, and OA is oxidized by h⁺, 2) H⁺ is reduced by e⁻, resulting in the formation of AHS over Rh particles and 3) the aromatic ring of BA is successively hydrogenated by AHS over Rh particles, resulting in the formation of CCA. Since CCA was formed in the presence of H₂ in the dark at 298 K, AHS would be essentially the same as that formed in the photocatalytic process. Self-coupling of AHS resulted in H₂ evolution. The rate of H₂ production increased after consumption of BA, which means that the active species formed on Rh are active for ring hydrogenation of BA.

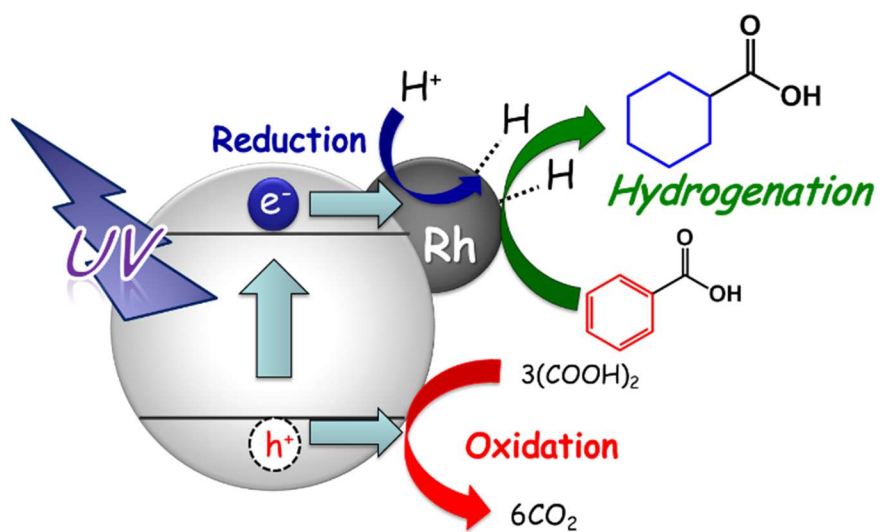


Figure 9 Expected reaction process of photocatalytic hydrogenation of BA to CCA over Rh-TiO₂.

4.4. Conclusions

The author examined photoinduced ring hydrogenation of BA in an aqueous suspension of metal (M)-loaded TiO₂ in the presence of OA under an H₂-free condition. Among the metal-loaded TiO₂ samples examined in this study, Rh-TiO₂ showed distinctive photocatalytic activity for the largest production of CCA, and apparent quantum efficiency reached 16% at 360 nm. A large amount of OA molecules was adsorbed on Rh-TiO₂ in water, contributing to efficient hole scavenging under light irradiation, and the reaction rate for CCA formation was mainly determined by the amount of BA adsorbed. Ring hydrogenation of BA to CCA under the present conditions consisted of two processes: 1) photocatalytic production of AHS and 2) thermocatalytic hydrogenation of BA over Rh particles.

References

1. P. T. Anastas and J. C. Warner, *Green Chemistry: Theory and Practice*, Oxford University Press, **1998**.
2. M. A. Fox and M. T. Dulay, *Chem. Rev.*, **1993**, *93*, 341-357.
3. G. Palmisano, V. Augugliaro, M. Pagliarob and L. Palmisano, *Chem. Commun.*, **2007**, 3425-3437.
4. G. Palmisano, E. Garcia-Lopez, G. Marci, V. Loddo, S. Yurdakal, V. Augugliaro and L. Palmisano, *Chem. Commun.*, **2010**, *46*, 7074-7089.
5. F. Mahdavi, T. C. Bruton and Y. Li, *J. Org. Chem.*, **1993**, *58*, 744-746.
6. V. Brezova, A. Blažkova, I. Šurina, B. Havlinova, *J. Photochem. Photobio. A*, **1997**, *107*, 233-237.
7. J. L. Ferry and W. H. Glaze, *Langmuir*, **1998**, *14*, 3551-3555.
8. V. Makarova, T. Rajh, M. C. Thurnauer, A. Martin, P. A. Kemme and D. Cropek, *Environ. Sci. Tech.*, **2000**, *34*, 4797-4803.
9. V. Brezova, P. Tarabek, D. Dvoranova, A. Staško and S. Biskupič, *J. Photochem. Photobio. A: Chem.*, **2003**, *155*, 179-198.
10. H. Tada, T. Ishida, A. Takao and S. Ito, *Langmuir*, **2004**, *20*, 7898-7900.
11. H. Tada, T. Ishida, A. Takao, S. Ito, S. Mukhopadhyay, T. Akita, K. Tanaka and H. Kobayashi, *ChemPhysChem*, **2005**, *6*, 1537-1543.
12. S. O. Flores, O. R.-Bernij, M. A. Valenzuela, I. Cordova, R. Gomez and R. Gutierrez, *Top. Catal.*, **2007**, *44*, 507-511.
13. H. Kominami, S. Iwasaki, T. Maeda, K. Imamura, K. Hashimoto, Y. Kera and B. Ohtani, *Chem. Lett.*, **2009**, *15*, 410-411.
14. K. Imamura, S. Iwasaki, T. Maeda, K. Hashimoto, B. Ohtani and H. Kominami, *Phys. Chem. Chem. Phys.*, **2011**, *13*, 5114-5119.

15. K. Imamura, T. Yoshikawa, K. Hashimoto and H. Kominami, *Appl. Catal. B, Environ.*, **2013**, 134–135, 193-197.
16. K. Imamura, K. Hashimoto and H. Kominami, *Chem. Commun.*, **2012**, 48, 4356-4358.
17. M. Fukui, A. Tanaka, K. Hashimoto and H. Kominami, *Chem. Lett.*, **2016**, 45, 985-987.
18. K. Imamura, T. Yoshikawa, K. Nakanishi, K. Hashimoto and H. Kominami, *Chem. Commun.*, **2013**, 49, 10911-10913.
19. K. Imamura, Y. Okubo, T. Ito, A. Tanaka, K. Hashimoto and H. Kominami, *RSC Adv.*, **2014**, 4, 19883-19886.
20. H. Kominami, S. Yamamoto, K. Imamura, A. Tanaka and K. Hashimoto, *Chem. Commun.*, **2013**, 49, 4558-4560.
21. H. Kominami, M. Higa, T. Nojima, T. Ito, K. Nakanishi, K. Hashimoto and K. Imamura, *ChemCatChem*, **2016**, 8, 2019-2022.
22. B. S. Moore, H. Cho, R. Casati, E. Kennedy, K. A. Reynolds, U. Mocek, J. M. Beale and H. G. Floss, *J. Am. Chem. Soc.*, **1993**, 115, 5254-5266.
23. N. Perret, X. Wang, J. J. Delgado, G. Blanco, X. Chen, C. M. Olmos, S. Barnal and M. A. Keane, *J. Catal.*, **2014**, 317, 114-125.
24. T. Harada, S. Ikeda, Y. H. Ng, T. Sakata, H. Mori, T. Torimoto, and M. Matsumura, *Adv. Funct. Mater.*, **2008**, 18, 2190–2196.
25. Z. Jiang, G. Lan, X. Liu, H. Tang and Y. Li, *Catal. Sci. Technol.*, **2016**, 6, 7259-7266.
26. X. Wen, Y. Cao, X. Qiao, L. Niu, L. Huo and G. Bai, *Catal. Sci. Technol.*, **2015**, 5, 3281-3287.
27. H. Wang and F. Zhao, *Int. J. Mol. Sci.*, **2007**, 8, 628-634.

Chapter 5

Ruthenium and palladium bimetallic system achieving functional parity with a rhodium co-catalyst for TiO₂-photocatalyzed ring hydrogenation of benzoic acid

5.1. Introduction

Ring hydrogenation of benzoic acid (BA) is an important chemoselective reaction. Cyclohexanecarboxylic acid (CCA) formed by hydrogenation of BA is an important intermediate of pharmaceutical and related compounds¹. In the case of hydrogenation of BA, benzaldehyde and benzyl alcohol can also be formed by reduction of the carboxyl group². Ring hydrogenation of BA was achieved by (thermo)catalytic reaction over a metal catalyst³⁻⁶. However, these catalytic reactions require dihydrogen (H₂) gas as a hydrogen source. Since the use of H₂ gas has a risk of explosion, special care should be paid during the reactions. Therefore, a catalytic system for ring hydrogenation without the use of H₂ gas is desired.

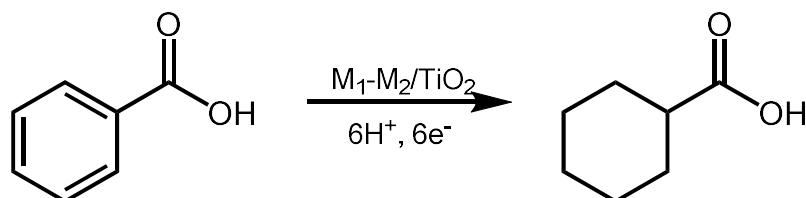
Since photocatalytic reactions are almost consistent with the concept of green chemistry⁷, substance conversion using photocatalysts has recently attracted the attention of researchers in the fields of organic chemistry, physical chemistry and material chemistry⁸. Kominami *et al.* reported that various photocatalytic reductions (hydrogenations) successfully occur under an H₂-free condition. In those studies, Kominami *et al.* succeeded in selective and chemoselective photocatalytic reduction of nitrobenzenes, sulfoxides, aldehydes and epoxides over metal-free TiO₂⁹⁻¹³ and photocatalytic hydrogenation of C=C, C≡C and C≡N bonds over metal-loaded TiO₂¹⁴⁻¹⁶. Very recently, the author also found that BA was chemoselectively

hydrogenated to CCA in an aqueous suspension of a rhodium (Rh)-loaded TiO₂ photocatalyst in the presence of oxalic acid as a hole scavenger¹⁷. These photocatalytic systems do not require H₂ gas as a reducing agent; therefore, the reaction does not require a pressure-tight reactor. Since Rh is a rare and expensive element, a photocatalyst having a smaller Rh content or a photocatalyst having another abundant element is favorable from the viewpoint of “Element Strategy”. In the same study¹⁷, the author also confirmed that TiO₂ having metal co-catalysts other than Rh exhibited no activity in photocatalytic ring-hydrogenation of BA.

Recently, it was reported that a catalyst having two elements exhibits higher activity and selectivity than those of catalysts consisting of single elements. For example, ruthenium (Ru)–palladium (Pd) alloy nanoparticles showed higher activity than the activities of single element catalysts such as Ru, Pd and Rh¹⁸. It has been proposed that the characteristics of an alloy catalyst are different from those of single element catalysts. There are also reports on photocatalysts consisting of a co-catalyst alloy¹⁹⁻²⁰. The effect of alloying co-catalysts on reduction of nitrobenzene was examined, and copper (Cu) and silver (Ag) alloy nanoparticles loaded on a zirconium oxide photocatalyst showed a different selectivity from those of Ag- and Cu-loaded photocatalysts¹⁹. In the case of photocatalytic oxidation of carbon monoxide, TiO₂ having a Pt-Ru alloy showed higher activity than those of Pt/TiO₂, Ru/TiO₂ and Pt-TiO₂-Ru (in which Pt and Ru were separately loaded)²⁰.

In this study, the author prepared TiO₂ photocatalysts having two kinds of metal co-catalyst that were inactive for the reaction when used solely and then used these photocatalysts for ring hydrogenation of BA under an H₂-free condition (Scheme 1). Among many combinations, the author found that CCA was formed when Ru and Pd were loaded on TiO₂. The author also characterized this photocatalyst to understand the reason why ring hydrogenation of BA occurred over an Ru and Pd

bimetallic system.



Scheme 1 Ring hydrogenation of BA in an aqueous suspension of TiO_2 having two kinds of co-catalyst under H_2 -free condition.

5.2. Experimental

5.2.1. Preparation of TiO_2 having two elements as a co-catalyst

By using a photodeposition method, two elements chosen from gold (Au), Ag, Cu, Pd and Ru were loaded on TiO_2 (P 25) and the total amount of the two elements was fixed to be 1.0 mol%. The TiO_2 powder was suspended in 10 cm^3 of an aqueous methanol solution (50 vol%) containing metal sources in a test tube. $HAuCl_4$, $AgNO_3$, $CuCl_2$, $PdCl_2$ and $RuCl_3$ were used as metal sources. The test tube was sealed with a rubber septum under argon (Ar) and then photoirradiated for 240 min at $\lambda > 300$ nm by a 400-W high-pressure mercury arc (Eiko-sha, Osaka) with magnetic stirring in a water bath continuously kept at 298 K. The resulting powder was washed repeatedly with distilled water and dried for 2 h in vacuo. Hereafter, these samples are designated as M_1-M_2/TiO_2 , where M_1 and M_2 are two elements loaded on TiO_2 . After the photodeposition, the filtrate was analyzed by atomic absorption spectrometry (AAS) using a Shimadzu AA-6200 or inductively coupled plasma atomic emission spectroscopy (ICP-AES) using Shimadzu ICPS-7500. These analyses confirmed that each co-catalyst was almost quantitatively loaded on TiO_2 . When the ratio of M_1-M_2/TiO_2 samples is discussed, the samples are shown as M_1X-M_2Y/TiO_2 , where X

and Y represent the ratio of M_1 and M_2 in the samples.

For comparison, TiO_2 having core-shell nanoparticles (Pd core-Ru shell, shown as Pd@Ru/ TiO_2 hereafter) was prepared by using a two-step photodeposition method^{21, 22}. TiO_2 powder was suspended in 10 cm^3 of an aqueous methanol solution (50 vol%) containing PdCl_2 in a test tube. The test tube was sealed with a rubber septum under Ar and then photoirradiated for 60 min under the same conditions as those for the photodeposition described above. Then an aqueous solution of RuCl_3 was injected into the test tube, and the mixture was photoirradiated by the same mercury arc for 180 min. The resulting powder was washed repeatedly with distilled water and dried for 2 h in vacuo. In the case of Pd@Ru/ TiO_2 , the contents of Pd and Ru were the same (0.50 mol%).

5.2.2. Characterization

Morphology of M_1X - M_2Y / TiO_2 samples was observed using a JEOL JEM-2100F transmission electron microscope (TEM) operated at 200 kV in the Joint Research Center (JRC) of Kindai University. X-ray photon spectroscopy (XPS) spectra of the samples were measured by using a Shimadzu/KRATOS AXIS-NOVA ESCA in the JRC. Ru and Pd K-edge XAFS spectra of the as-prepared Ru-Pd/ TiO_2 photocatalyst and reference samples (Pd foil, PdO, Ru powder and RuO_2) were recorded at the BL01B1 beamline at the SPring-8 (Japan Synchrotron Radiation Research Institute, Hyogo, Japan) in the transmission mode at ambient temperature. A typical data reduction procedure (e.g., background removal and normalization) was carried out with Athena(version 0.9.25).

5.2.3. Photocatalytic reaction

In a typical run, the prepared photocatalyst (50 mg) was suspended in 5 cm^3 of

water containing BA (*ca.* 50 μmol) and oxalic acid (OA, *ca.* 300 μmol) as a hole scavenger in a test tube, which was sealed with a rubber septum and then photoirradiated under Ar at 298 K with the high-pressure mercury arc (Eiko-sha, Osaka). The amounts of BA and CCA were determined with an FID-type gas chromatograph (GC-2025, Shimadzu) equipped with a DB-1 column. Chlorobenzene was used as an internal standard sample. Chlorobenzene (7 mm^3) and diethyl ether (2 cm^3) were added to the reaction solution (3 cm^3). After the mixture had been stirred, BA and CCA in the diethyl ether phase were analyzed. The amounts of BA and CA were determined from the ratios of the peak areas to the peak area of chlorobenzene. The amount of H_2 as the reduction product of protons (H^+) was determined with a TCD-type gas chromatograph (GC-8A, Shimadzu) equipped with an MS-5A column.

5.3. Results and Discussion

5.3.1. *Effects of the combination of two elements as a co-catalyst on ring hydrogenation*

Figure 1 shows the effects of the combination of two elements on yields of CCA produced in photocatalytic ring hydrogenation of BA in aqueous suspensions of $M_{150}-M_{250}/TiO_2$ under irradiation of UV light for 30 min. No hydrogenation of BA occurred when only one element was used ($M_1 = M_2$ in Figure 1). Most of the combinations of two elements also resulted in no formation of CCA, which is generally explained by no hydrogenation of BA in the single use of elements, i.e., no synergy effect was obtained in these combinations. Very interestingly, CCA was formed when Ru and Pd were simultaneously loaded on TiO_2 , indicating that photocatalytic ring hydrogenation of BA was possible without the use of an Rh co-catalyst. An interesting point is that Ru and Pd were inactive for hydrogenation when used solely.

To understand photocatalytic CCA formation over $Ru_{50}-Pd_{50}/TiO_2$, samples having different Ru-Pd ratios were prepared and then used for photocatalytic ring hydrogenation of BA. Figure 2 shows the effect of Ru-Pd ratio on yields of CCA and H_2 in the reaction. In all cases, H_2 was formed as the product of reduction of H^+ by photogenerated electrons ($2H^+ + 2e^- = H_2$), indicating that Ru and Pd did not lose catalysis for H_2 evolution. No CCA was formed when Ru or Pd was solely used as shown at both ends of Figure 2 (also shown in Figure 1, see $M_1 = M_2 = Pd$ and $M_1 = M_2 = Ru$). Ring hydrogenation of BA occurred only when Ru and Pd were simultaneously loaded on TiO_2 . Figure 2 also shows that CCA was formed in a wide range of Ru-Pd ratios. There are some possibilities for explaining the activity of the Ru-Pd/ TiO_2 photocatalyst for ring hydrogenation, and the Ru-Pd/ TiO_2 photocatalyst was characterized and evaluated in detail.

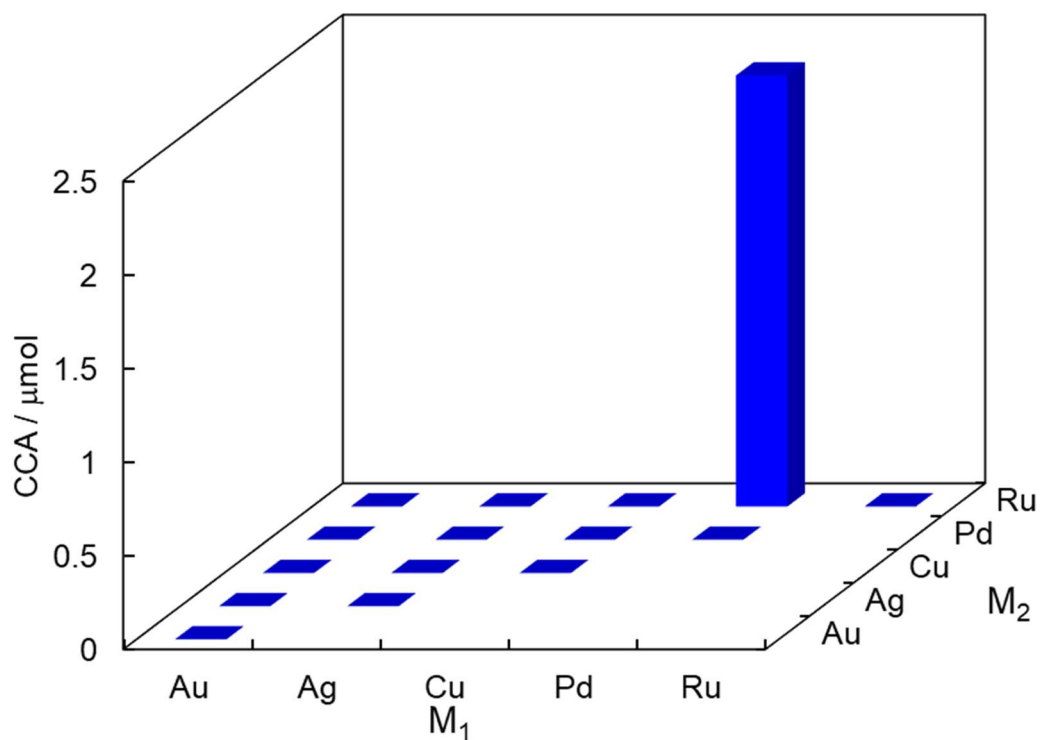


Figure 1 Effects of the combination of two elements as co-catalysts (1.0 mol%) on the yields of CCA produced in photoinduced ring hydrogenation of BA in aqueous suspensions of M₁-M₂/TiO₂ under irradiation of UV light for 30 min.

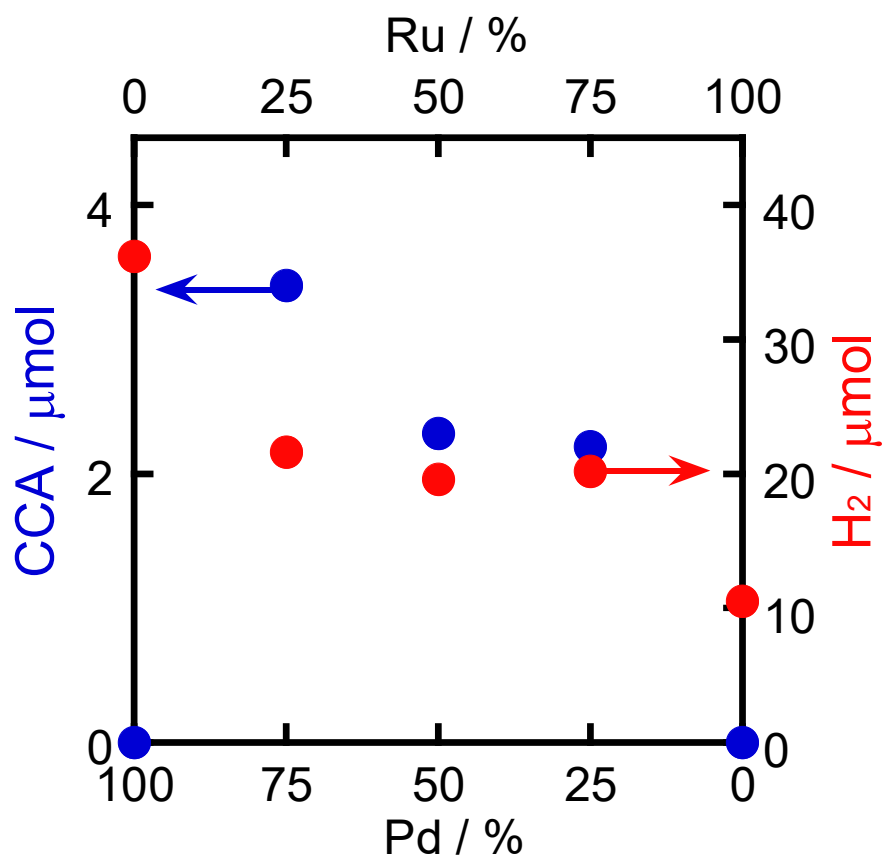


Figure 2 Effect of the ratio of Ru and Pd on CCA and H₂ formed in photocatalytic ring-hydrogenation of BA in an aqueous solution containing OA.

5.3.2. TEM observation

TEM photographs of Ru/TiO₂, Pd/TiO₂ and RuX-PdY/TiO₂ samples and particle size distributions of these samples are shown in Figures 3 and 4, respectively. Figures 3(a) and 3(e) show TEM photographs of Ru/TiO₂ and Pd/TiO₂, respectively. Nanoparticles of Ru and Pd were observed in Ru/TiO₂ and Pd/TiO₂, and the average diameters were determined to be 2.0 nm and 3.2 nm, respectively (Figures 4(a) and 4(e)). Figures 3(b), 3(c) and 3(d) show TEM photographs of Ru75-Pd25/TiO₂, Ru50-Pd50/TiO₂ and Ru25-Pd75/TiO₂, respectively. From these photographs, the average diameters were determined to be 3.1 nm, 3.4 nm and 4.3 nm, respectively (Figures 4(b), 4(c) and 4(d)).

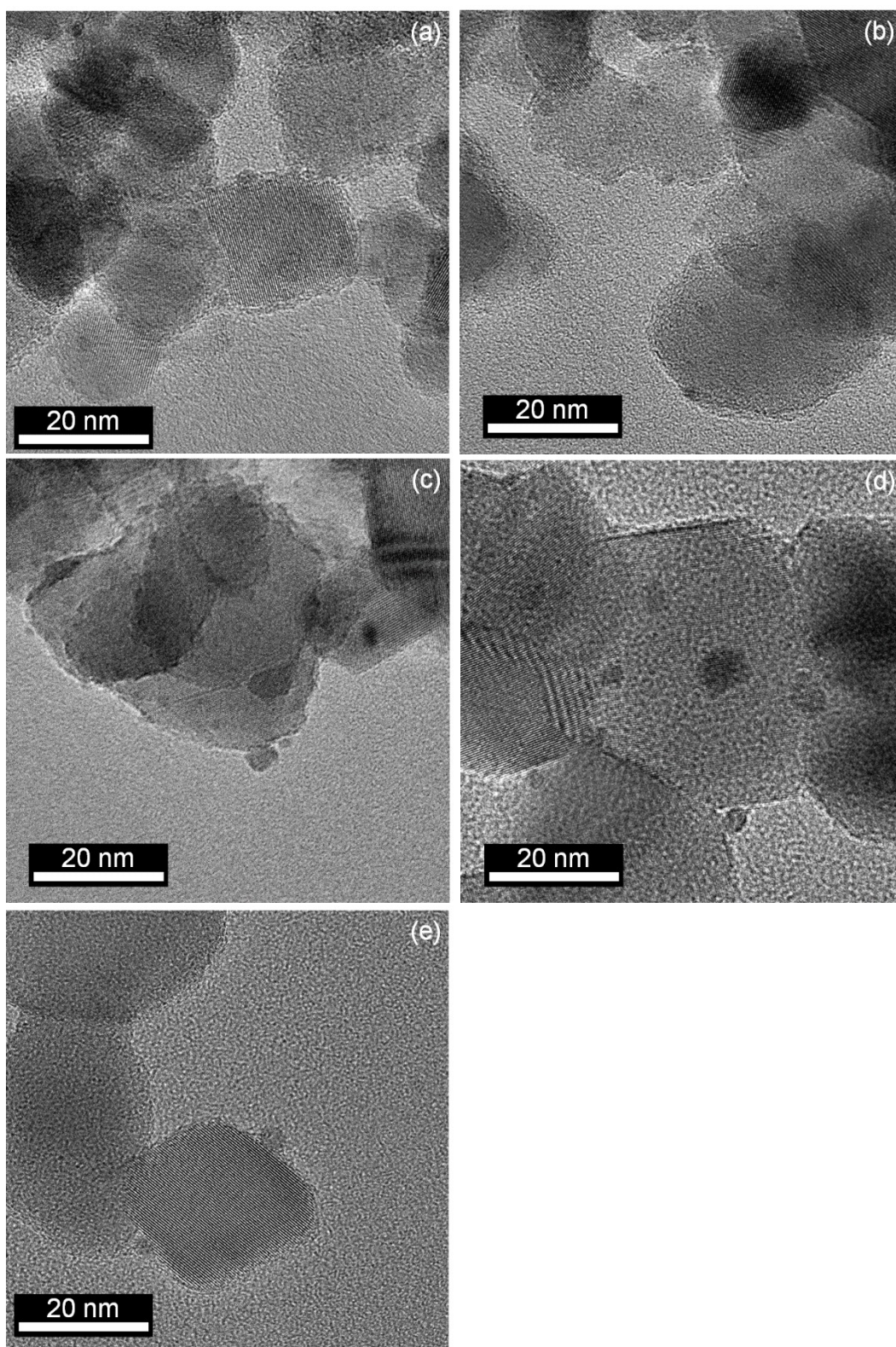


Figure 3 TEM images of (a) Ru/TiO₂, (b) Ru75-Pd25/TiO₂, (c) Ru50-Pd50/TiO₂, (d) Ru25-Pd75/TiO₂, and (e) Pd/TiO₂.

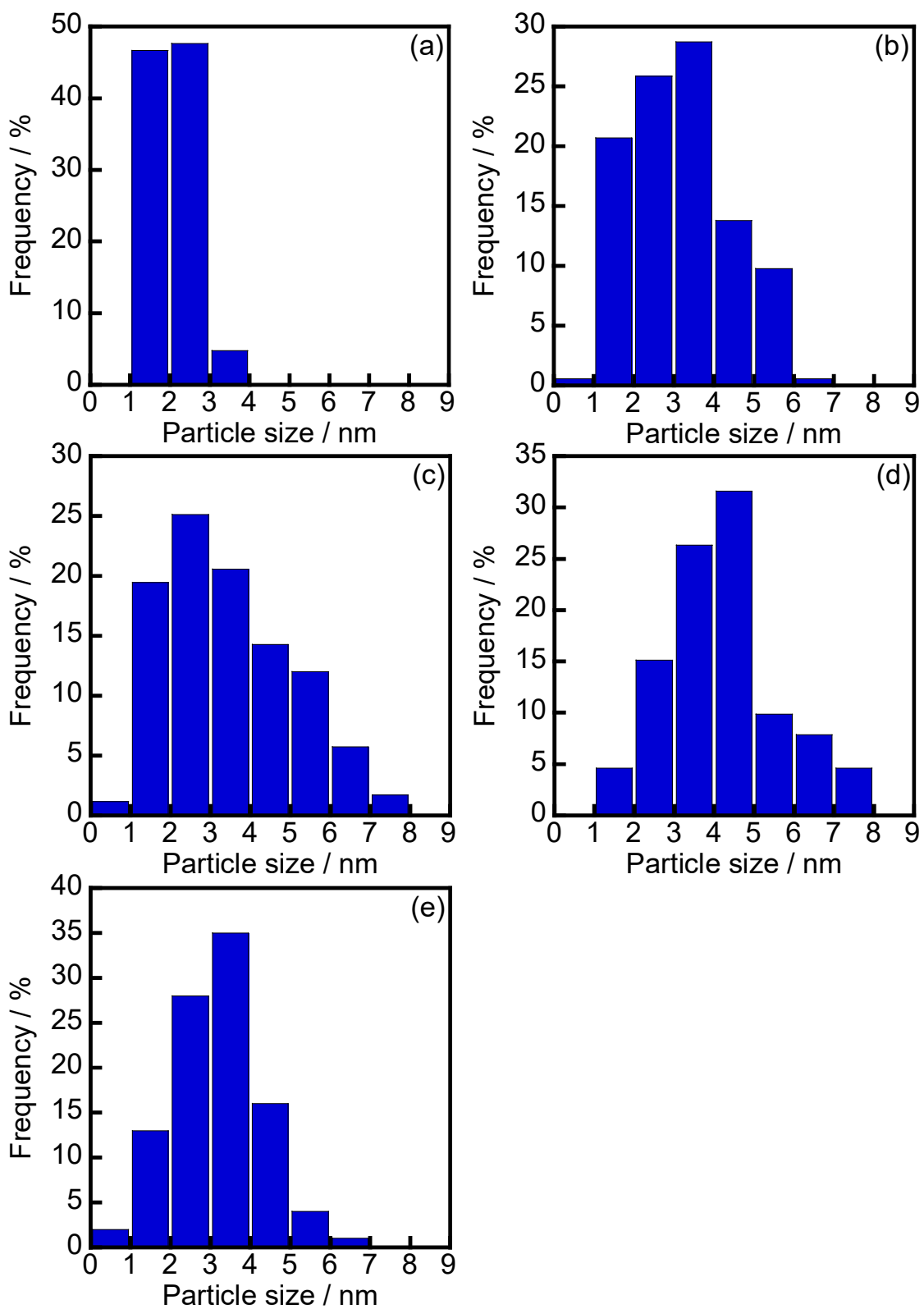


Figure 4 Particle size distributions of (a) Ru/TiO₂, (b) Ru₇₅-Pd₂₅/TiO₂, (c) Ru₅₀-Pd₅₀/TiO₂, (d) Ru₂₅-Pd₇₅/TiO₂, and (e) Pd/TiO₂.

5.3.3. XPS analysis

XPS was used to obtain information on the particles loaded on TiO₂, as shown in Figure 3, and XPS spectra of various samples (RuX-PdY/TiO₂) and reference samples (Pd foil, PdO powder, Ru metal powder and RuO₂ powder) around (a) Pd 3d and (b) Ru 3d components are shown in Figure 5. No peak due to Pd (3d) was observed in the spectrum of Ru/TiO₂ and no peak due to Ru (3d_{5/2}) was observed in the spectrum of Pd/TiO₂. In the spectra of the Pd foil and PdO powder as reference samples, 3d_{5/2} and 3d_{3/2} peaks of Pd⁰ were observed at 335.4 and 340.7 eV, and the peaks of Pd²⁺ were observed at 337.0 and 342.4 eV. The surfaces of Pd particles in Ru-free Pd/TiO₂ were in a metallic state. In the spectra of RuX-PdY/TiO₂, the peak intensity gradually decreased with a decrease in Pd content in the samples and the peak top slightly shifted to the higher binding energy region in all samples, indicating that the Pd species near the surface of particles in RuX-PdY/TiO₂ is in an electron-deficient state (Pd^{δ+}). In the spectra of Ru powder and RuO₂ as reference samples, the 3d_{5/2} peak of Ru⁰ was observed at 279.6 eV, and the peak of Ru⁴⁺ was observed at 280.8 eV. In the spectrum of Pd-free Ru/TiO₂, since the peak was observed at 280.8 eV, the surfaces of Ru particles in Pd-free Ru/TiO₂ were in an oxidized state (Ru⁴⁺). Since the photodeposition provides a strongly reductive condition, the Ru precursor is loaded in the metallic state on the surface of TiO₂. The change in the oxidation state of surface Ru species from zero to +4 means that metallic Ru species on the surfaces of particles partly oxidized during the washing and drying processes under air. Actually, the peak was broad compared with that of RuO₂, indicating that an Ru species in a lower oxidation state is also present near the surface of Ru particles. An increase in the peak at around 279.6 eV was observed in the spectra of Ru75-Pd25/TiO₂ and Ru50-Pd50/TiO₂, indicating that an Ru species in the metallic state is partly present on the surfaces of particles in these samples. The state and distribution of Ru and Pd

species in the particles loaded on TiO₂ and the functions as co-catalysts for ring hydrogenation will be discussed on the basis of results of XPS and XANES in the next section and on the basis of results of additional photocatalytic reactions in the following section.

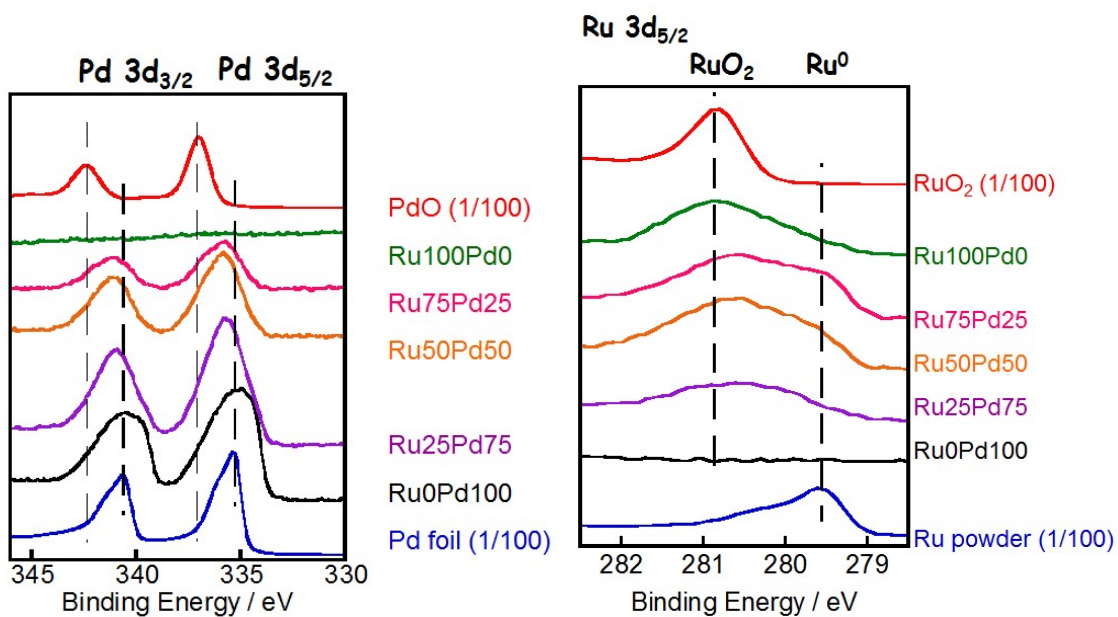


Figure 5 XPS spectra of various samples (RuX-PdY/TiO₂) and reference samples (Pd foil, PdO, Ru metal powder and RuO₂) around (a) Pd 3d and (b) Ru 3d components.

5.3.4. XANES analysis

To obtain bulk information about particles loaded on TiO₂, XANES spectra of the samples shown in the previous section were analyzed. Pd K-edge XANES spectra of Pd/TiO₂ and RuX-PdY/TiO₂ are shown in Figure 6(a) together with spectra of Pd foil and PdO powder as references. XANES spectra of Pd/TiO₂ and Ru-Pd/TiO₂ were similar to that of Pd foil, indicating that most of the Pd species in these samples were in the Pd⁰ state. Considering the results of XPS analysis, it can be concluded that only the Pd species near the surface of particles was in a slightly electron-deficient state. Ru K-edge XANES spectra of Ru/TiO₂ and RuX-PdY/TiO₂ are shown in Figure 6(b) together with spectra of Ru powder and RuO₂ powder as references. Ru/TiO₂ and RuX-PdY/TiO₂ showed XANES spectra of which the shapes included both spectra of Ru and RuO₂. The results of XPS and XANES analyses indicated that both metallic and oxidized Ru species were present in RuX-PdY/TiO₂. Since the results of XPS (surface information) and XANES (bulk information) were similar, the author reached the idea that Ru species were present near the surface of particles formed on the surface of TiO₂. Reduction potentials of Pd²⁺/Pd and Ru³⁺/Ru were 0.951 V²³ and 0.599 V²⁴, respectively, suggesting that Pd²⁺ was preferentially reduced and deposited as Pd metal particles on the surface of TiO₂ followed by the deposition of Ru metal on the Pd particles. During the washing and drying processes, parts of metallic Ru were oxidized to RuO₂, resulting in co-existence of metallic and oxidized states of RuX-PdY/TiO₂. These results suggest that RuX-PdY/TiO₂ had a Pd core-Ru shell-like structure and that this structure contributes to the ring hydrogenation activity of the RuX-PdY/TiO₂ photocatalyst.

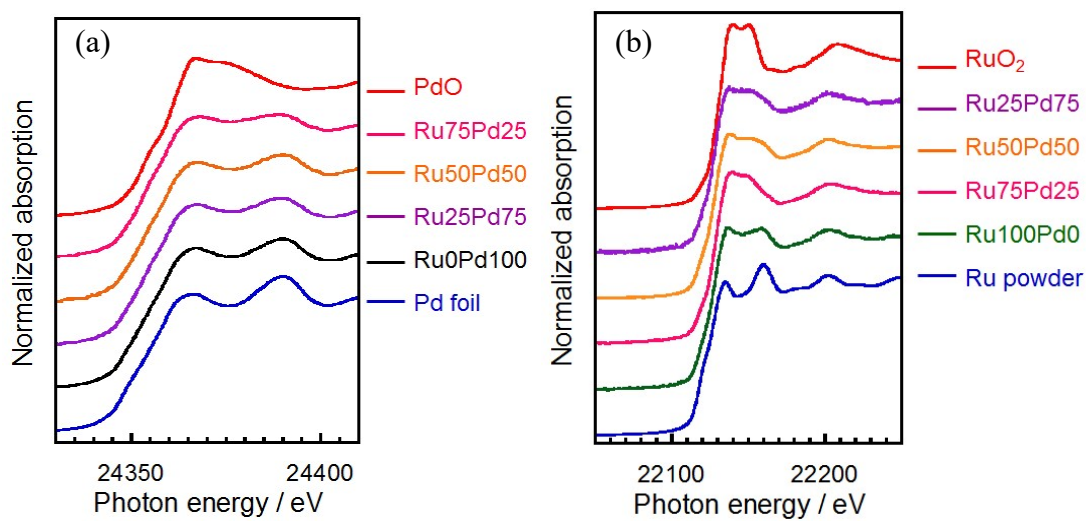


Figure 6 (a) Pd K-edge and (b) Ru K-edge XANES spectra of Pd foil, PdO, Ru metal powder, RuO₂ and various samples (RuX-PdY/TiO₂).

5.3.5. Ring hydrogenation over different types of photocatalyst with the same compositions

To investigate the effect of the combination of Ru and Pd, Pd@Ru/TiO₂, i.e., TiO₂ having a Pd core and an Ru shell (see experimental section) prepared by the two-step photodeposition method, was used for this reaction under the same conditions other than the photocatalyst. The results are shown in Figure 7(b). As expected, Pd@Ru/TiO₂ produced CCA in this reaction as well as RuX-PdY/TiO₂, and the catalytic performance was almost the same (including H₂ evolution) as that of Ru50-Pd50/TiO₂ (Figure 7(a) same at Pd 50% in Figure 2), suggesting that Ru50-Pd50/TiO₂ has a structure similar to that of Pd@Ru/TiO₂. For comparison, Ru/TiO₂ (25 mg, Ru content: 1.0 mol%) and Pd/TiO₂ (25 mg, Pd content: 1.0 mol%) were simultaneously used in this reaction under the same conditions other than the photocatalyst, and the results are shown in Figure 7(c). Although almost the same amounts of H₂ were formed, no ring hydrogenation of BA to CCA occurred in the mixture of Ru/TiO₂ and Pd/TiO₂. These results provided important information about the structure exhibiting photocatalytic activity for ring-hydrogenation of BA, i.e., the co-existence of Ru and Pd in one particle, most likely a Pd core-Ru shell-like structure, is very important.

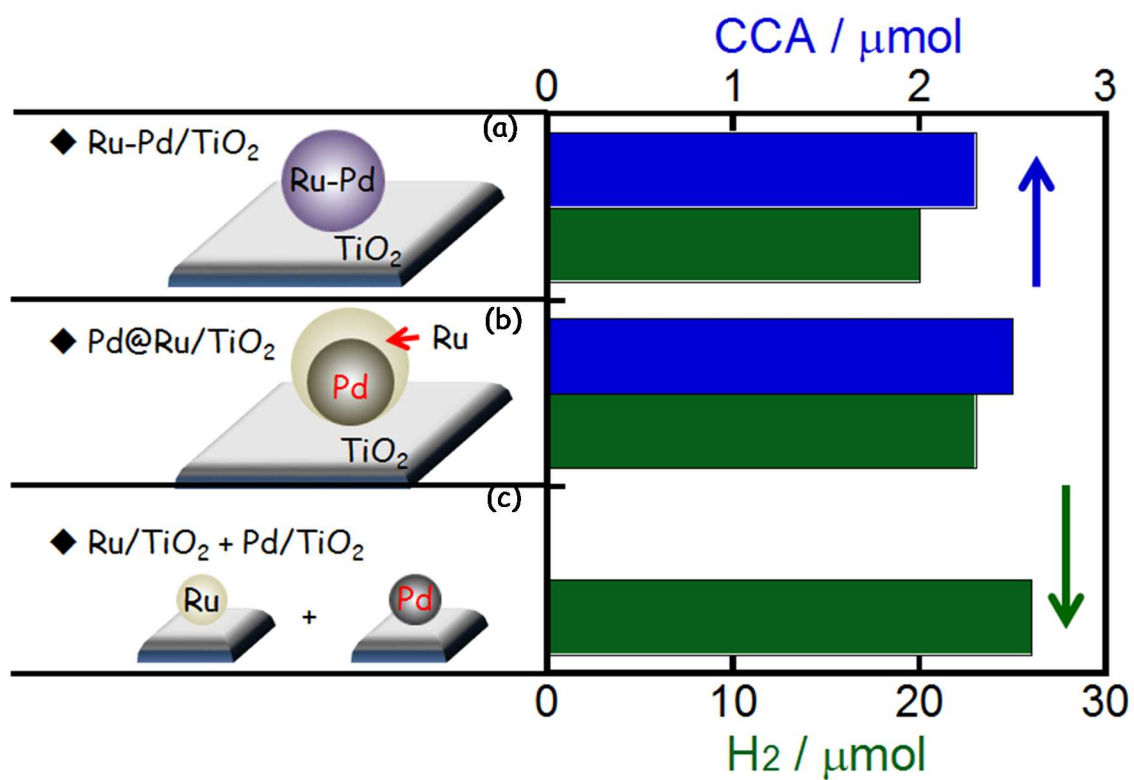


Figure 7 Amounts of CCA and H₂ formed in photocatalytic ring-hydrogenation of BA over (a) Ru₅₀-Pd₅₀/TiO₂, (b) Pd@Ru/TiO₂, and (c) a mixture of Ru/TiO₂ and Pd/TiO₂.

5.3.6. Effect of H₂ treatment of Pd-free Ru/TiO₂ on photocatalytic ring hydrogenation

In order to clarify the active sites of ring hydrogenation of BA, Ru/TiO₂ was treated in H₂ gas at 573 K for 2 h and then used for ring hydrogenation under the same conditions. Since this reduction process requires no post-treatment such as washing and drying, the time of exposure to air can be minimized and the reduced samples can be immediately used for the photocatalytic reaction. Interestingly, CCA was formed over Pd-free hydrogen-treated Ru/TiO₂ as shown in Figure 8, although the reaction rate was much lower than those of RuX-PdY/TiO₂. This result suggests that Ru⁰ loaded on TiO₂ acts as active sites for ring hydrogenation.

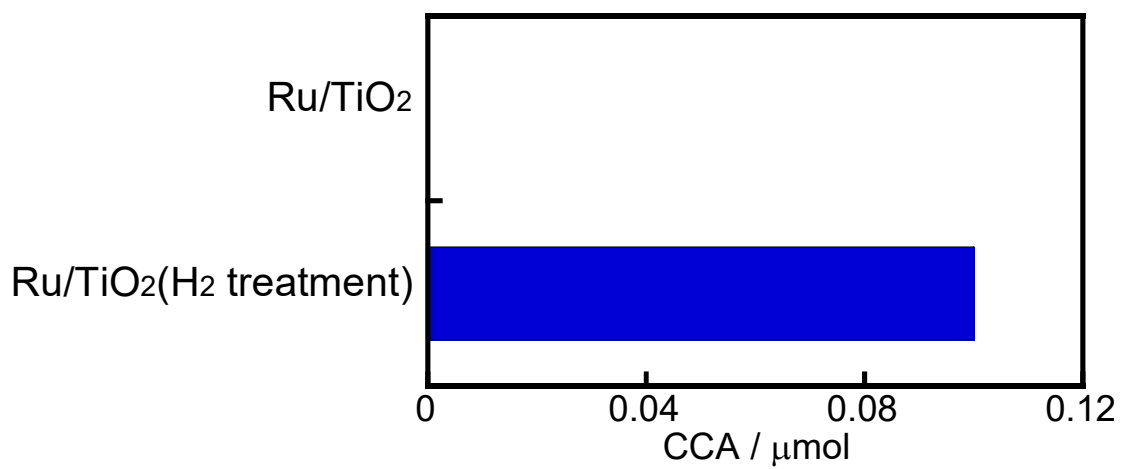


Figure 8 Effect of H₂ treatment of Ru/TiO₂ samples on CCA formation in photocatalytic ring-hydrogenation of BA with 30-min photoirradiation from a high-pressure mercury arc.

5.3.7. Functions of Ru and Pd in photocatalytic ring hydrogenation

Based on the results of characterization of RuX-PdY/TiO₂ and evaluation of photocatalytic activity in ring hydrogenation, the expected structure of RuX-PdY/TiO₂ is shown in Figure 9. In the particles loaded on TiO₂, Ru is mainly distributed on the outer surface of the particles and most of the Pd is distributed inside the particles, i.e., a core-shell-like structure is formed. However, the results of XPS and XANES suggest that the core-shell structure is incomplete and parts of Pd may be exposed outside. Some of the surface Ru is oxidized to Ru⁴⁺ by oxygen in air and some of the surface Ru is stabilized as a metallic state probably by the contribution of Pd located near Ru. The stabilized metallic Ru acts as active sites for photocatalytic ring hydrogenation of BA. The presence of a slightly electron-deficient Pd species suggests that electrons are donated to Ru species, resulted in the stabilization of metallic Ru. As shown in the author's previous paper, Ru/TiO₂ was inactive for this reaction. Strictly speaking, this expression is not correct; surface-oxidized Ru/TiO₂ was inactive. The obtained results indicate that stabilization of metallic Ru is difficult due to oxidation by oxygen and can be achieved by co-use of Pd. This study also revealed a new function of Pd, i.e., stabilizer of Ru in a metallic state.

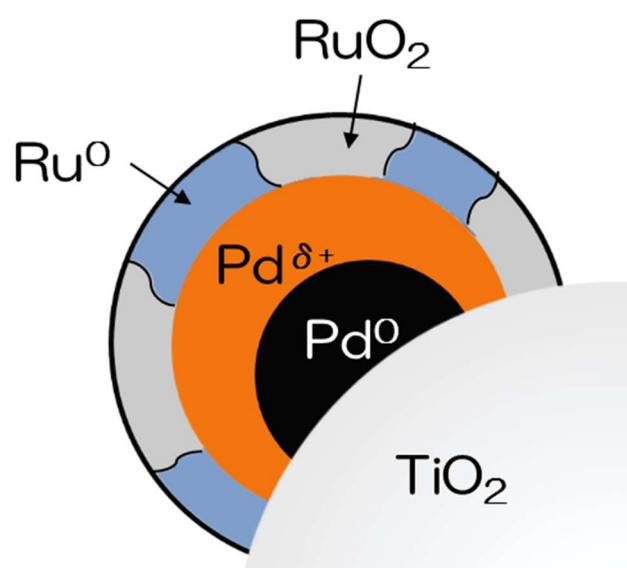


Figure 9 The expected structure of RuX-PdY/TiO₂.

5.4. Conclusions

The author examined ring hydrogenation of BA over a TiO₂ photocatalyst having two kinds of elements as a co-catalyst under H₂-free conditions. Single use of a co-catalyst (Au, Ag, Cu Pd and Ru) and also simultaneous use of co-catalysts in most cases resulted in no hydrogenation, whereas CCA was successfully formed over the Ru-Pd/TiO₂ photocatalyst, indicating that ring hydrogenation was achieved without the use of an Rh co-catalyst. Results of XPS and XANES suggest that Ru and RuO₂ in the particles loaded on TiO₂ are mainly distributed on the outer surface of the particles, and most of the metallic Pd is distributed inside the particles and stabilizes some of the Ru in a metallic state. Photocatalytic reactions suggested that the stabilized metallic Ru acts as active sites for photocatalytic ring hydrogenation of BA.

References

1. B. S. Moore, H. Cho, R. Casati, E. Kennedy, K. A. Reynolds, U. Mocek, J. M. Beale and H. G. Floss, *J. Am. Chem. Soc.*, **1993**, *115*, 5254-5266.
2. N. Perret, X. Wang, J. J. Delgado, G. Blanco, X. Chen, C. M. Olmos, S. Barnal and M. A. Keane, *J. Catal.*, **2014**, *317*, 114-125.
3. T. Harada, S. Ikeda, Y. H. Ng, T. Sakata, H. Mori, T. Torimoto, and M. Matsumura, *Adv. Funct. Mater.*, **2008**, *18*, 2190–2196.
4. Z. Jiang, G. Lan, X. Liu, H. Tang and Y. Li, *Catal. Sci. Technol.*, **2016**, *6*, 7259-7266.
5. X. Wen, Y. Cao, X. Qiao, L. Niu, L. Huo and G. Bai, *Catal. Sci. Technol.*, **2015**, *5*, 3281-3287.
6. H. Wang and F. Zhao, *Int. J. Mol. Sci.*, **2007**, *8*, 628-634.
7. P. T. Anastas and J. C. Warner, *Green Chemistry: Theory and Practice*, Oxford University Press, 1998.
8. M. A. Fox, M. T. Dulay, *Chem. Rev.*, **1993**, *93*, 341-357.
9. K. Imamura, K. Hashimoto, H. Kominami, *Chem. Commun.*, **2012**, *48*, 4356-4358.
10. H. Kominami, K. Nakanishi, S. Yamamoto, K. Imamura and K. Hashimoto, *Catal. Commun.*, **2014**, *54*, 100-103.
11. M. Fukui, A. Tanaka, K. Hashimoto and H. Kominami, *Chem. Lett.*, **2016**, *45*, 985-987.
12. H. Kominami, S. Yamamoto, K. Imamura, A. Tanaka, K. Hashimoto, *Chem. Commun.*, **2013**, *49*, 4558-4560.
13. H. Kominami, M. Higa, T. Nojima, T. Ito, K. Nakanishi, K. Hashimoto, K. Imamura, *ChemCatChem*, **2016**, *8*, 2019-2022.
14. K. Imamura, T. Yoshikawa, K. Nakanishi, K. Hashimoto, H. Kominami, *Chem. Commun.*, **2013**, *49*, 10911-10913.

15. K. Imamura, Y. Okubo, T. Ito, A. Tanaka, K. Hashimoto, H. Kominami, *RSC Adv.*, **2014**, *4*, 19883-19886.
16. K. Nakanishi, A. Tanaka, K. Hashimoto, H. Kominami, *Phys. Chem. Chem. Phys.*, **2017**, *19*, 20206-20212.
17. K. Nakanishi, R. Yagi, K. Imamura, A. Tanaka, K. Hashimoto, H. Kominami, *Catal. Sci. Technol.*, **2018**, *8*, 139-146.
18. K. Kusada, H. Kobayashi, R. Ikeda, Y. Kubota, M. Takata, S. Toh, T. Yamamoto, S. Matsumura, N. Sumi, K. Sato, K. Nagaoka, H. Kitagawa, *J. Am. Chem. Soc.*, **2014**, *136*, 1864-1871.
19. Z. Liu, Y. Huang, Q. Xiao, H. Zhu, *Green Chem.*, **2016**, *18*, 817-825.
20. T. Zhang, S. Wang, F. Chen, *J. Phys. Chem. C*, **2016**, *120*, 9732-9739.
21. H. Tada, A. Takao, T. Akita, K. Tanaka, *ChemPhysChem*, **2006**, *7*, 1687-1691.
22. A. Tanaka, K. Hashimoto, H. Kominami, *ChemCatChem*, **2011**, *3*, 1619-1623.
23. W. H. Haynes, D. R. Lide, Eds., *CRC Handbook of Chemistry and Physics*, *92th Edition*, CRC press: U. S. A., **2011**, 5-83.
24. I. Povar, O. Spinu, *J. Electrochem. Sci. Eng.*, **2016**, *6*, 145-153.

General conclusions

In this work, photocatalytic chemoselective reduction of oxygen containing compounds under hydrogen-free condition was developed and the application to conversion of sulfur-containing compounds and biomass-derived compounds was studied. In addition, photocatalyst according to the “elemental strategy” was also developed. This thesis, which consists of 5 chapters, is a summary of the author’s work.

In chapter 1, photocatalytic deoxygenation of sulfoxides to corresponding sulfides was examined in acetonitrile suspensions of bare TiO₂ particles at room temperature without the use of a metal co-catalyst and toxic reagents. The present photocatalytic method can be applied for deoxygenation of various sulfoxides to corresponding sulfides. Chemoselective reduction of phenyl vinyl sulfoxide to phenyl vinyl sulfide was also achieved because the metal-free TiO₂ photocatalyst had no ability for hydrogenation of the C=C double bond. From chapter1, the author found that TiO₂ photocatalyst can be applied to chemoselective reduction of sulfur-containing compounds.

In chapter 2, FAL was chemoselectively and quantitatively converted to FOL in alcohol suspensions of a TiO₂ photocatalyst under metal-free and hydrogen-free conditions. Oxidation of 2-pentanol to 2-pentanone simultaneously occurred with a high stoichiometry, and various alcohols such as glycerol and ethanol were used for this reaction, indicating that double up-grading of FAL and alcohol was possible. From chapter 2, the author found that biomass upgrading is possible by using photocatalyst.

In chapter 3, the author examined photocatalytic hydrogenation of furan, a representative heterocyclic compound and a compound derived from biomass, in an alcoholic suspension of metal-loaded TiO₂ under an H₂-free condition, in which alcohol

worked as a solvent, electron donor and hydrogen source. Hydrogenation of furan to THF under the present condition consisted of two processes: 1) photocatalytic production of active hydrogen species and 2) thermocatalytic hydrogenation of furan over Pd particles. Biomass-related alcohols (ethanol, butanol and glycerol) can also be used for hydrogenation of furan. From chapter 3, the author found that photocatalytic hydrogenation is not limited to hydrocarbons and can be applied to oxygen-containing heterocyclic compounds.

In chapter 4, the author examined photoinduced ring hydrogenation of BA in an aqueous suspension of metal-loaded TiO₂ in the presence of OA under an H₂-free condition. A large amount of OA molecules was adsorbed on Rh-TiO₂ in water, contributing to efficient hole scavenging under light irradiation, and the reaction rate for CCA formation was mainly determined by the amount of BA adsorbed. From chapter 4, it was revealed that ring hydrogenation is achieved over Rh-TiO₂ photocatalyst and that the adsorption of the substrate is an important factor for the reaction.

In chapter 5, the author examined ring hydrogenation of BA over a TiO₂ photocatalyst having two kinds of elements as a co-catalyst under H₂-free conditions. Single use of a co-catalyst (Au, Ag, Cu Pd and Ru) and also simultaneous use of co-catalysts in most cases resulted in no hydrogenation, whereas CCA was successfully formed over the Ru-Pd/TiO₂ photocatalyst, indicating that ring hydrogenation was achieved without the use of an Rh co-catalyst. Characterization of the photocatalyst suggests that the stabilized metallic Ru acts as active sites for photocatalytic ring hydrogenation of BA. From chapter 5, the author shows the possibility that bimetallic system consisting of two inactive co-catalysts can be used in replace a precious co-catalyst.

In summary, photocatalytic chemoselective reduction of oxygen containing compounds under hydrogen-free condition was achieved. This thesis provides further

possibility of photocatalytic reactions, especially, more difficult reaction and chemoselective reaction.

Regarding the future prospects and possibility for this work, the author is considering applications of visible light responsive photocatalyst for the effective utilization of sun light, biomass upgrading by photocatalytic oxidation and reduction for the accumulation of solar energy, and the development of more advantageous photocatalyst based on elemental strategy using elements with a large Clarke number (carbon, nitrogen and iron).

Publication list

Chapter 1

Photocatalytic deoxygenation of sulfoxides to sulfides over titanium(IV) oxide at room temperature without use of metal co-catalysts

H. Kominami, K. Nakanishi, S. Yamamoto, K. Imamura, K. Hashimoto

Catal. Commun., **2014**, *54*, 100-103.

Chapter 2

Photocatalytic selective hydrogenation of furfural to furfuryl alcohol over titanium(IV) oxide under metal-free and hydrogen-free conditions at room temperature

K. Nakanishi, A. Tanaka, K. Hashimoto, H. Kominami

Chem. Lett., **2018**, *47*, 254-256.

Chapter 3

Photocatalytic hydrogenation of furan to tetrahydrofuran in alcoholic suspensions of metal-loaded titanium(IV) oxide without addition of hydrogen gas

K. Nakanishi, A. Tanaka, K. Hashimoto, H. Kominami

Phys. Chem. Chem. Phys., **2017**, *19*, 20206-20212.

Chapter 4

Ring hydrogenation of aromatic compounds in aqueous suspensions of an Rh-loaded TiO₂ photocatalyst without use of H₂ gas

K. Nakanishi, R. Yagi, K. Imamura, A. Tanaka, K. Hashimoto, H. Kominami

Catal. Sci. Technol., **2018**, *8*, 139-146.

Chapter 5

Ruthenium and palladium bimetallic system achieving functional parity with a rhodium co-catalyst for TiO₂-photocatalyzed ring hydrogenation of benzoic acid

K. Nakanishi, R. Yagi, H. Asakura, A. Tanaka, K. Hashimoto, T. Tanaka, H. Kominami

To be submitted.

Other publication list

1. Copper-modified titanium dioxide: a simple photocatalyst for the chemoselective and diastereoselective hydrogenation of alkynes to alkenes under additive-free conditions

H. Kominami, M. Higa, T. Nojima, T. Ito, K. Nakanishi, K. Hashimoto, K. Imamura
ChemCatChem, **2016**, *8*, 2019-2022.

2. Chemoselective reduction of nitrobenzenes having other reducible groups over titanium(IV) oxide photocatalyst under protection-, gas-, and metal-free conditions

K. Imamura, K. Nakanishi, K. Hashimoto, H. Kominami
Tetrahedron, **2014**, *70*, 6134-6139.

3. Photocatalytic reduction of benzonitrile to benzylamine in aqueous suspensions of palladium-loaded titanium(IV) oxide

K. Imamura, T. Yoshikawa, K. Nakanishi, K. Hashimoto, H. Kominami
Chem. Commun., **2013**, *49*, 10911-10913.

4. Simultaneous and stoichiometric water oxidation and Cr(VI) reduction in aqueous suspensions of functionalized plasmonic photocatalyst Au/TiO₂-Pt under irradiation of green light

A. Tanaka, K. Nakanishi, R. Hamada, K. Hashimoto, H. Kominami
ACS Catal., **2013**, *3*, 1886-1891.

Acknowledgments

This present thesis is the summary of the results of the author's work during 2013-2018 at the Program in Molecular and Material Engineering, Interdisciplinary Graduate School of Science and Engineering, Kindai University. This work was partially supported by Japan Society for the Promotion of Science (JSPS) for a Research Fellowship for young scientists.

The author wishes to express his sincere gratitude to *Professor Hiroshi Kominami*, Department of Applied Chemistry, School of Science and Engineering, Kindai University, for his invaluable guidance, suggestions and innumerable instructions throughout this work.

The author wishes to express his sincere gratitude to *Assistant Professor Atsuhiko Tanaka*, Department of Applied Chemistry, School of Science and Engineering, Kindai University, for his invaluable guidance, suggestions and innumerable instructions throughout this work during 2016-2018.

The author would like to state appreciation to *Senior scientist Keiji Hashimoto*, School of Science and Engineering, Kindai University, for his helpful discussion and comments.

The author thanks Dr. Kazuya Imamura, Mr. Satoshi Yamamoto, Mr. Ryosuke Yagi, and all the member of Professor Kominami's laboratory for their helpful discussion and valuable collaborations.

Finally, the author deeply thanks his parents Kensuke and Nakako Nakanishi, and his sister Saori Yoneda, for their continuous encouragements and supports.

Kousuke Nakanishi

2018